

# **PROCESS DESIGN OF OPTIMAL REACTOR NETWORKS USING ATTAINABLE REGION APPROACH**

**Dual Degree Project Report**

**Submitted in the Partial Fulfillment of the Requirement for the Degree  
of**  
**MASTER OF TECHNOLOGY**  
**in**  
**CHEMICAL ENGINEERING**  
**by**  
**SUSHRUT SHENDRE**  
**(Roll No. 11D020007)**

**Guide: Prof. Arun Moharir**



**DEPARTMENT OF CHEMICAL ENGINEERING  
INDIAN INSTITUTE OF TECHNOLOGY  
BOMBAY 400076  
JUNE 2016**

## **ACCEPTANCE CERTIFICATE**

Department of Chemical Engineering

Indian Institute of Technology, Bombay

The project report entitled “Process Design of Optimal Reactor Networks using Attainable Region Approach” submitted by Mr. Sushrut Shendre (Roll No. 11D020007) may be accepted for being evaluated.

Date: June 22, 2016

Guide: Prof. Arun Moharir

.....

Examiner: Prof. Jayesh Bellare

.....

Chairperson & Examiner: Prof. Mani Bhushan

.....

## **ACKNOWLEDGEMENT**

I sincerely express my gratitude to my project guide Prof. Arun Moharir for his immense support and guidance during the course of this study. His valuable suggestions and timely progress reviews helped me to construct my work.

Sushrut Shendre

11D020007

## **DECLARATION**

I declare that this report represents my ideas in my own words and I have made sure that whenever information, figures or equations from outside sources are included in the report, they have been properly cited and referenced to the original source. I also admit that I have adhered to all principles of academic honesty and integrity and have not falsified any data/fact/source in my submission. I understand that any violation of the above will call for disciplinary action by the Institute and can evoke penal action from sources, which have not been properly cited, or from whom permission has not been taken when needed.

Sushrut Shendre

11D020007

## ABSTRACT

Reactor or a reactor network is a very important component in any process flowsheet. Maximization of value creation can be achieved only if the reactor network is correctly predicted and set up. In this study, we arrive at optimal reactor networks using the profound concept of Attainable Region. The Attainable Region (AR) is a complete set of product compositions that can be obtained by using any reactor network possible for a given reaction scheme and feed composition. We construct the AR using plug flow reactor (PFR) and continuous stirred tank reactor (CSTR) trajectories and mixing lines in a stage-wise procedure using the rate vector method. The user might either directly provide us with a desired product concentration or with an objective function in terms of the product composition which should be optimized. In the case of latter, we set up an optimization problem that can enable us to find the optimum value of this objective function and the product concentration that gives this optimized value. Once we have the product concentration of interest, we check whether it can be attained or not, i.e., whether the point corresponding to this concentration lies inside/on the AR or outside respectively. If the point lies outside, the concentration cannot be attained by simple reactor systems and would require separation systems in addition to the reactor network. If the point lies inside/on the AR, the concentration is attainable and we devise strategies to find the reactor network and its design that will allow us to attain this concentration, by tracing back the trajectories and regions we constructed while constructing the AR. We further look for other possibilities of reactor networks and their respective designs which can meet the same objective and follow this by setting up a cost optimization problem to arrive at the optimal reactor network. A generic algorithm to construct the AR for any reaction scheme, its associated kinetics and feed composition, and to find the optimal reactor network for any desired concentration (if attainable) has been proposed in this study.

## TABLE OF CONTENTS

<b>Chapter No.</b>	<b>Title</b>	<b>Page No.</b>
	Acknowledgement	iii
	Abstract	v
	List of Figures and Tables	vii
	Abbreviations and Nomenclature	xi
<b>1</b>	<b>INTRODUCTION</b>	<b>1</b>
1.1	Overview of Attainable Region	1
1.2	Motivation behind this study	15
1.3	Outline of the study	16
<b>2</b>	<b>LITERATURE SURVEY</b>	<b>17</b>
2.1	Rate Vector Method	17
2.2	Linear Programming Method	18
2.3	Infinite DimEnsionAl State-space (IDEAS) model	20
<b>3</b>	<b>CONSTRUCTION OF ATTAINABLE REGION</b>	<b>22</b>
3.1	Constructing Attainable Region (Van de Vusse)	23
3.2	2D projections of the Attainable Region	33
3.3	Different feed compositions	35
3.4	Other reaction schemes: Trambouze and Denbigh kinetics	39
3.5	Attainable Regions after applying restrictions of feed availability and reactor volume	44
<b>4</b>	<b>OPTIMAL REACTOR NETWORK DESIGN USING ATTAINABLE REGION</b>	<b>65</b>
4.1	To know whether the required point can be attained or not	65
4.2	Reactor Network Design to attain the desired point	67
4.3	Optimal Reactor Network	77
4.4	Optimization of user-defined objective functions	95
<b>5</b>	<b>CONCLUSIONS</b>	<b>107</b>
	<b>REFERENCES</b>	<b>111</b>

## LIST OF FIGURES

Figure No.	Title	Page No.
1.1	Attainable Region for $A \leftrightarrow B$ with a 50-50 mixture of A and B as feed	2
1.2	Attainable Region for $A \leftrightarrow B$ with pure B as feed	2
1.3	Attainable Region for $A \rightarrow B$ with pure A as feed	3
1.4	Concentration profiles of the species as a function of residence time for the reaction $A \rightarrow B \rightarrow C$	3
1.5	PFR line for $A \rightarrow B \rightarrow C$ in $C_A-C_B$ concentration space	4
1.6	PFR line for $A \rightarrow B \rightarrow C$ in $C_A-C_C$ concentration space	5
1.7	PFR line for $A \rightarrow B \rightarrow C$ in $C_B-C_C$ concentration space	5
1.8	PFR and CSTR lines for $A \rightarrow B \rightarrow C$ in $C_A-C_B$ concentration space	6
1.9	PFR and CSTR lines for $A \rightarrow B \rightarrow C$ in $C_A-C_B$ concentration space	8
1.10	The concept of mixing process in the AR	10
1.11	Attainable Region showing the basic processes of reaction and mixing	11
1.12	Multiple reactor network choices to attain points P and Q	12
2.1	Flowsheet for CSTR 'i' in linear programming method (Kauchali et. al. 2001)	18
2.2	Flowsheet for the Infinite DimEnsionAl State-space model (Burri et. al., 2001)	20
3.1	Candidate AR obtained after Stage 1 – Van de Vusse reaction scheme	25
3.2	Rate vectors at different points on the normal Stage 1 trajectory	27
3.3	Candidate AR obtained after Stage 2	28
3.4	Rate vectors at different points on the CSTR trajectory from the initial feed point	30
3.5	Candidate AR obtained after stage 3	31
3.6	Final Attainable Region for the Van de Vusse reaction scheme (black); the blue and green trajectories represent the normal PFR and CSTR trajectories from the given feed point	32
3.7	Attainable Region for the Van de Vusse reaction scheme as obtained in previous work (Glasser and Hildebrandt, 1997)	32
3.8	2D projection of the AR in A v/s C space	34
3.9	2D projection of the AR in A v/s D space	34
3.10	AR plot for Van de Vusse reaction scheme with feed as [0.9 0.1 0 0]	35
3.11	AR plot for Van de Vusse reaction scheme with feed as [0.5 0.5 0 0]	36
3.12	AR plot for Van de Vusse reaction scheme with feed as [0.2 0.8 0 0]	36
3.13	AR plot for Van de Vusse reaction scheme with feed as [0.9 0 0.1 0]	36
3.14	AR plot for Van de Vusse reaction scheme with feed as [0.1 0 0.9 0]	37
3.15	AR plot for Van de Vusse reaction scheme with feed as [0.9 0 0 0.1]	37
3.16	AR plot for Van de Vusse reaction scheme with feed as [0.25 0.25 0.25 0.25]	37
3.17	AR plot for Van de Vusse reaction scheme with feed as [0 1 0 0]	38
3.18	AR plot for Van de Vusse reaction scheme with feed as [0 0.5 0.5 0]	38
3.19	AR plot for Van de Vusse reaction scheme with feed as [0 0.5 0 0.5]	38
3.20	AR plot for Van de Vusse reaction scheme with feed as [0 0.5 0.25 0.25]	39
3.21	Candidate AR plot for Trambouze reaction scheme – Stage 1	41

3.22	Candidate AR plot for Trambouze reaction scheme – Stage 2	41
3.23	AR plot for Trambouze reaction scheme – Stage 3	42
3.24	AR plot for Trambouze reaction scheme – from literature (Wang et. al., 2006)	42
3.25	AR plot for Denbigh reaction scheme	43
3.26	The model for a single CSTR	45
3.27	AR plot for a single CSTR of volume 1 m <sup>3</sup> and maximum feed available of 1m <sup>3</sup> /s (Van de Vusse reaction scheme)	47
3.28	Comparison of ARs with and without feed & volume constraints	48
3.29	AR plot for a single CSTR of volume 0.5 m <sup>3</sup> and maximum feed available of 1m <sup>3</sup> /s (Van de Vusse reaction scheme)	48
3.30	AR plot for a single CSTR of volume 0.1 m <sup>3</sup> and maximum feed of 1m <sup>3</sup> /s (VdV reaction scheme)	49
3.31	AR plot for a single CSTR of volume 0.05m <sup>3</sup> and maximum feed of 1m <sup>3</sup> /s (VdV reaction scheme)	49
3.32	AR plot for a single PFR of volume 1 m <sup>3</sup> and maximum feed available of 1m <sup>3</sup> /s (Van de Vusse reaction scheme)	50
3.33	AR plot for a single PFR of volume 0.5 m <sup>3</sup> and maximum feed of 1m <sup>3</sup> /s (VdV reaction scheme)	50
3.34	AR plot for a single PFR of volume 0.1 m <sup>3</sup> and maximum feed of 1m <sup>3</sup> /s (VdV reaction scheme)	50
3.35	AR plot for a single PFR of volume 0.05 m <sup>3</sup> and maximum feed of 1m <sup>3</sup> /s (VdV reaction scheme)	51
3.36	PFR and CSTR plots for the AR under feed availability and reactor volume restrictions	51
3.37	Two reactor series model	52
3.38	AR for two reactor model under feed and volume constraints for VdV reaction scheme – case 1	54
3.39	AR for two reactor model under feed and volume constraints for VdV reaction scheme – case 2	54
3.40	AR for two reactor model under feed and volume constraints for VdV reaction scheme – case 3	55
3.41	AR for two reactor model under feed and volume constraints for VdV reaction scheme – case 4	55
3.42	Two reactor parallel model	56
3.43	AR for two reactor model under feed and volume constraints for VdV reaction scheme – case 5	56
3.44	AR for two reactor model under feed and volume constraints for VdV reaction scheme – case 6	56
3.45	AR for two reactor model under feed and volume constraints for VdV reaction scheme – case 7	57
3.46	Final AR for two reactor model under feed and volume constraints for VdV reaction scheme	57
3.47	Comparison of the ARs for one and two reactor models under restrictions of feed and volume	58
3.48	Three reactor model – Arrangement 1	58
3.49	Three reactor model – Arrangement 2	59
3.50	Three reactor model – Arrangement 3	59
3.51	Three reactor model – Arrangement 4	59
3.52	ARs for all combinations of R <sub>1</sub> and R <sub>2</sub> in Arrangement 1 of three reactor model	60

3.53	ARs for all combinations of $R_1$ and $R_2$ in Arrangement 2 of three reactor model	61
3.54	ARs for all combinations of $R_1$ and $R_2$ in Arrangement 3 of three reactor model	62
3.55	ARs for all combinations of $R_1$ and $R_2$ in Arrangement 4 of three reactor model	63
3.56	Final AR for three reactor model under feed and volume constraints for VdV reaction scheme	63
4.1	Stage 1 region for VdV reaction scheme showing the point required (red) in Illustration 4.2.1(a)	68
4.2	The reactor network to obtain the point desired in Illustration 4.2.1(a)	68
4.3	Stage 1 region for VdV reaction scheme showing the point required (red) in Illustration 4.2.1(b)	69
4.4	The reactor network to attain the point desired in Illustration 4.2.1(b)	70
4.5	Stage 1 region for VdV reaction scheme showing the point required (red) in Illustration 4.2.2	70
4.6	The reactor network required to attain the point desired in Illustration 4.2.2	71
4.7	AR plot for VdV Vusse reaction scheme showing the point required (P) in Illustration 4.2.3	72
4.8	The reactor network required to attain the point desired in Illustration 4.2.3	73
4.9	AR plot for VdV Vusse reaction scheme showing the point required (R) in Illustration 4.2.4	74
4.10	The reactor network required to attain the point desired in Illustration 4.2.4	74
4.11	AR plot for Van de Vusse reaction scheme showing the point required (red) in Illustration 4.2.5	75
4.12	The reactor network required to attain the point desired in Illustration 4.2.5	76
4.13	AR plot for Van de Vusse reaction scheme showing the point required (red) in Illustration 4.2.6	76
4.14	The reactor network required to attain the point desired in Illustration 4.2.6	77
4.15	Alternate strategies to attain the required point(red) – Illustration 4.3.1	78
4.16	Alternate reactor network to attain the example discussed in Illustration 4.2.1	79
4.17	Possible reactor networks to attain the point (0.4576,0.0070) in the VdV reaction scheme	80
4.18	Alternate strategies to attain the required point(red) – Illustration 4.3.2	81
4.19	Alternate reactor network to attain the example discussed in Illustration 4.2.2	81
4.20	Possible reactor networks to attain the point (0.6999,0.0042) in the VdV reaction scheme	82
4.21	Strategies to attain point Q – Illustration 4.3.3	83
4.22	Reactor network design to attain point Q in Illustration 4.3.3	83
4.23	Non-optimal reactor network to attain the point in Illustration 4.3.2	84
4.24	Stage 1 normal and convexified curves for the reaction scheme 2A->B->C showing the required point (red) and the multiple strategies that can be used to attain it	85

4.25	One of the possible reactor networks required to attain the point desired in Illustration 4.3.4	85
4.26	Coupled Attainable Region plot and the optimal reactor network scheme to traverse the boundary for the Van de Vusse reaction scheme	87
4.27	Optimal Reactor Network for the Van de Vusse reaction scheme	88
4.28	Comparison of our results with those of Metzger and Glasser. (a)Attainable region from previous study. (b) Attainable region from our results (c) Optimal Reactor Network from previous study (d) Optimal Reactor Network from our results. Figure 11(a) and 11(c) cited from 'Teaching Reaction Engineering using the Attainable Region; Matthew J. Metzger, Benjamin J. Glasser	89
4.29	AR plot for the Van de Vusse reaction scheme and its various trajectories and regions	90
4.30	The AR plot the Van de Vusse reaction scheme for the kinetics as given in Example 4.4.1	97
4.31	Reactor network to attain the point desired	98
4.32	Reactor network required to attain the point desired in Example 4.4.1- Case 1	99
4.33	Reactor network required to attain the point desired in Example 4.4.1- Case 2	99
4.34	Reactor network required to attain the point desired in Example 4.4.1- Case 3	99
4.35	Reactor network required to attain the point desired in Example 4.4.1- Case 4	100
4.36	The AR plot the Trambouze reaction scheme for the kinetics as given in Example 4.4.2	102
4.37	The AR plot the alpha-Pinene reaction scheme for the kinetics as given in Example 4.4.3	103
4.38	The reactor network required to attain the point desired in Example 4.4.3	104
4.39	The AR plot the Denbigh reaction scheme for the kinetics as given in Example 4.4.4	105
4.40	The reactor network required to attain the point desired in Example 4.4.4	106
5.1	Summary of the study	110

## LIST OF TABLES

Table No.	Title	Page No.
3.1	Areas of the convex candidate ARs after various stages	31
4.1	Reactor networks for various curves/regions of the Attainable Region	91
4.2	Parameters for Van de Vusse reaction scheme	99
4.3	Summary of results for Van de Vusse reaction scheme	101
4.4	Summary of results for $\alpha$ -Pinene reaction scheme	104
4.5	Summary of results for Denbigh reaction scheme	106

## ABBREVIATIONS

AR	Attainable Region
PFR	Plug Flow Reactor
CSTR	Continuous Stirred Tank reactor
DSR	Differential Stream Reactor
IDEAS	Infinite DimEnsionAl State-space model
VdV	Van de Vusse

## NOMENCLATURE

Symbol	Name (Units)	First used on Page No.
a	Fraction of feed which goes in the reactor(dimensionless)	71
$c_i$	Composition at CSTR exit ( $\text{kg}/\text{m}^3$ )	18
$c_{\text{low}}$	Lower limit on the composition ( $\text{kg}/\text{m}^3$ )	19
$c_{\text{out}}$	Composition at network outlet ( $\text{kg}/\text{m}^3$ )	19
$c_{\text{up}}$	Upper limit on the composition ( $\text{kg}/\text{m}^3$ )	19
C	Concentration ( $\text{kmol}/\text{m}^3$ )	1
d	column vector of the constant terms in the equations	96
frac	Fraction ranging from 0 to 1	45
$FC_i^0$	Component inlet flowrate ( $\text{kg}/\text{s}$ )	18
$F_i$	Total feed to the $i^{\text{th}}$ CSTR ( $\text{m}^3/\text{s}$ )	18
k	Rate constant (units vary with order)	4
K	Number of network outlet streams (dimensionless)	20
m	Slope (dimensionless)	94
M	vector form of the coefficients of x and y coordinates in the equations	96
p	Required point	65
P	Number of network inlet streams (dimensionless)	20
$Q_{ij}$	Flowrate at exit of CSTR $i$ entering CSTR $j$ ( $\text{m}^3/\text{s}$ )	18
$Q_{i,\text{out}}$	Flowrate at exit of CSTR $i$ sent to outlet of network ( $\text{m}^3/\text{s}$ )	18
$Q_{0,i}$	Amount of feed entering the CSTR $i$ ( $\text{m}^3/\text{s}$ )	18
$Q_{0,\text{out}}$	Amount of feed bypassing all CSTRs ( $\text{m}^3/\text{s}$ )	18
r	Rate vector ( $\text{mol}/\text{m}^3\text{s}$ )	26
R	Reactor (dimensionless)	52
s	Fraction of feed bypassed (dimensionless)	7
t	variable in terms of which the objective function is described	96
u	Flow parameter in IDEAS model ( $\text{m}^3/\text{s}$ )	20
$U_f$	Lower bound on volume ( $\text{m}^3$ )	19

$U_v$	Upper bound on volume ( $m^3$ )	19
$V_i$	Volume of CSTR $I$ ( $m^3$ )	18
$w$	Flow parameter used in IDEAS model ( $m^3/s$ )	20
$x$	Flow parameter used in IDEAS model ( $m^3/s$ )	20
$X$	Matrix for storing normal trajectory data points (dimensionless)	25
$y$	Flow parameter used in IDEAS model ( $m^3/s$ )	20
$Y$	Matrix for storing convexified curve data points (dimensionless)	25
$y_i$	Binary variable (dimensionless)	20
$z_{mn}$	Flow joining $m$ to $n$ ( $m^3/s$ )	20

### Greek Symbols:

$\alpha$	Concentration parameter in IDEAS model ( $kg/m^3$ )	21
$\beta$	Cost associated with mixing or reactor operation (\$)	80
$\gamma$	Concentration parameter in IDEAS model ( $kg/m^3$ )	21
$\epsilon$	Concentration parameter in IDEAS model ( $kg/m^3$ )	21
$\Psi$	Cost coefficient in IDEAS model (\$)	21
$\tau$	Residence time (s)	4
$v$	Flow rate ( $kg/m^3$ )	45
$\omega$	Cost coefficient in IDEAS model (\$)	21
$\chi$	Cost coefficient in IDEAS model (\$)	21
$\zeta$	Cost coefficient in IDEAS model (\$)	21
$\Omega$	Concentration parameter in IDEAS model ( $kg/m^3$ )	21

# CHAPTER 1

## INTRODUCTION

### 1.1. Overview of Attainable Region

The concept of Attainable Region (AR) theory was originally introduced by Horn in 1964. It is defined as a product concentration space which can be achieved by any possible reactor network, which may include Plug Flow Reactors (PFRs), Continuous Stirred Tank Reactors (CSTRs), bypass, recycle and their combinations, from a single or multiple feeds. (Glasser and Hildebrandt, 1997; Godorr et al., 1999; Hildebrandt and Glasser, 1990; Hildebrandt et al., 1990). Suppose we are being provided with a feed. Now if employ any number of reactors in any series or parallel combination, the set of all possible product combinations that we can achieve is called the Attainable Region.

We introduce the concept of AR by taking a simple reaction which is as follows



where  $A$  and  $B$  represent the two species involved in the reaction. The arrow  $\leftrightarrow$  represents that the reaction is reversible. Suppose the feed is a 50-50 mixture of  $A$  and  $B$  with both concentrations as  $0.5 \text{ kmol/m}^3$ . The equilibrium constant is unity.

Here, we see that the composition is at equilibrium from the beginning itself given that the feed is a 50-50 mixture of  $A$  and  $B$  and the equilibrium constant is unity. The composition remains the same and does not change by reaction. Irrespective of the reactor type and size, the concentration of both the species remains unchanged. Thus, the AR in this case is just a point and is thus zero dimensional. When plotted in a two dimensional space  $C_A - C_B$ , where  $C_i$  represents the concentration of species  $i$ , it is just a point,  $(0.5,0.5)$  as shown in Fig. 1.1.

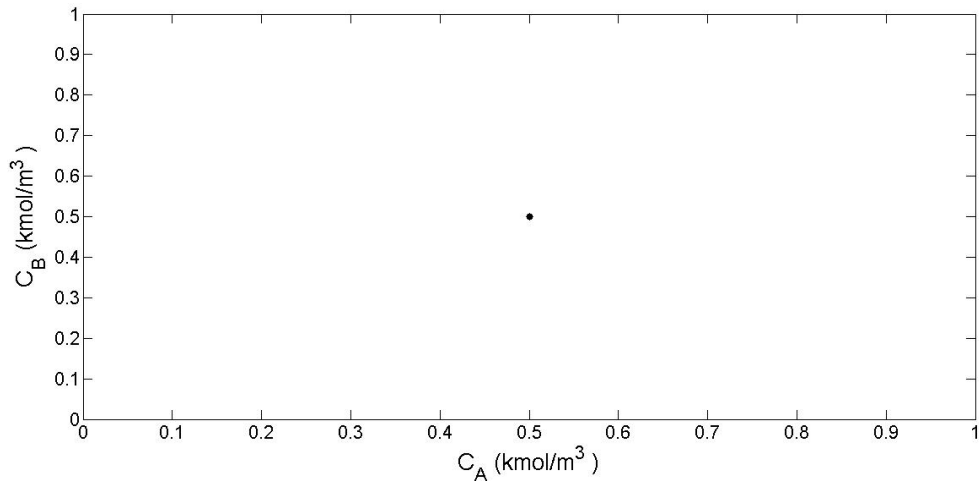


Fig. 1.1. Attainable Region for  $A \leftrightarrow B$  with a 50-50 mixture of A and B as feed

Now, suppose the feed is pure B instead, its concentration being  $1 \text{ kmol/m}^3$ . The AR for such a feed is a straight line joining the feed point, which in the  $C_A - C_B$  space is  $(0,1)$  and the equilibrium point,  $(0.5,0.5)$ , as shown in Fig. 1.2.

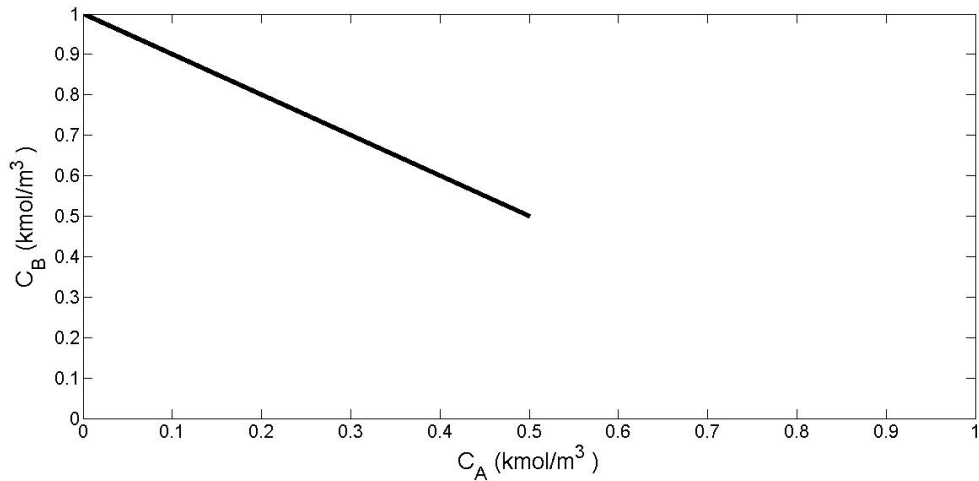


Fig. 1.2. Attainable Region for  $A \leftrightarrow B$  with pure B as feed

Now, if we use pure A with its concentration as  $1 \text{ kmol/m}^3$  as the feed, with the above reaction as irreversible, then as reactor space time increases, pure A will react to form B and finally, we will be left with only pure B. Thus, the AR in this case will be a straight line joining the points corresponding to the feed  $(1,0)$  and the final point  $(0,1)$ . It is shown in Fig. 1.3.

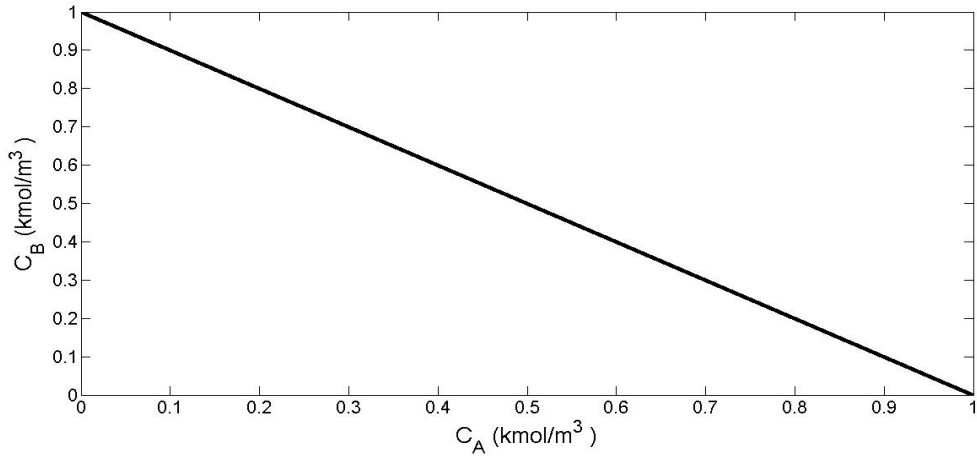
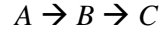


Fig. 1.3. Attainable Region for  $A \rightarrow B$  with pure A as feed

As we saw in the previous trivial looking examples, the ARs were quite simple. The potential of AR in reactor network design evolves as one gets into multiple series-parallel reactions, with the simplest of them being an irreversible series reaction



The feed is pure A, its concentration being  $1 \text{ kmol/m}^3$ . Both the reactions are first order and the rate constants for both the reactions are taken as  $1 \text{ s}^{-1}$ . The concentration space is three dimensional here and the AR resides in this three dimensional space. However, for the ease of visualization, the AR is displayed in two dimensional space using concentrations of any two species involved in the reaction. So if we consider a plug flow reactor (PFR) and allow the above reaction to proceed for a considerable space time, the concentration profiles for A, B and C as a function of space time,  $\tau$  are obtained as shown in Fig. 1.4.

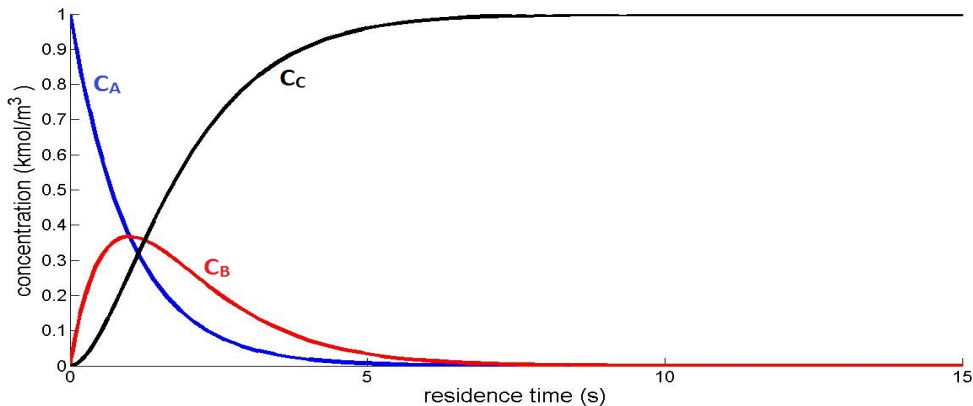


Fig. 1.4. Concentration profiles of the species as a function of space time for the reaction  $A \rightarrow B \rightarrow C$

These profiles were derived using the PFR equations:

$$\frac{dC_A}{d\tau} = -k_1 C_A \quad (1.1)$$

$$\frac{dC_B}{d\tau} = k_1 C_A - k_2 C_B \quad (1.2)$$

$$\frac{dC_C}{d\tau} = k_2 C_B \quad (1.3)$$

The equations basically govern how fast the components involved in the reaction are getting consumed/created, where  $C_i$  represent the concentration of species  $i$ .  $\tau$  represents the space time and  $k_1$  and  $k_2$  represent the rate constants.

Now, these equations can also be used to construct a  $C_B$  v/s  $C_A$  plot over the range of space time. This curve is called a reactor line and is as shown in Fig. 1.5.

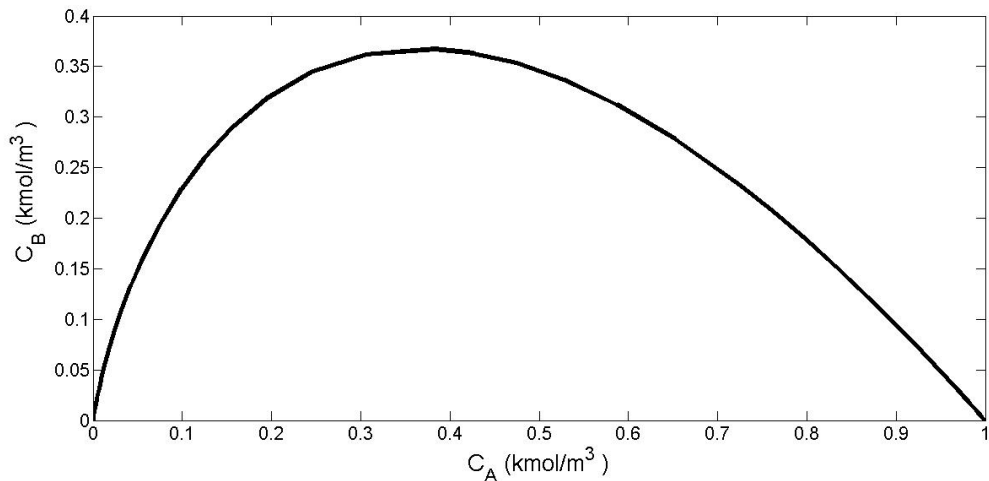


Fig. 1.5. PFR line for  $A \rightarrow B \rightarrow C$  in  $C_A$ - $C_B$  concentration space

This representation in two dimensions is by no means limited to two particular species. We can also construct  $C_C$  v/s  $C_A$  and  $C_C$  v/s  $C_B$  plots, as are shown in Fig. 1.6. and Fig. 1.7.

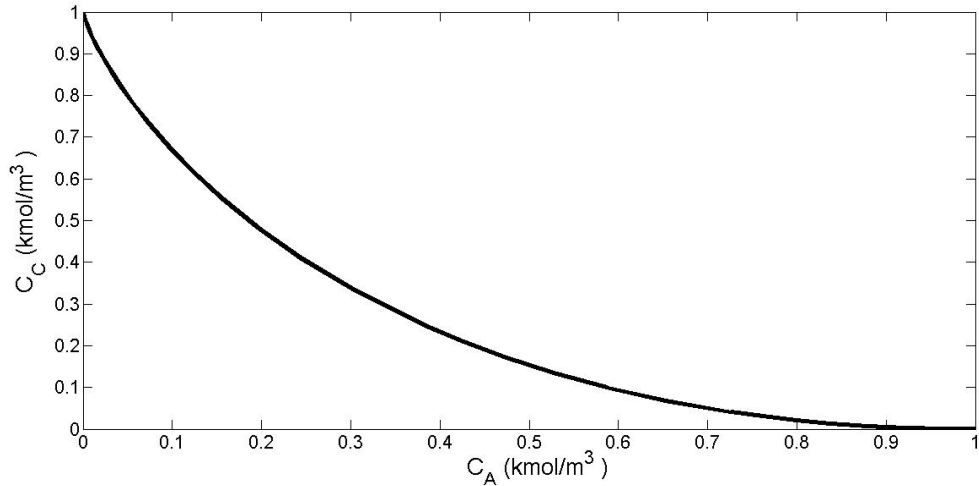


Fig. 1.6. PFR line for  $A \rightarrow B \rightarrow C$  in  $C_A$ - $C_C$  concentration space

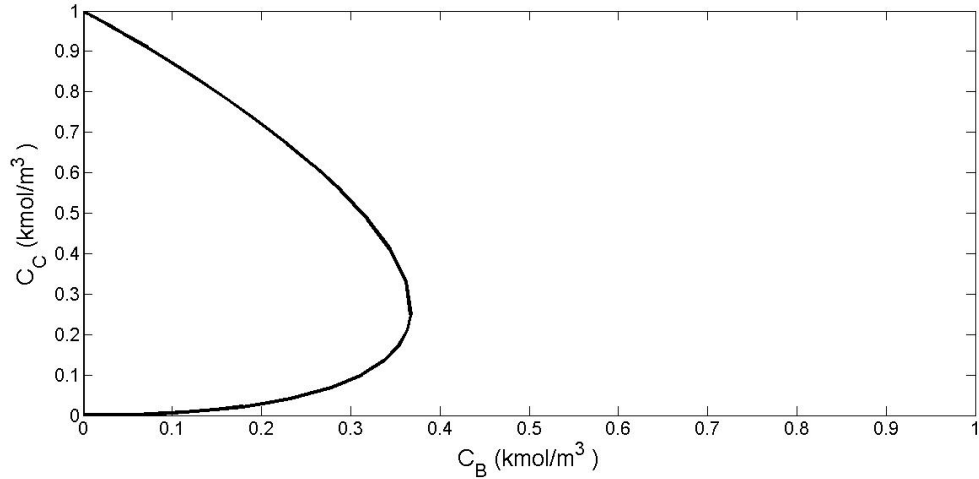


Fig. 1.7. PFR line for  $A \rightarrow B \rightarrow C$  in  $C_B$ - $C_C$  concentration space

We now look at some of the properties that are useful in the construction of AR.

**A point in AR concentration space representing the feed point is always included in the AR.**

Since the feed point is already available to us, we can achieve this point in the output if we choose to employ no reactor at all. Thus, the feed is always part of the AR. This can be clearly seen from Fig. 1.1 – 1.3 and Fig. 1.5 – 1.7.

**A point in the AR concentration space representing infinite space time is also included in the AR.**

By infinite space time, we mean that the space time is large enough that the reactions go to completion. For reversible reactions, this would mean that the reaction has reached the equilibrium point. Thus, if we operate any reactor for infinite space time, the concentration we get is obviously attainable.

From Fig. 1.1, we see that the point (0.5,0.5) which was the equilibrium point, is attainable. For the reaction scheme  $A \rightarrow B \rightarrow C$ , the concentrations of species,  $A$ ,  $B$  and  $C$  at infinite space time are 0, 0 and 1 kmol/m<sup>3</sup> respectively since  $A$  would be get continuously get depleted, and the intermediate specie,  $B$  which is formed initially, also gets converted to  $C$ , once  $A$  is completely depleted. From Fig. 1.5–1.7, we see that the concentrations of  $A$ ,  $B$  and  $C$ , corresponding to infinite space time, are included in the AR.

Now, for the reaction scheme mentioned above, we can also generate a continuous stirred tank reactor (CSTR) line. The CSTR equations are given as:

$$C_A - C_A^0 = \tau(-k_1 C_A) \quad (1.4)$$

$$C_B - C_B^0 = \tau(k_1 C_A - k_2 C_B) \quad (1.5)$$

$$C_C - C_C^0 = \tau(k_2 C_B) \quad (1.6)$$

where  $C_i^0$  denotes the concentration of specie  $i$  in the feed.

The  $C_B$  v/s  $C_A$  plot for a CSTR line is shown in Fig. 1.8. along with the PFR line obtained earlier.

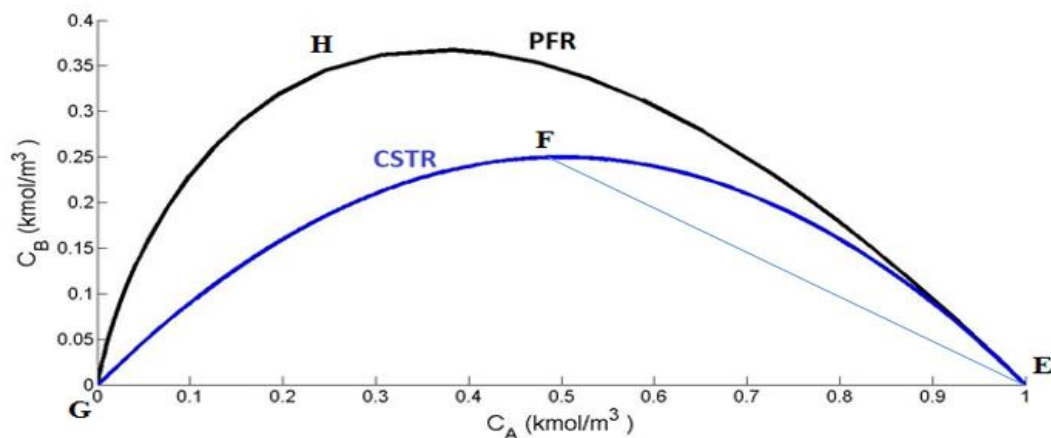


Fig. 1.8. PFR and CSTR lines for  $A \rightarrow B \rightarrow C$  in  $C_A$ - $C_B$  concentration space

Thus, the two lines indicate all the possible product combinations which are attainable using one and only one PFR or CSTR. That is, all points on the curve, EFG, can be attained by operating a CSTR. As we increase the CSTR space time, we traverse along EFG. Similarly, all points on the curve EHG can be attained by operating a PFR.

Now, suppose we have a CSTR operating at a certain space time so as to obtain point F. Now, we bypass the feed such that the fraction of feed being bypassed is  $s$  and that being sent to the reactor is  $1 - s$ . The mixed cup concentration, which is the concentration obtained when the bypassed feed is mixed with the concentration at the reactor exit, will be a point lying on the line segment EF. The exact location of this point will split EF in two parts, one of fractional length  $s$  towards F, and the other of fractional length  $1 - s$  towards E. This can be appreciated by simple mass balance. Thus, changing the value of  $s$  from 0 to 1 allows us to traverse from F along FE towards E. The extreme cases can be understood very easily. When  $s$  is 0, no feed is being bypassed, i.e. the mixed cup concentration is the same as that of reactor exit, i.e. point F. When  $s$  is 1, all the feed is being bypassed and none of it enters the reactor. Thus, the mixed cup concentration is same as that of the feed, i.e. point E. Thus, when the value of  $s$  is near to 0, we get points close to F, and when the value of  $s$  is close to 1, we get points close to E. The mixed cup concentration is given by the mixing rule.

$$\overline{C_{mixedcup}} = s\overline{C_1} + (1 - s)\overline{C_2} \quad (1.7)$$

where  $s$  is the mixing fraction and  $\overline{C_{mixedcup}}$ ,  $\overline{C_1}$  and  $\overline{C_2}$  are concentrations vectors representing the mixed cup concentration, concentration of the feed (bypassed) and the concentration at the reactor exit respectively.

Thus, we saw that all points on the line segment EF can be attained by operating a CSTR with bypass. Now, if we change the location of point F by changing the reactor space time and allow it to traverse along the blue curve, each of the line segments connecting it to the feed point can be attained. Thus, all the points under the blue curve and thus the whole area under the blue curve can be attained by the same configuration, which is, operating a CSTR with bypass. For different points, the parameters that change are the space time at which the CSTR is operated and the fraction of feed being bypassed.

Similarly, the whole area under the black curve can be attained by operating a PFR with bypass. Thus, for points lying under the blue curve, i.e. points inside the region EFGE can be attained by two strategies, either by operating a CSTR with bypass, or a PFR with bypass. Points inside the

region EFGHE cannot be attained by operating a CSTR with bypass. Either we have to operate a PFR with bypass, or we have to mix the outputs of a PFR and a CSTR operating in parallel. The latter will be explained shortly.

Bypassing the feed is not the only way to understand this concept. Let us take points I and J, as shown in Fig. 1.9. Both of these points can be attained by operating a CSTR at certain space times. Now, if we mix the concentrations corresponding to these points such that the respective fractions are  $s$  and  $1 - s$ , we attain a point on the line segment IJ. The physical implication is that, to attain this point, we have to operate two CSTRs in parallel and mix their outputs in a certain proportion.

The exact location of this point is determined by finding the mixed cup concentration. As we vary the value of  $s$  from 0 to 1, we attain all the points lying on the line segment JI. Now, if we alter the positions of points I and J to other points on the blue curve, we can attain all points on all such line segments. All such line segments span the entire area under the curve and thus, we can comment that the whole area under the blue curve can be attained and the way to do this is operating two CSTRs in parallel and mixing their outputs.

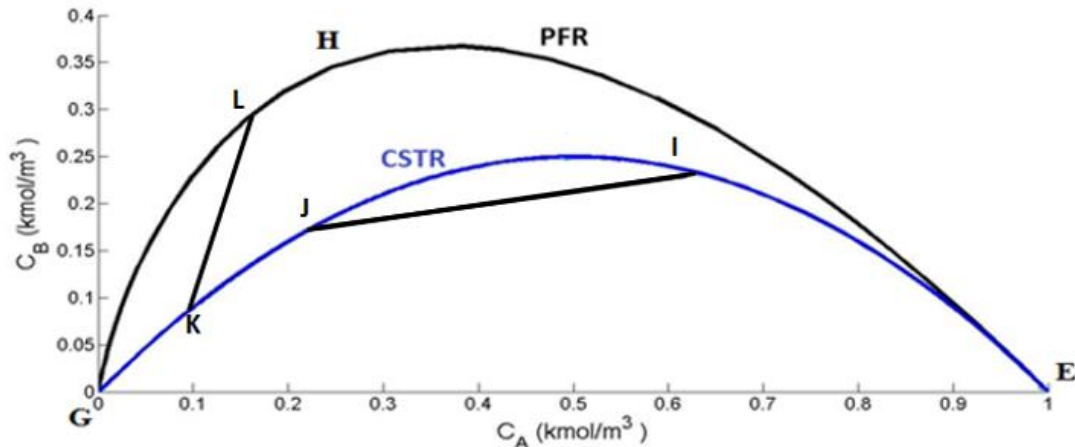


Fig. 1.9. PFR and CSTR lines for  $A \rightarrow B \rightarrow C$  in  $C_A$ - $C_B$  concentration space

Let us revisit points inside the region between the CSTR and PFR reaction lines. We take two points K and L such that they lie on the CSTR and PFR reactor lines respectively. Now, suppose we mix the concentrations corresponding to these points such that the fraction corresponding to points K and L is  $s$  and  $1 - s$  respectively, then the mixed cup concentration will be a point lying on the line segment KL. By changing the value of this fraction  $s$ , we can attain all points on the line segment KL. Similarly, by changing the location of points K and L, we can attain all the points

inside the region EIJKGHE. Thus, operating a PFR and a CSTR in parallel such that their outputs are mixed can enable us to attain all the points inside the region EIJKGHE.

The arguments discussed above also result in another conclusion that if two points are attainable, then all points on the line joining these two points are also attainable, which is our next property:

**The Attainable Region is convex, i.e. for a given feed and rate constants, if two points are attainable, then all the points on the line joining these two points are also attainable.** (Glasser et al., 1987; Glasser and Hildebrandt, 1997; Glasser et al., 1994; Godorr et al., 1994; Hildebrandt and Glasser, 1990; Hildebrandt et al., 1990)

However, we must note that, these reactor lines, may not constitute the complete AR as AR allows using any type and number of reactors in any arrangement, and for now, we have considered only one reactor.

We take another example. Consider the elementary reaction scheme where a species *A* forms *B* obeying second order kinetics. *B* further forms *C* obeying first order kinetics.



The rate constants for the reactions,  $k_1$  and  $k_2$  are taken to be  $1 \text{ m}^3/\text{kmol/s}$  and  $1 \text{ s}^{-1}$ , and the feed is pure *A* with its concentration as  $1 \text{ kmol/m}^3$ .

For the reaction scheme discussed above, the expressions for the change in concentration with residence time for a plug flow reactor (PFR) are as follows:

$$\frac{dC_A}{d\tau} = -k_1 C_A^2 \quad (1.8)$$

$$\frac{dC_B}{d\tau} = k_1 C_A^2 - k_2 C_B \quad (1.9)$$

$$\frac{dC_C}{d\tau} = k_2 C_B \quad (1.10)$$

Thus, the expressions above show us the rates at which the components are getting consumed/created where  $C_i$  represent the concentration of species *i*.

Fig. 1.10. shows in black the reaction line obtained by solving the PFR equations. So, all the points lying on the black curve can be attained by operating a PFR for a certain residence time. We have already looked at how the points under the reaction line can be obtained. Now, we look at point K. Clearly, there is no line segment originating from the feed point and joining K such that if it is

extrapolated away from K, it will intersect the curve. Thus, bypassing the feed is not an option here. However, we see from the figure that there are two points  $K'$  and  $K''$  such that the line segment joining these two points contains the point K. Now, we know that points  $K'$  and  $K''$  can be attained by operating PFR for certain residence times. So if we operate two PFRs in parallel such that the concentration of outputs of these reactors correspond to points  $K'$  and  $K''$ , and their outputs are mixed in a certain proportion, we get the concentration corresponding to point K. In other words, we operate two PFRs in parallel such that the outputs at the exits of these reactors have concentrations corresponding to points  $K'$  and  $K''$ .

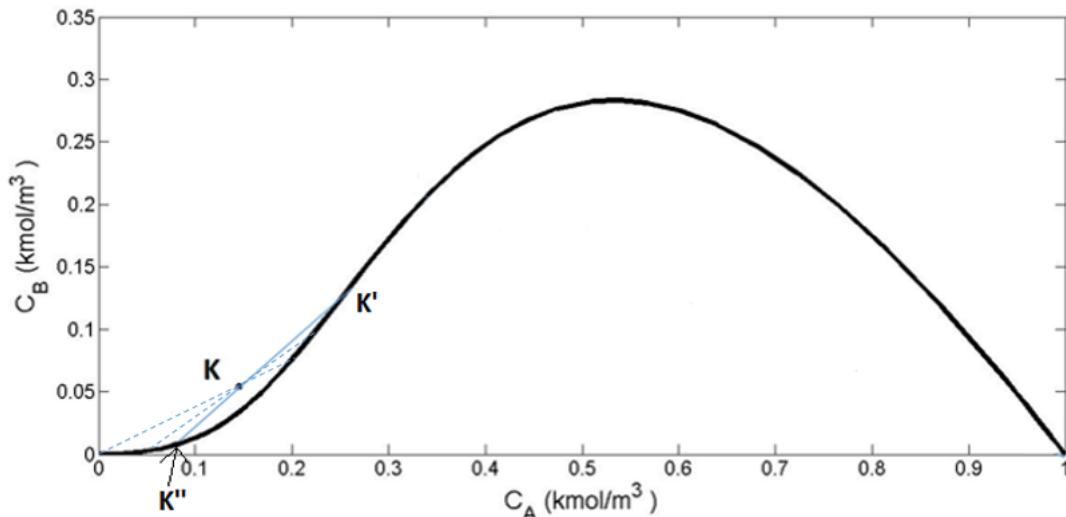


Fig. 1.10. The concept of mixing process in the AR

As can be seen, points like K lie in the concave region of the curve obtained by solving the reactor equations. Proceeding similarly, we see that there are multiple possibilities for  $K'$  and  $K''$ , as shown by the dashed lines. Similarly, if we consider all such points that lie in the concave region and construct line segments that pass through these points, we can get an extended region which is attainable (by operating two reactors in parallel). This extended region is shown in Fig. 1.11. The blue curve shows us the curve obtained by solving the reactor equations. The black line shows the boundary up to which the points can be attained using mixing. This area, which includes the area under the reaction curve and also the extended area which can be availed by mixing, comprises what is known as the convex hull.

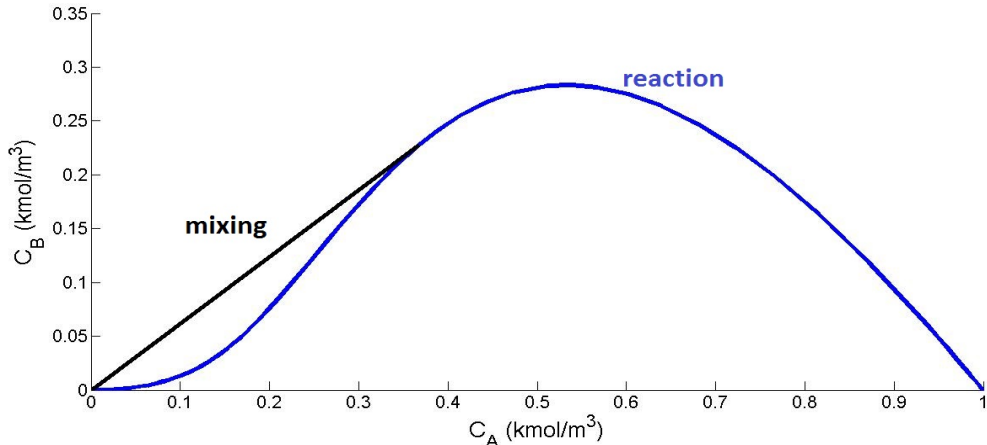
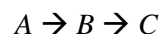


Fig. 1.11. Attainable Region showing the basic processes of reaction and mixing

Thus, for no restrictions on the reactor network parameters, the AR is convex. The lapse in convexity at certain regions that may arise is taken care of by the mixing process. We will see later in Chapter 3, that under restrictions of feed availability and the volume of reactor(s), this proposition of convexity is challenged.

Studies have shown that once the Attainable Region is obtained, the reactor network can be determined and optimized. In fact, designing reactor networks is one of the main practical reasons of developing AR. The basic reactor systems are PFR and CSTR. Only CSTRs, PFRs, and mixing lines are sufficient to construct an AR. The PFR trajectory is such that the reaction vector is defined to be tangent to the trajectory at every point on the AR. Similarly, The CSTR vector is defined as the vector addition of the feed and negative of the concentration vector at the point of interest. (Feinberg, 1999; Hildebrandt and Glasser, 1990; Omtveit et al., 1994; Rooney et al., 2000) Some studies also demonstrate the incorporation of Differential Stream Reactors (DSRs) as a reactor system, which act as crucial precursors to PFRs. DSR is an ideal PFR such that a feed is distributed along its length. (Feinberg, 2000)

Having discussed some of the key basic elements of the AR theory, we are now in a position to appreciate the need to find an optimal reactor network and the usefulness of AR in doing that. We revisit the series reaction



The CSTR and PFR lines are shown in Fig. 1.12. First, we can easily comment that a point which lies outside the CSTR curve can never be attained using a CSTR. Similarly, a point lying outside

of the PFR curve can never attained using a PFR. Next, all points on the CSTR and PFR curves can be attained by operating a CSTR or PFR respectively, at certain residence time.

Now, let us consider a point P lying inside the PFR but outside the CSTR boundary. As we saw earlier, this point can be attained by bypassing the feed such that the concentration at the PFR exit corresponds to point P' (red solid line). But, this is the not the only possible solution. We can attain the points P'' and P''' by operating two separate PFRs at their respective required residence times in parallel and mix their outputs in a certain proportion such that we get point P. Also, the points P'' and P''' can lie anywhere on the PFR curve such that P lies on the line segment joining them and thus, there are multiple possibilities for the position of the pair of P'' and P''', some of which are shown by dashed red lines in the figure. Another possibility is operating a CSTR and PFR in parallel, the corresponding representation of which is shown by the line segment KL. So, we clearly see that for attaining point P, there are multiple reactor networks that can be employed.

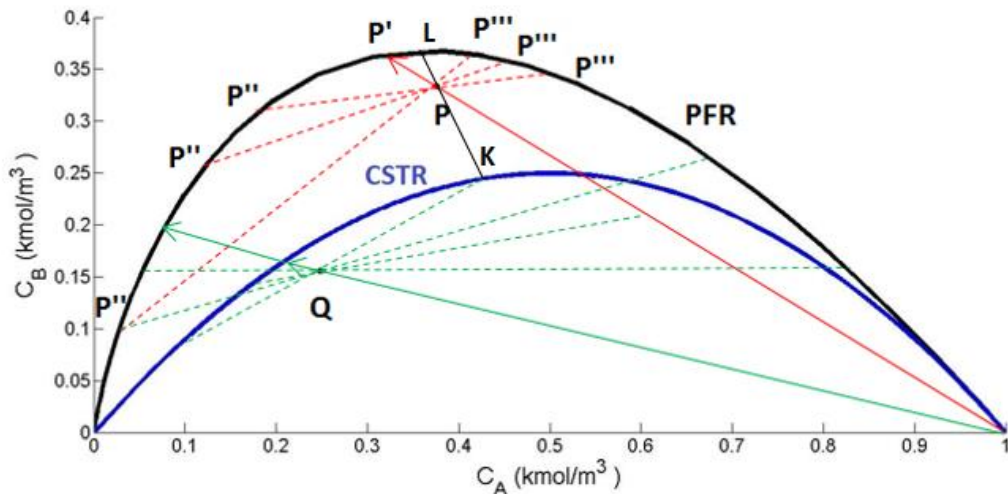


Fig. 1.12. Multiple reactor network choices to attain points P and Q

Further, if we consider point Q which lies under both the CSTR and PFR curves, we can see from the figure that we have the possibility of bypassing feed to a CSTR or bypassing feed to a PFR, as shown by solid green lines. Also, there are possibilities of parallel operation of two CSTRs and parallel operation of two PFRs, as shown by dashed green lines.

Thus, knowing the AR enables us to see whether the concentration corresponding to the point can be attained or not. As per the price functions of the various species involved in a reaction, any point

inside or on the AR can be the required point. The AR now presents us with multiple choices of reactor networks so as to attain this point. Since there are multiple choices, there comes a need to come up with an optimal solution that would basically reduce our costs.

In this study, we are mainly concerned with the Attainable Region for isothermal systems, i.e. all the reactors in the network operate isothermally and at the same temperature. Also, the feed is assumed to be available at this temperature. Also, it is assumed that the generation and absorption of heat is handled by the heat exchange network such that the reactors are maintained at the designated temperature. Although our work is primarily concerned with isothermal systems, the AR concept can also be applied to non-isothermal systems. The industrial significance of exothermic reversible reactions is huge. But for such systems, the optimum reactor requires high initial temperature and low exit temperatures to enable high conversion rates. The AR technique comes in handy as it provides optimum ways to achieve efficient temperature fall. For such systems, the Attainable Region has been used to find the optimal reactor networks for elementary as well as complex kinetics. As in isothermal systems, the boundary of the AR tells us the combination of reactors and the process parameters that are needed to attain those outputs. It has proved to be a highly accurate technique in predicting the process design. Studies also show the applicability of the AR concept to reversible exothermic systems where allowance of external cooling and heating with constant temperature utilities is made. Also, including minimization of utilities as an optimization parameter, the AR technique can be used to arrive at designs which operate at lower cost, and at the same time, deliver high conversions. (Hopley et al., 1996; Nicol et al., 2001; Nicol et al., 1997) Also, by assessing the thermodynamic properties of the species involved, a wide range of reactions that could take place in a complex system, such as water gas shift reaction, can be determined. (Okonye et al., 2012)

The application of AR approach has by no means been limited to chemical reactor design. Various fields have incorporated the principles of AR to good effect. To appreciate the importance of the AR approach, we take a look at a few of its vast applications.

The AR concept has found its relevance in the crystallization and purification sector. AR laws are used to find out the range of product properties, which can be changed by manipulating the variables and/or changing the device. Also, for a specific crystallization device, kinetics and initial concentration, the AR concept has been used to find what particle sizes can be attained. (Vetter et al., 2014)

AR theory has also been used in reactive distillation. It is used to find the attainable selectivity for different conversions for series and parallel combination of reactions. The systems considered were non-azeotropic ideal systems. The analysis was extended to single binary azeotrope systems, and multi-stage reactive rectification with total reflux and reactive stripping with total reboil models. (Agarwal et al., 2008a; Agarwal et al., 2008b; Amte et al., 2012; Amte et al., 2011)

AR concept has also been used in studying the grinding ability of platinum ore. The focus was to reduce the grinding period and energy to achieve certain product characteristics. Also, given a desired size range, efforts were made to maximize the product within that range. Thus, it was postulated that the AR technique can be used to improve mill performance. Objectives included maximization of breakage, mass fraction of the product within a desired size range, and energy minimization. (Danha et al., 2015) The applications of the AR analysis have been extended to communiton. (Khumalo et al., 2006)

Work has also been done to use the AR technique in continuous ball milling. The work has been centered on how to modify the conditions to achieve the desired product characteristics, such as size. Parameters investigated are slurry concentration, feed flow rate, energy required, and ball size distribution. (Mulenga and Chimwani, 2013)

The AR analysis for chemical reactor networks has been used for production of bioethanol. Minimization of residence time was targeted. (Scott et al., 2013)

Using AR as a benchmark for finding attainable product concentrations has been exploited in water gas reaction. The process has been studied using the conventional method, along with iso-state algorithm and linear programming. (Kauchali et al., 2004)

In binary distillation, the AR theory has been used to find the effect of including costs for controlling the reflux ratio. Also, the reflux ratio has been changed along the distillation column length to examine the results. (Kauchali et al., 2000)

The AR concept has been used to prove that polymers of higher molecular weights can be produced than are produced in the industry. (Smith and Malone, 1997)

## 1.2. Motivation behind this study

Reactor or a network of reactors is a very important part of a chemical process flowsheet. It is where the low priced reactants get converted to high valued products and thus contributes the most in value creation. In any chemical reaction scheme, the value that is created depends on the type of reactors, their arrangement, and other parameters like residence time of each reactor and streams that are bypassed or recycled. Thus, prediction of the reactor network that gives us the maximum value is very vital in the operation of the plant. Wrong prediction of the type and/or arrangement of reactor(s) and even incorrect estimation of parameters can lead to huge losses, especially when the value is sensitive to the concentration of a particular single species. This has prompted researchers to work towards finding techniques towards achieving this reactor network and the design that will lead to maximum profit. Several of these include mathematical formulation of Mixed Integer Non-Linear Programming problems. On account of problems of convergence and high computational efforts required, another stream of work has been targeted towards achieving the optimal reactor network through use of the Attainable Region approach. The main benefits of the Attainable Region approach are that it is computationally efficient and also it is easy to visualize.

Having understood the importance of optimal reactor network and AR as an efficient method to achieve that, we aim to build an AR generator, wherein we just have to give the reaction scheme, the kinetics (order and rate constants of each reaction) and the feed concentration as the inputs, and we get the fully constructed Attainable Region such that the concentrations of species corresponding to points outside this closed convex shape cannot be achieved no matter which type of reactor(s), which arrangement of reactor(s) or what set of parameters we use. We follow this with an algorithm to find possible reactor networks, wherein we just have to enter the coordinates of the point corresponding to the concentration of species we want to obtain and we get the reactor network and its design specifying the type of reactors (CSTR or PFR), the arrangement (series or parallel or coupled), and the parameters (residence time, streams bypassed, streams mixed, mixing fraction) that would be required to attain the required point.

Knowledge of the values (prices) associated with various products and reactants allows us to use the AR obtained from the AR generator to find such a concentration that would maximize our earnings. The reactor network required to attain this concentration can then be found out. Since it is a geometrical approach, the AR method can be easily visualized. Even without numerical

solutions, one can easily understand how the concentrations get changed with respect to the processes of reaction and mixing. Any constraints that a user may have can be included fairly easily and solved for using this approach. Also, these can be pictured geometrically at the same time.

### 1.3. Outline of the study

This report is structured as follows: In Chapter 2, we present the Literature Survey explaining the various methods aimed at construction of the Attainable Region, namely the rate vector method, linear programming method and the Infinite Dimensional State-space method. In Chapter 3, we elaborate the rate vector method and explain how the complete AR can be obtained. We present the cases for Van de Vusse, Trambouze and Denbigh reaction schemes. We compare our results with the results obtained in previous studies to arrive at the accuracy and generality of the AR generator. We also present the methodology to construct the AR under constraints of feed availability and reactor volume. In Chapter 4, we present a way to obtain possible reactor networks for a required concentration, given a reaction scheme and its kinetics (order and rate constants of reactions) and feed, using the AR. This is followed by framing cost reduction problems so as to find the optimal reactor network. This is followed by optimization problems, where we look at the optimization of a user-defined objective function for a given reaction scheme and then find the optimal reactor network to achieve the concentration that gives this optimized value. Lastly, we conclude our study in Chapter 5.

## CHAPTER 2

### LITERATURE SURVEY

Having looked at the concept of Attainable Region and its vast applicability, we look at few of the methods in the literature aimed at the construction of AR. As will be seen later, correct construction of AR is very vital as the purpose of AR is to provide all concentrations that can be attained. Incorrect construction of the AR may lead to exclusion of some of the possible product compositions. In such a case, the very definition of the AR would be invalidated. Also, incorrect construction of AR may lead to a non-optimal solution for the user-defined price function and ultimately may lead to reduction of value. In the following sections, we look at three methods used in the construction of AR, namely, the Rate Vector method, the Linear Programming method and the Infinite Dimensional State-space (IDEAS) method. The Rate Vector has just been briefed in this chapter and will be explained in detail in Chapter 3.

#### **2.1. Rate Vector method**

This is the conventional method used for the construction of ARs. This is based on the properties of the rate vectors of CSTRs and PFRs. The algorithm starts by constructing a PFR trajectory from the feed point. The obtained curve is then convexified. What we mean by a convexified curve is that all points on or within the boundary of the curve can be obtained on a line segment connecting two points. In other words, for a convexified curve, if any two points lying inside/on the curve are connected with a line segment, then all the points on the line segment must lie inside/on the curve. If the initial PFR trajectory is not convex, then it is convexified and the physical implication of the new points is that they are obtained by mixing two streams corresponding to the two points between which the line segment is drawn. The obtained region is called as candidate AR. Now, we check whether the PFR rate vectors at all points are directed out of the surface of the convex hull. If yes, then the obtained hull is the final AR. If no, then we construct CSTRs from various feed points in

the concavity on the PFR trajectory and convexify each such trajectory. This may extend the candidate AR. If it does, we look at whether CSTR rate vectors at all points are directed inside the new candidate AR. If yes, then we have the final AR. If no, then we construct PFR trajectories from various feed points on the concavities on the CSTR curve, and convexify them. This may further extend the region. This is repeated until there is no further extension. (Hildebrandt and Glasser, 1990)

The knowledge of how all the points are obtained on the AR while constructing it gives us the necessary information about the reactor network and the corresponding operating strategies to achieve the same. The method is explained further in Section 3.1, where a detailed step-by-step construction is shown.

## 2.2. Linear Programming Method

In this method, a large set of grid points is defined. The constraints for such a programming problem are the overall and component mass balances. Fig. 2.1 shows the flowsheet for a CSTR series model. Feed to CSTR  $i$  can come from any upstream or downstream CSTR. The model also permits for bypass, recycle and mixing. Although the model comprises of only CSTRs, the concept can be extended to PFRs as they can be approximated as multiple CSTRs in series. If there are side streams, then it can be approximated as a DSR. (Kauchali et al., 2002)

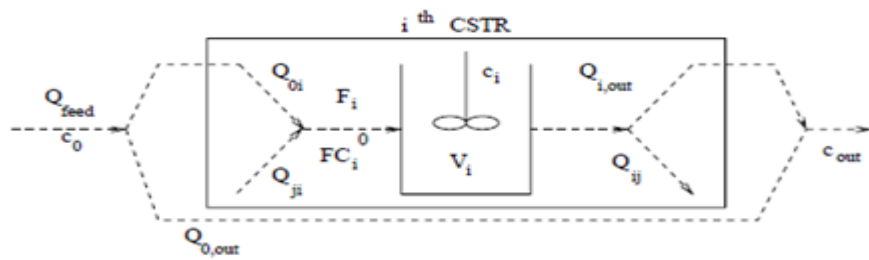


Fig. 2.1. Flowsheet for CSTR ' $i$ ' in linear programming method. (Kauchali et al., 2002)

In Fig. 2.1,  $F_i$  and  $FC_i^0$  refer to the total feed to the  $i^{th}$  CSTR and the component inlet flowrate respectively.  $Q_{0i}$ ,  $Q_{0,out}$ ,  $Q_{ij}$  and  $Q_{i,out}$  refer to the amount of feed entering the CSTR, feed bypassing all CSTRs, flowrate at the exit of CSTR  $i$  entering CSTR  $j$ , flowrate at the exit of CSTR  $i$  sent to

the outlet of the network respectively.  $V_i$  is the volume of CSTR  $i$ .  $c_i$  is the composition at CSTR exit, and  $c_{out}$  is the composition at the network outlet.

The AR is obtained by maximizing the exit concentration subject to the following conditions:

$$F_i c_i - F C_i^0 = V_i R_i \quad (2.1)$$

$$F_i = \sum_j Q_{ji} + Q_{0i} \quad (2.2)$$

$$F_i = \sum_j Q_{ij} + Q_{i,out} \quad (2.3)$$

$$F C_i^0 = \sum_j Q_{ji} c_j + Q_{0i} c_0 \quad (2.4)$$

$$1 = \sum_i Q_{0i} + Q_{0,out} \quad (2.5)$$

$$1 = \sum_i Q_{i,out} + Q_{0,out} \quad (2.6)$$

$$c_{out} = \sum_i Q_{i,out} c_i + Q_{0,out} c_0 \quad (2.7)$$

$$c_{low} \leq c \leq c_{up} \quad (2.8)$$

$$i, j \in I \quad (2.9)$$

$$F_i, F C_i^0, Q_{ij}, Q_{0i}, Q_{i,out}, Q_{0,out}, V_i \geq 0 \quad (2.10)$$

After obtaining the AR, the following Mixed Integer Linear Programming (MILP) problem is executed to determine the structure involving the fewest CSTRs.

$$\min \sum_i y_i \quad (2.11)$$

such that the constraints are given by Eq. 2.1-2.10 along with

$$V_i \leq U_v y_i \quad (2.12)$$

$$F_i \leq U_f y_i \quad (2.13)$$

$$y_i = \{0,1\} \quad (2.14)$$

$$F_i, F C_i^0, Q_{ij}, Q_{0i}, Q_{i,out}, Q_{0,out}, V_i \geq 0 \quad (2.15)$$

The objective function is to minimize the sum of binary variables  $y_i$ .  $y_i$  is equivalent to 0 for an empty CSTR, and is 1 otherwise.  $U_v$  and  $U_f$  are upper and lower bounds on the volume of  $i^{th}$  CSTR.

### 2.3. Infinite DimEnsionAl State-space (IDEAS) method

The method model is decomposed into two blocks. The first is the reactor operator (often abbreviated as ROP). It considers all possible inlet streams and processing conditions such as residence time and temperature, and transforms them into all possible outlet streams. The second is the distribution network (DN), which accounts for mixing, bypass and recycle. This provision extends the concentration space at reactor operator exit. The overall result is the generation of a convex and feasible concentration space region. (Burri et al., 2002)

Fig. 2.2 represents the flowsheet for the IDEAS model. The terms in the parenthesis denote the flow and concentration respectively, i.e., for each parenthesis  $(i, j)$ ,  $i$  represents the flow rate of the stream and  $j$  represents the concentrations of the components.  $z$  denotes the distribution network such that  $z_{mn}$  represents the flow joining  $m$  from  $n$ .

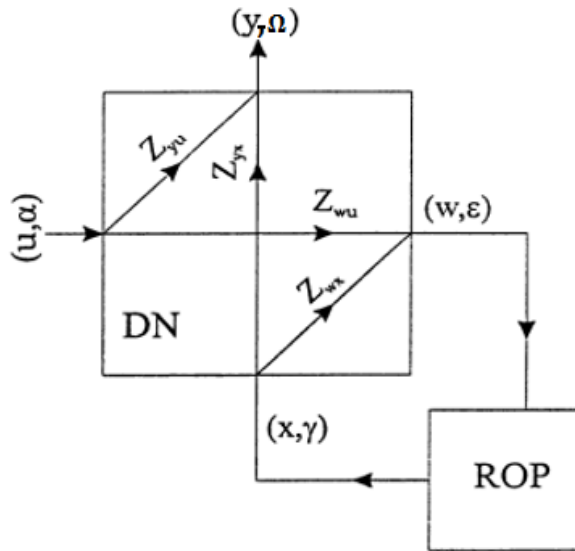


Fig. 2.2. Flowsheet for the Infinite DimEnsionAl State-space model (Burri et al., 2002)

We now look at the problem constraints.  $K$  denotes the number of network outlet streams and  $P$  denotes the number of network inlet streams.

$$u(k) = \sum_{i=1}^K z_{yu}(i, k) + \sum_{i=1}^K z_{wu}(i, k) \quad \forall k = 1, 2, \dots, P \quad (2.16)$$

$$y(i) = \sum_{k=1}^P z_{yu}(i, k) + \sum_{k=1}^P z_{yx}(i, k) \quad \forall i = 1, 2, \dots, K \quad (2.17)$$

$$w(i) = \sum_{k=1}^P z_{wu}(i, k) + \sum_{k=1}^P z_{wx}(i, k) \quad \forall i = 1, 2, \dots, \infty \quad (2.18)$$

$$x(k) = \sum_{i=1}^K z_{yx}(i, k) + \sum_{i=1}^K z_{wx}(i, k) \quad \forall k = 1, 2, \dots, \infty \quad (2.19)$$

$$\epsilon(i)w(i) = \sum_{k=1}^P \alpha(k)z_{wu}(i, k) + \sum_{k=1}^P \gamma(k)z_{wx}(i, k) \quad \forall i = 1, 2, \dots, \infty \quad (2.20)$$

$$y^l(i) \leq y(i) \leq y^u(i) \quad \forall i = 1, 2, \dots, K \quad (2.21)$$

$$\Omega^l(i)y(i) \leq \sum_{k=1}^P \alpha(k)z_{yu}(i, k) + \sum_{k=1}^P \gamma(k)z_{yx}(i, k) \leq \Omega^u(i)y(i) \quad \forall k = 1, 2, \dots, K \quad (2.22)$$

We now have the objective function as mentioned below subject to the constraints listed in Eq. 2.16 - 2.22

$$\begin{aligned} & \sum_{i=1}^{\infty} [\varphi(i)u(i) + \psi(i)y(i) + \omega(i)w(i) + \chi(i)x(i) \\ & + \sum_{l=u,x} \sum_{m=y,w} \sum_{k=1}^{\infty} \zeta_{ml}(i, k)z_{ml}(i, k)] \end{aligned} \quad (2.23)$$

where  $\varphi$ ,  $\psi$ ,  $\omega$ ,  $\chi$  and  $\zeta$  are the respective cost coefficients. By appropriate selection of the coefficients, various objectives such as maximization of concentration, yield, selectivity etc. can be formulated.

$$cost = \inf \text{Eq. 2.23} \quad (2.24)$$

subject to Eq. 2.16 – 2.22.

Thus, we looked at the methods discussed in the literature used in the construction of AR. While making a decision as to which method we need to choose, factors that come into picture are computational efforts required in the method, its ease of visualization and how it would aid in finding the reactor networks. Keeping these in mind, the Rate Vector method is used.

## CHAPTER 3

# CONSTRUCTION OF ATTAINABLE REGION

Having looked at the methods to arrive at the Attainable Region, we choose the conventional method (i.e. the Rate Vector method) in our study. The reason for this choice is that the linear programming and IDEAS methods take a reactor or a reactor network and then solve the optimization function and thus find the AR only with respect to that reactor network. However, AR is the set of all points corresponding to concentrations that can be attained by a combination of any type and arrangement of reactors and their various parameters (residence time, bypass). Thus, many simulations would have to be performed to see which reactor network gives us the complete AR. This would increase the computational efforts required. The rate vector method overcomes these problems as it takes a systematic approach towards finding the complete AR as will be discussed in Section 3.1, taking fairly lesser computational efforts. Also, being a geometric method, effects of choice of reactors and the process of mixing can be easily visualized and understood. As we shall see in Chapter 4, it is fairly convenient to derive the optimal reactor network policy using the Attainable Region obtained from this method.

Before moving into the detailed construction of AR using the Rate Vector method, we first highlight the major steps involved. We first begin by drawing a PFR trajectory from the feed point. By a PFR trajectory, we mean the trajectory obtained by solving the PFR equations for the given reaction scheme and kinetics. We look for concavities in this trajectory and convexify them. The product compositions falling in this additional region retrieved in the convexification process are attainable by feed bypass or by employing two reactors in parallel, as was discussed earlier. Further, from these points of concavity, we look whether CSTR trajectories and their respective convexified regions would extend the region already covered by the convexified PFR region. This is repeated until there are no concavities and thus no further possibility of region extension. This final region is our AR. So, we see that the presence of concavities and extension of region using a bypass and/or more than one reactors in series/parallel are the two important aspects that come into picture. Usually, for simple reactions, the PFR trajectory itself is convex and thus the complete AR. If it is not convex, the convexified PFR region is found to be the AR for such simple reaction schemes. But, in practical situations, this may not be the case. Thus, to appreciate the Rate Vector method,

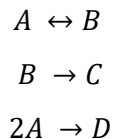
we need a reaction scheme and its kinetics that presents concavities in the initial stages such that the need of convexification can be seen. Also, it must allow the later stages to extend the region so that there is a need of having more than one reactor to construct the complete AR. Reactions and kinetics given by Van de Vusse (VdV) is one such reaction scheme having reversible as well as irreversible reactions and also series and parallel reactions. Also, it is one of the most studied reaction schemes in the literature. (Glasser and Hildebrandt, 1997; Metzger and Glasser, 2007; Chitra and Govind, 1981) In Section 3.1, we show a detailed step by step construction of AR for the Van de Vusse reaction scheme. We also show how the method has been incorporated in a tool called the AR Generator, which as the name suggests, finds the complete AR for any user given reaction scheme and kinetics. By making use of this method, we have made the tool generic in nature. That is to say, it works for a reaction scheme that can have any number of reactions, any type of reactions (reversible or irreversible; series or parallel), any order of the reactions, and can have any value of the rate constants. Also, the accuracy of this tool is then verified by comparing it to previous literature works. This is followed by two more case studies, namely the Trambouze and Denbigh reaction schemes.

We have to note that the case studies are chosen such that they aid in the illustration of our objectives. This by no means is a limitation of our methodology and altering the reaction schemes and/or kinetics does not change the methodology presented. The tool works for any reaction scheme and kinetics other than the ones discussed in this study. Thus, the tool works for any reaction scheme and kinetics thrown by the user and gives correct results. The simulations have been performed using *MATLAB*.

### 3.1. Constructing Attainable Region for Van de Vusse reaction scheme

We now present a step-by-step analysis of the generation of the AR for the Van de Vusse reaction scheme.

Van de Vusse reaction scheme:



The reactions are elementary and the ' $\leftrightarrow$ ' sign implies that the reaction is reversible.

$k_1$  = rate constant for the reaction of  $A$  going to  $B$  =  $1\text{ s}^{-1}$

$k_2$  = rate constant for the reaction from  $B$  to  $A$  =  $5 \text{ s}^{-1}$

$k_3$  = rate constant for the reaction  $B \rightarrow C = 10 \text{ s}^{-1}$

$k_4$  = rate constant for the reaction  $2A \rightarrow D = 100 \text{ m}^3 \text{ kmol}^{-1} \text{ s}^{-1}$

The feed is pure  $A$  and its concentration is  $1 \text{ kmol m}^{-3}$ .

While running the simulations, the residence time was varied from 0 to a very large value (in our simulations: 20000 s) for both the PFR and the CSTR. The step size taken to go from 0 to this value is not equal. The steps are taken such that the trajectories and regions obtained are smooth. At the same time, we keep in mind that the computational efforts required are not too high. So, these decisions were made keeping in mind the computational efforts required such that the accuracy of the results was not compromised.

**Stage 1:** We construct the trajectory for a PFR from the feed point. This is then convexified in the sense that mixing between the various points is accounted for, such that the region gets extended.

The PFR equations for the Van de Vusse reaction scheme are:

$$\frac{dC_A}{d\tau} = -k_1 C_A + k_2 C_B - k_4 C_A^2 \quad (3.1)$$

$$\frac{dC_B}{d\tau} = k_1 C_A - k_2 C_B - k_3 C_B \quad (3.2)$$

$$\frac{dC_C}{d\tau} = k_3 C_B \quad (3.3)$$

$$\frac{dC_D}{d\tau} = k_4 C_A^2 \quad (3.4)$$

Fig. 3.1 shows the candidate AR at this stage. By a candidate AR, we mean a region that is obtained at any intermediate stage. A candidate AR is just a candidate for the final AR and may or may not be the final AR. The 2-D figure is a plot of concentration of species  $B$  on y-axis and species  $A$  on x-axis. The trajectory PSRTJKL represents the normal trajectory obtained by the PFR, and the region PQRTJMLP represents its convexified region. We use the terminology normal trajectory in this work to mean the trajectory that is obtained by solving the equations of the reactor only and that no convexification is taken into account. We shall stick to this terminology in the future as well.

As can be seen, there are two regions where the normal trajectory has been convexified. The one towards the bottom left side in Fig. 3.1 has been redrawn on a magnified scale to appreciate the convexification in that region.

In our simulations, the ordinary differential equations are solved using the *ode15s* solver in *MATLAB*. The input arguments required are the equations, the time span for which we need to integrate and the initial conditions. We take the time (residence time) span from 0 to a very large value (in our simulations: 20000). The initial condition is taken as the available feed, which is [1 0 0]. The output arguments are the time (Residence time in our case since our equations are of the form  $\text{d}\text{el}(\text{concentration})/\text{d}\text{el}(\text{residence time})$ ) and the concentrations at the respective residence times, which basically constitute the normal trajectory data points. We store these data points in a matrix  $X_1$  and the residence time in a matrix  $T_1$ . For convexified region matrix, we look at the pair of points in  $X_1$  between which the normal trajectory was not convex. We eliminate the points between each such pair of points and obtain another matrix which stores the data points for the convexified region. We call this matrix  $Y_1$ . The subscript 1 denotes the stage number.

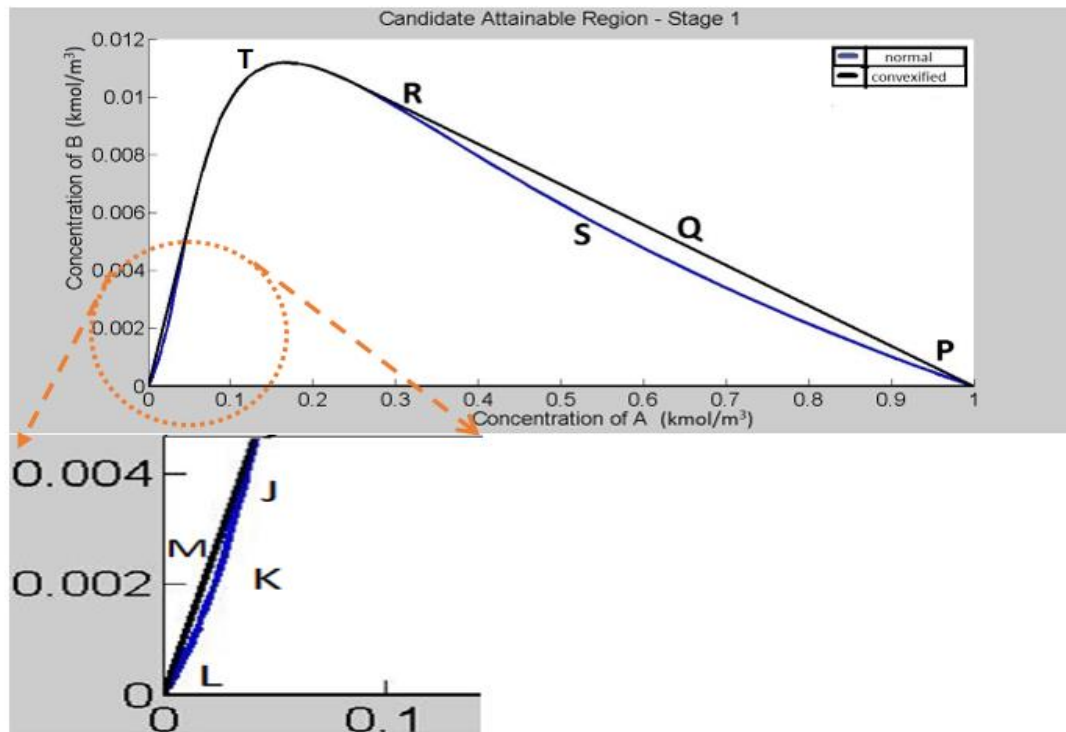


Fig. 3.1. Candidate AR obtained after Stage 1 – Van de Vusse reaction shceme

**Stage 2:** Having constructed the normal and convexified region, we observe from Fig. 3.1 that there are certain regions where the normal trajectories are concave and that they can be convexified. For example, the curves PSR and JKL have been convexified to PQR and JML respectively and thus have extended the region. These become our regions of interest in this stage. Our objective is to find whether taking points on the boundary of the normal trajectory in these regions as the feed points of a CSTR and drawing CSTR trajectories from such points further expands the candidate AR obtained in Stage 1. For all such trajectories, we also convexify them and check whether they extend their respective normal trajectories. Finally, we convexify the total region obtained. However, if there is no such point that extends the candidate AR obtained from Stage 1, we stop and have our final AR.

An efficient way to check which points are capable of extending the candidate AR is by examining the rate vectors. The rate vector at a point is a function of concentration of species at that point and tells us how fast the components get consumed or created. For a PFR, the steady state model for PFR is given by

$$\frac{d\bar{c}}{d\tau} = \bar{r}(\bar{c}) \quad (3.5)$$

where  $\bar{c}$  is the vector for the concentration of species at a certain residence time. Since the Van de Vusse reaction scheme has four components,  $A$ ,  $B$ ,  $C$  and  $D$ , the vector  $\bar{c}$  is given by

$$\bar{c} = [C_A \ C_B \ C_C \ C_D] \quad (3.6)$$

The concentration of all species is dependent on the residence time. Similarly, the rate vector  $\bar{r}$  is given by

$$\bar{r} = [r_A \ r_B \ r_C \ r_D] \quad (3.7)$$

Thus, for a PFR, we have

$$r_A = \frac{dC_A}{d\tau} \quad (3.8)$$

$$r_B = \frac{dC_B}{d\tau} \quad (3.9)$$

$$r_C = \frac{dC_C}{d\tau} \quad (3.10)$$

$$r_D = \frac{dC_D}{d\tau} \quad (3.11)$$

Thus,

$$\bar{r} = \left[ \frac{dC_A}{d\tau} \frac{dC_B}{d\tau} \frac{dC_C}{d\tau} \frac{dC_D}{d\tau} \right] \quad (3.12)$$

Using this equation and the PFR equations, we get

$$\bar{r} = [-k_1 C_A + k_2 C_B - k_4 C_A^2 \quad k_1 C_A - k_2 C_B - k_3 C_B \quad k_3 C_B \quad k_4 C_A^2] \quad (3.13)$$

The rate vector at a point on the PFR trajectory, in a two dimensional space, is the tangent ray originating from that point. The concavity in certain regions in the normal trajectory arises when such rate vectors in that region are directed towards intersecting the normal trajectory. So, we check whether the tangent at any point, when extended intersects the normal trajectory. Fig. 3.2 shows that the tangents drawn from points on the curve PSR (shown in red) intersect the normal trajectory. Beyond this region the tangents point outwards or lie along the normal trajectory (shown in green) and hence this region is not of interest in stage 2. The concavity towards the bottom left corner is not addressed in this figure.

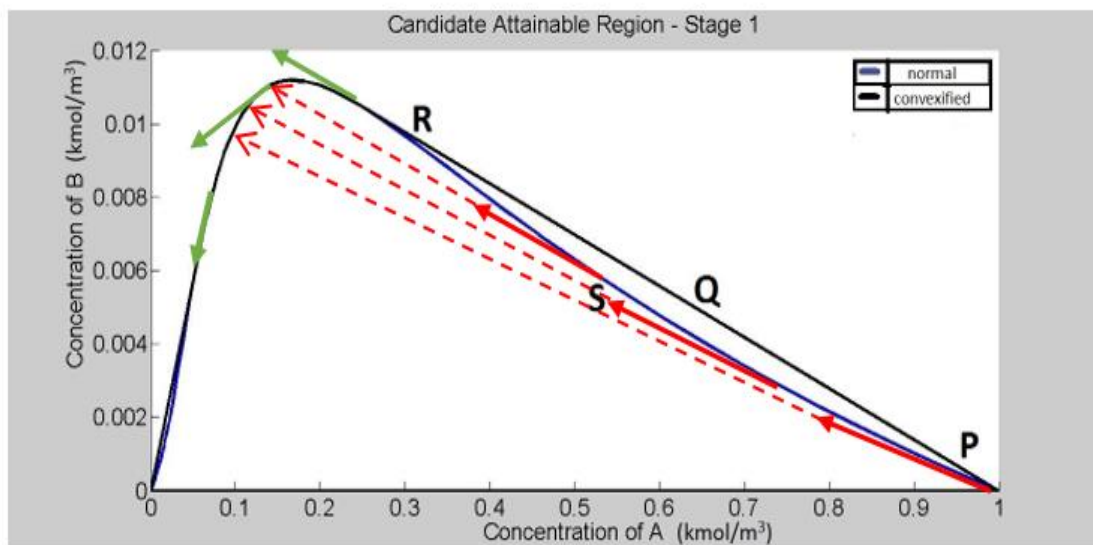


Fig. 3.2. PFR rate vectors at different points on the normal Stage 1 trajectory

We take the points where the tangent points into the normal curve as feed and draw CSTR trajectories and look whether the candidate AR obtained earlier is extended or not.

The CSTR equations for the Van de Vusse reaction scheme are given as:

$$C_A - C_A^0 = \tau(-k_1 C_A + k_2 C_B - k_4 C_A^2) \quad (3.14)$$

$$C_B - C_B^0 = \tau(k_1 C_A - k_2 C_B - k_3 C_B) \quad (3.15)$$

$$C_C - C_C^0 = \tau(k_3 C_B) \quad (3.16)$$

$$C_D - C_D^0 = \tau(k_4 C_A^2) \quad (3.17)$$

The trajectories and the candidate AR obtained at this stage is shown in Fig. 3.3.

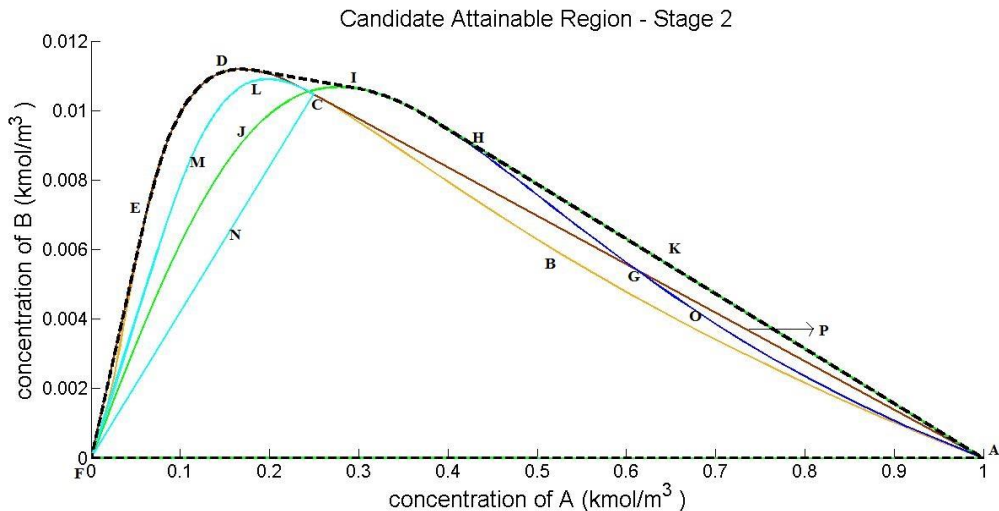


Fig. 3.3. Candidate AR obtained after Stage 2

ABCDEF represents the normal PFR trajectory from the first stage whereas APGCDEFA represents its convex region. For the second stage, we plot some intermediate curves that completely highlight our rationale behind the procedure. AOIGHIJF is the normal CSTR trajectory drawn from the available feed point (also a point where PFR rate vector points towards intersecting the trajectory), and AKHIJFA represents its convexified region. These regions extend the candidate AR obtained after Stage 1. Region CLMFNC represents a CSTR region drawn from a feed point at which the PFR rate vector did not point towards intersecting the normal trajectory and thus it can be seen that it does not extend the region. The region AKHIDEFA represents the region obtained by convexifying all the regions at this stage and is the candidate AR at Stage 2.

In our simulations, to solve the algebraic equations, we use the *fsolve* command in *MATLAB*, where the input arguments are the equations and the initial guess. The output arguments are the solved values. We pre-specify the residence time in an array that goes from 0 to a large step size (in our simulations: 20000 s) in steps so as to not compromise the smoothness (accuracy) of the curve, at

the same time, keeping the computational efforts under consideration, and then use the *fsolve* command to solve for each residence time. Another thing to note is that we have to repeat the calculations for different feed points that came up while convexifying the first stage points. We name the matrices as  $X_{2i}$  and  $Y_{2i}$ , where X and Y denote matrices for storing data points corresponding to normal trajectories and convexified regions respectively. The subscript 2 denotes the Stage 2 points.  $i$  denotes the  $i^{th}$  feed, from which the trajectories were constructed.

**Stage 3:** The steady state model for a CSTR is given by

$$\bar{c} - \bar{c}_0 = \tau \bar{r} \quad (3.19)$$

As discussed earlier,  $\bar{c}$  and  $\bar{r}$  are given as:

$$\bar{c} = [C_A \ C_B \ C_C \ C_D] \quad (3.20)$$

$$\bar{r} = [r_A \ r_B \ r_C \ r_D] \quad (3.21)$$

For a CSTR, we have

$$r_A = \frac{C_A - C_{A0}}{\tau} \quad (3.22)$$

$$r_B = \frac{C_B - C_{B0}}{\tau} \quad (3.23)$$

$$r_C = \frac{C_C - C_{C0}}{\tau} \quad (3.24)$$

$$r_D = \frac{C_D - C_{D0}}{\tau} \quad (3.25)$$

Thus,

$$\bar{r} = \left[ \frac{C_A - C_{A0}}{\tau} \quad \frac{C_B - C_{B0}}{\tau} \quad \frac{C_C - C_{C0}}{\tau} \quad \frac{C_D - C_{D0}}{\tau} \right] \quad (3.26)$$

Using this equation and the CSTR equations, we get

$$\bar{r} = [-k_1 C_A + k_2 C_B - k_4 C_A^2 \quad k_1 C_A - k_2 C_B - k_3 C_B \quad k_3 C_B \quad k_4 C_A^2] \quad (3.27)$$

The rate vector at a point in this case is a ray originating from the feed concentration towards the concentration corresponding to the point of interest. This ray should point inside the normal

trajectory at the point of origin. But, in concave regions, this ray points out of the normal trajectory at the point of origin.

So, we check whether any such ray towards any point on the normal trajectory from the feed point is directed outside of the normal trajectory at its origin. Out of the several trajectories obtained in Stage 2, we select the one with the initial feed point [1 0 0 0] as the feed point to show in the figure. Fig. 3.4. shows that in the concave region, the ray from feed to the points (red) directs outside of the normal trajectory at its origin. The green rays are directed towards the interior of the normal trajectory and thus such points are not of interest.

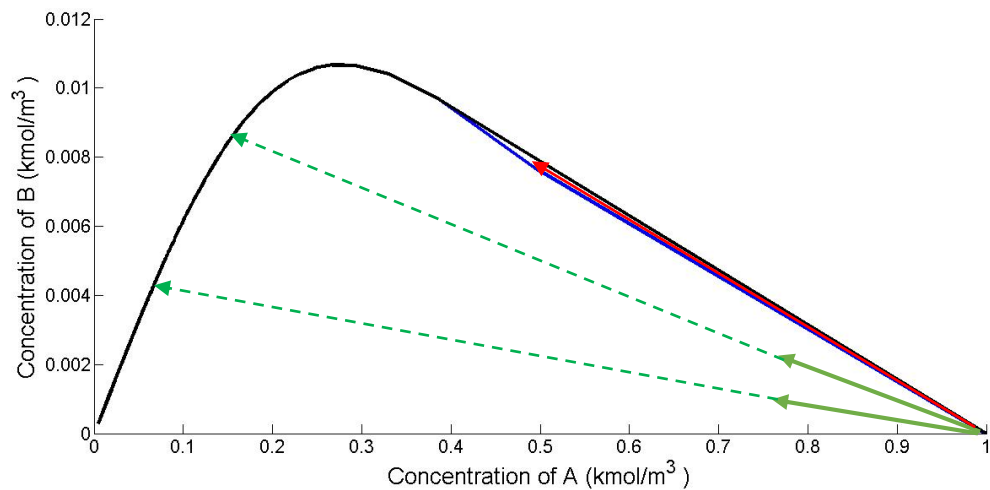


Fig. 3.4. Rate vectors at different points on the CSTR trajectory from the initial feed point

We construct all PFR trajectories with such feed points. All such trajectories obtained are convexified. In Fig. 3.5, we only show the trajectory that extended the candidate AR at Stage 2. It is shown by the magenta colored curve. In our simulations, the data points for the normal and convexified trajectories are stored in  $X_{3i}$  and  $Y_{3i}$  respectively. The subscript 3 denotes the Stage 3 points.  $i$  denotes the  $i^{th}$  feed, from which the trajectories were constructed.

Stage 2 and Stage 3 are repeated until no further extension of the region is possible. One way to ensure that no further extension is possible is to find the area/volume of the convex hull at each stage. In our simulations, the area is found by using the *convhull* command. This command finds the points on the normal trajectory which when connected by straight line segments, give us the convexified region. Also, it finds the area of this convex region.

When the area/volume at Stage  $i$  is equal to that at Stage  $i-1$ , we solve for Stage  $i+1$  and see whether this area/volume is equal to that of Stage  $i-1$ . If it is equal, the stop condition is imposed. Thus, when the area/volume of convex hull of the stages  $i-1$ ,  $i$  and  $i+1$  are equal, we say that  $i-1$  stages are enough to construct the AR.

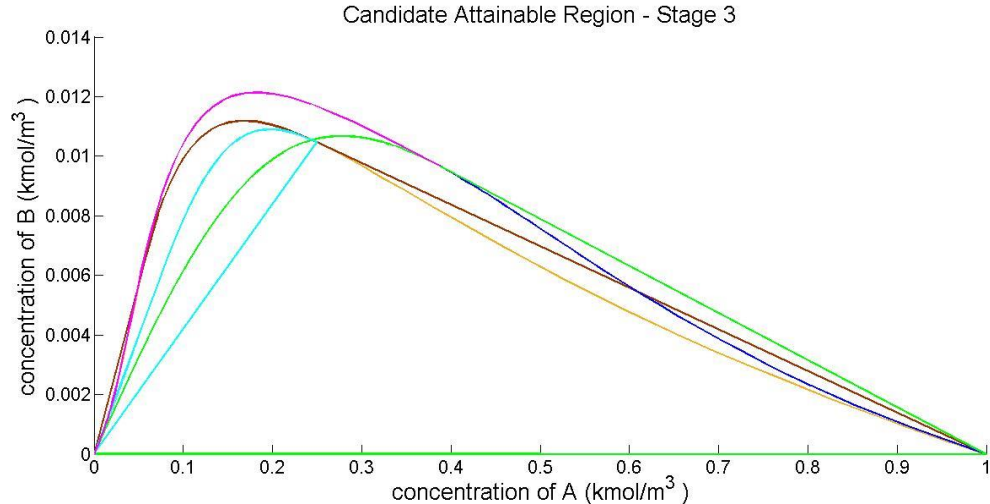


Fig. 3.5. Candidate AR obtained after stage 3

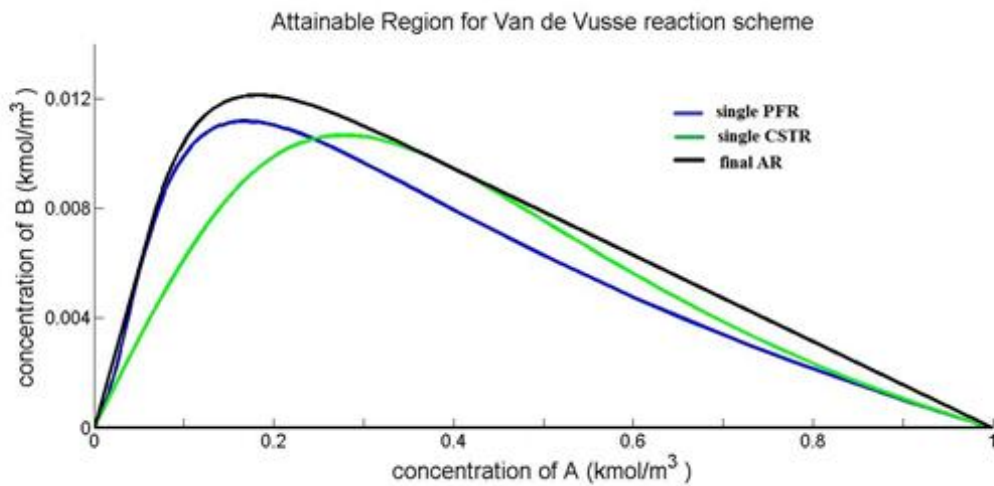
From Table 3.1. we see that the area of the convex hull is same for Stage 4 and Stage 3. Thus, the inclusion of any CSTR in Stage 4 has not extended the region obtained in Stage 3. We then solve for Stage 5 and look whether it extends the region. Since the area obtained after Stage 5 is equal to that obtained after Stage 3 and 4, we impose the stop condition.

Table. 3.1. Areas of the convex hull after various stages

Stage No.	Area	% change in area
1	$6.11 \times 10^{-3}$	
2	$6.59 \times 10^{-3}$	7.7760
3	$6.78 \times 10^{-3}$	2.8998
4	$6.78 \times 10^{-3}$	0
5	$6.78 \times 10^{-3}$	0

The final attainable region, beyond which no further extension is possible, is shown in Fig. 3.6. The final AR is shown in black. The figure also shows the trajectories obtained when a single PFR and a single CSTR is operated at the given feed point ( $C_{AO} = 1$ ,  $C_{BO} = C_{CO} = C_{DO} = 0$ ). They are shown in blue and green respectively. Thus, we can see clearly that the implementation of merely

a single reactor is not enough to obtain the final AR and that an intelligent combination of reactors may be required to obtain it.



*Fig. 3.6. Final Attainable Region for the Van de Vusse reaction scheme (black); the blue and green trajectories represent the normal PFR and CSTR trajectories from the given feed point*

Fig. 3.7. shows the AR obtained in a previous work. (Glasser and Hildebrandt, 1997)

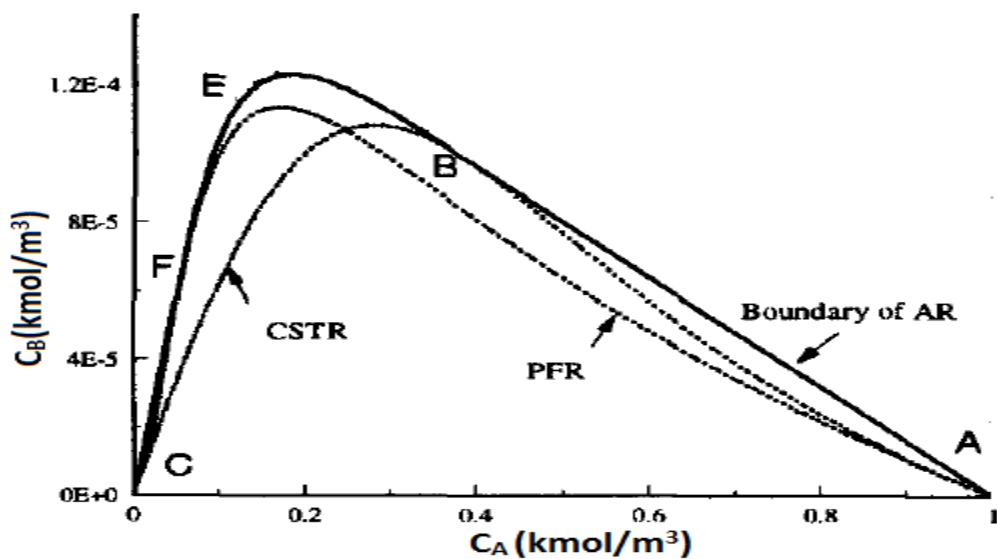


*Fig. 3.7. Attainable Region for the Van de Vusse reaction scheme as obtained in previous work (Glasser and Hildebrandt, 1997)*

We see that the qualitative nature of the AR obtained in our work exactly matches that by Glasser and Hildebrandt. The reason for the difference in the scales in the y-axis (a factor of 100) is that the value of  $k_1$  in their work was taken to be  $0.01 \text{ s}^{-1}$ , instead of  $1 \text{ s}^{-1}$  in our study.

The rationale behind choosing the Van de Vusse reaction scheme along with the specified kinetics, as stated earlier, is that they highlight most of the important aspects in the construction of AR. As was seen in Stages 1 and 2, they depict the concavities that can be obtained in the normal trajectories and the need to make them convex. Also, they facilitate the use of more than one reactor in the construction of the complete AR in such a way that it can be visualized on the two dimensional plots.

Also, as a result of the use of these kinetics, various regions are created, which require the use of different reactor network configurations, as will be seen in Chapter 4.

### 3.2. 2D projections of the Attainable Region

We have thus far investigated the projection of the AR in the  $(C_A, C_B)$  plane. However, as stated earlier, AR can be plotted in any two dimensions that one wishes for. Thus, to obtain different projections of the AR, we undergo the same methodology for the two dimensions one wishes to plot the AR in. Plotting the AR in any two dimensions will not alter the methodology presented in Section 3.1.

So, we now look at the projections in  $(C_A, C_C)$  and  $(C_A, C_D)$  planes. Fig. 3.8 shows the projection of the AR in the  $(C_A, C_C)$  plane. The blue colored trajectories correspond to PFR whereas the green colored trajectories correspond to CSTR. The black curve corresponds to the final AR projection on the  $(C_A, C_C)$  plane.

Looking at Fig. 3.8, we can now see the importance of the region RS in Fig. 3.6. We can see that for the CSTR, the concentration of  $C$  is increasing in the region corresponding to RS in Fig. 3.6. Thus, if we ignore and do not include the slight convexification of the region RS, we could have missed out on a lot of attainable concentrations of species  $C$ .

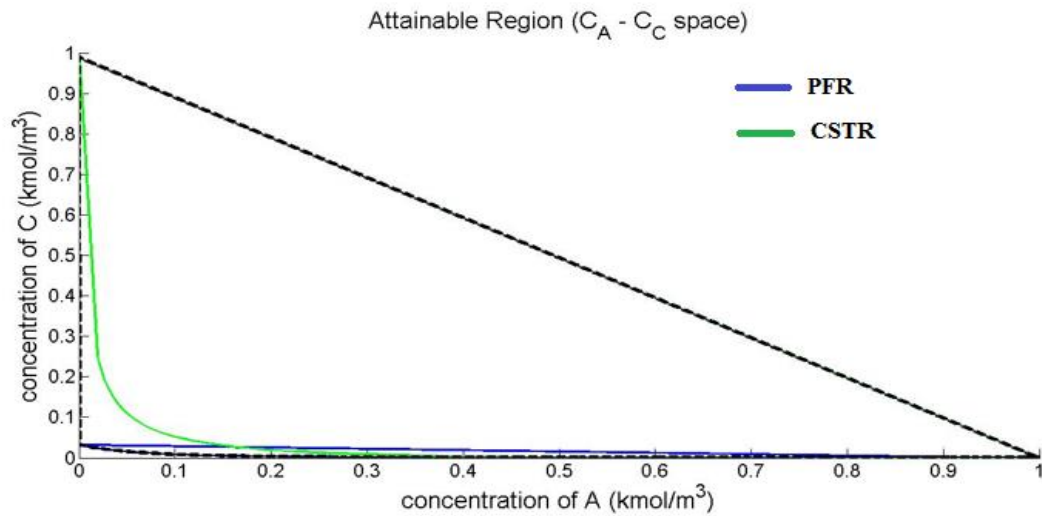


Fig. 3.8. 2D projection of the AR in  $C_A$ - $C_C$  space

Similarly, Fig. 3.9. shows the projection the AR on the  $(C_A, C_D)$  plane. The color scheme is same as the previous one.

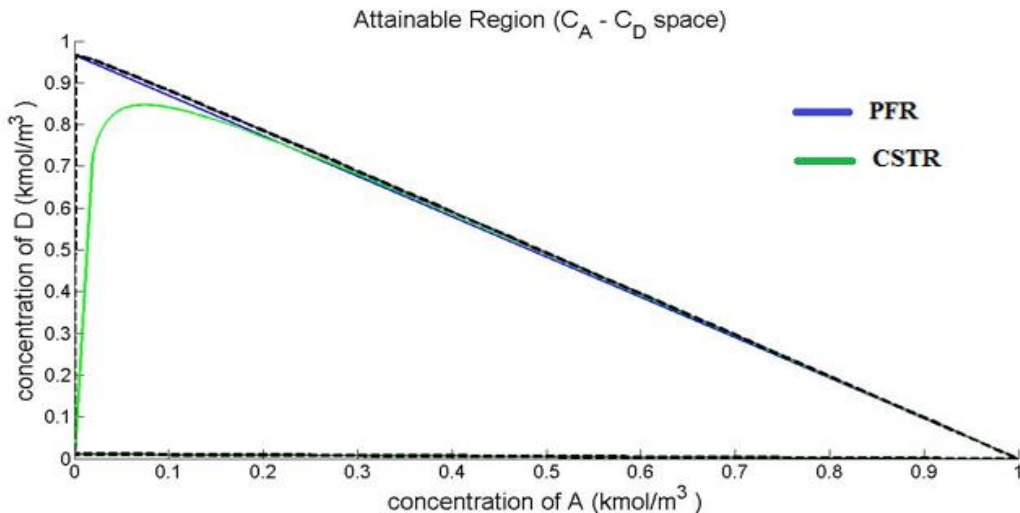


Fig. 3.9. 2D projection of the AR in  $C_A$ - $C_D$  space

Looking at Fig. 3.9. we can see that for the CSTR, the concentration of species  $D$  is decreasing in the region corresponding to RS in Fig. 3.6. Thus, the region RS in Fig. 3.6. may come in handy in a situation where  $D$  is the unwanted/least economical product. Thus, it becomes clear that it is important to look at the projections of AR on each plane.

Another reason for this study is that it highlights the flexibility of our tool. The construction of reactor lines and their convexification (if needed), and similarly, the incorporation of further stages can be shown in any two dimensional space. The methodology does not change based on which two dimensions we want to plot the AR in.

### 3.3. Different feed compositions

So far, we have demonstrated the construction of AR for the Van de Vusse reaction scheme and kinetics with the available feed being pure A and its concentration being 1 kmol/m<sup>3</sup>. We may not always have this feed. The choice of feed that is given depends on the user. Thus, it is important that our tool can construct the ARs for any given feed. Since the equations governing the PFR and CSTR depend on the initial concentration, i.e. the feed, the trajectories obtained are different for different feeds. Thus, the whole structure of the AR gets changed. Our tool is capable of handling any feed that is given by the user. The figures below show the ARs obtained when different feeds are used. Changing the feed composition does not alter the methodology presented.

#### 3.3.1. Feed composition: [0.9 0.1 0 0]

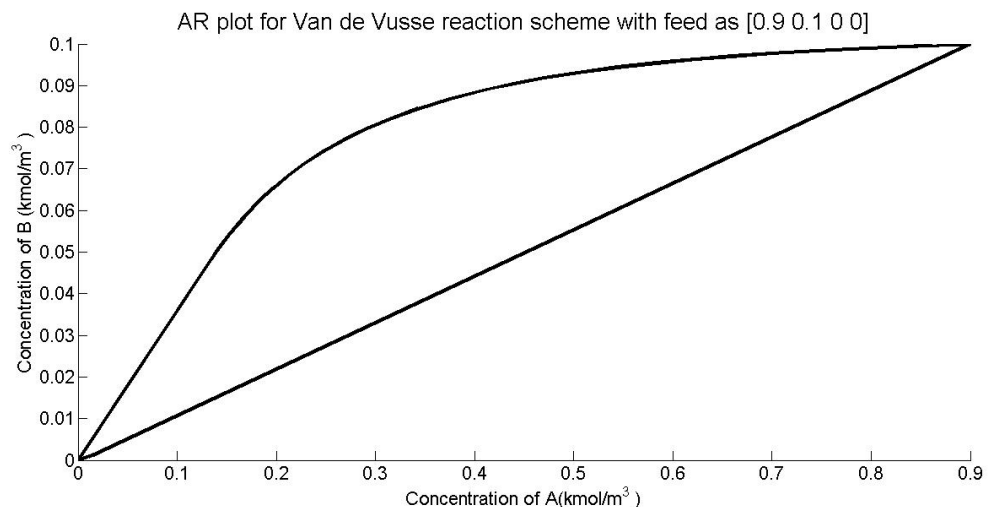


Fig. 3.10. AR plot for Van de Vusse reaction scheme with feed as [0.9 0.1 0 0]

### 3.3.2. Feed composition: [0.5 0.5 0 0]

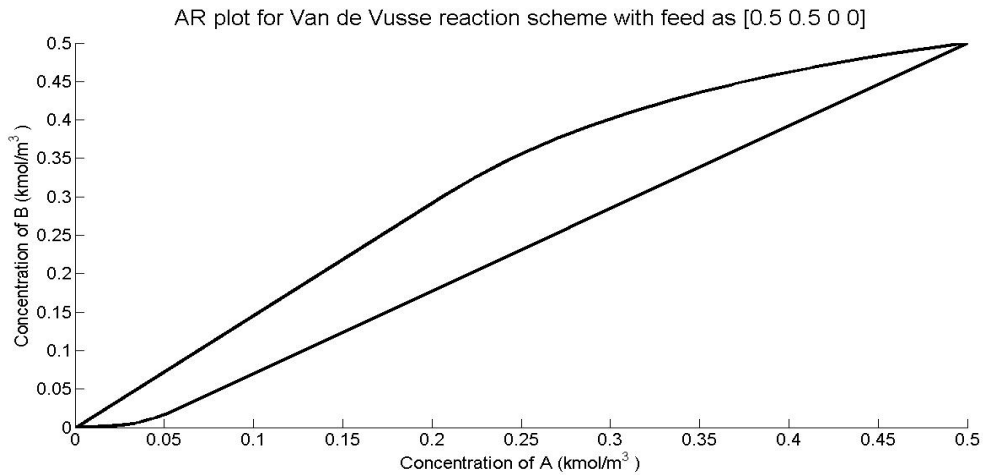


Fig. 3.11. AR plot for Van de Vusse reaction scheme with feed as [0.5 0.5 0 0]

### 3.3.3. Feed composition: [0.2 0.8 0 0]

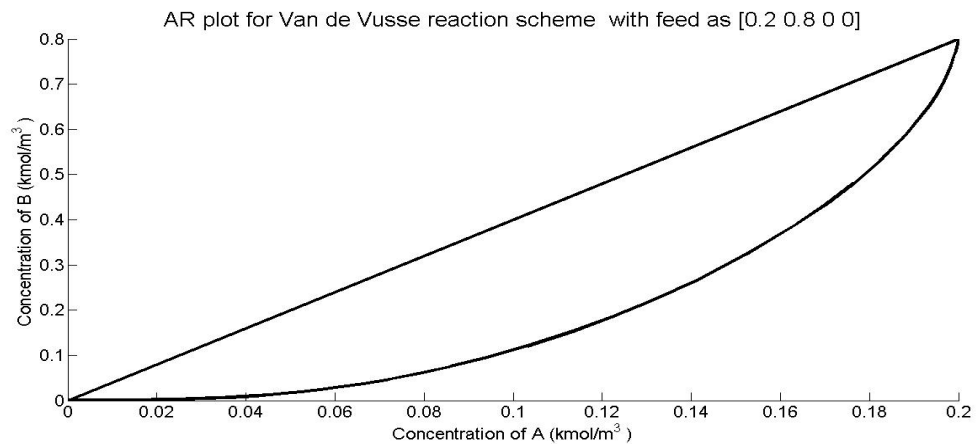


Fig. 3.12. AR plot for Van de Vusse reaction scheme with feed as [0.2 0.8 0 0]

### 3.3.4. Feed composition: [0.9 0 0.1 0]

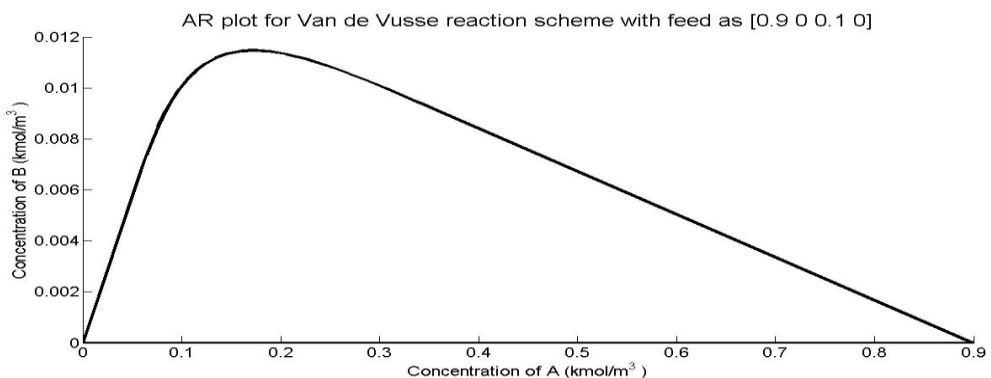


Fig. 3.13. AR plot for Van de Vusse reaction scheme with feed as [0.9 0 0.1 0]

### 3.3.5. Feed composition: [0.1 0 0.9 0]

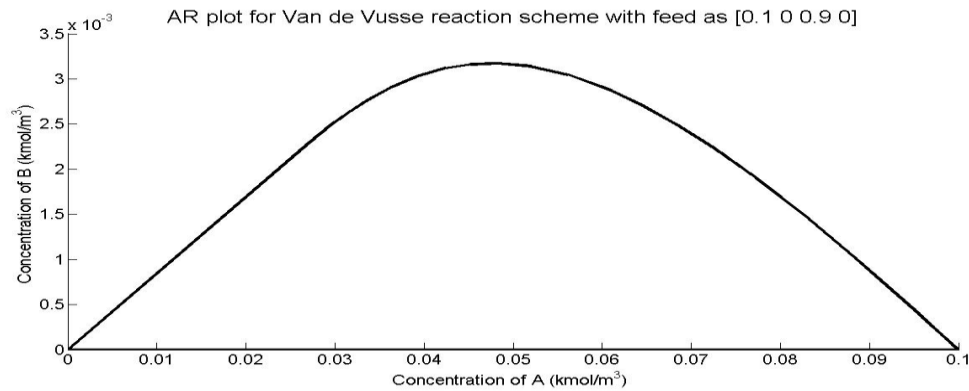


Fig. 3.14. AR plot for Van de Vusse reaction scheme with feed as [0.1 0 0.9 0]

### 3.3.6. Feed composition: [0.9 0 0 0.1]

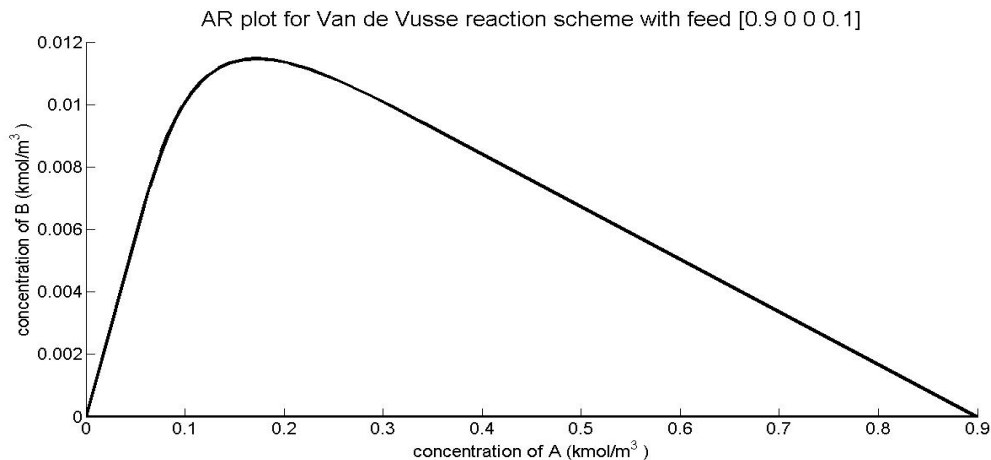


Fig. 3.15. AR plot for Van de Vusse reaction scheme with feed as [0.9 0 0 0.1]

### 3.3.7. Feed composition: [0.25 0.25 0.25 0.25]

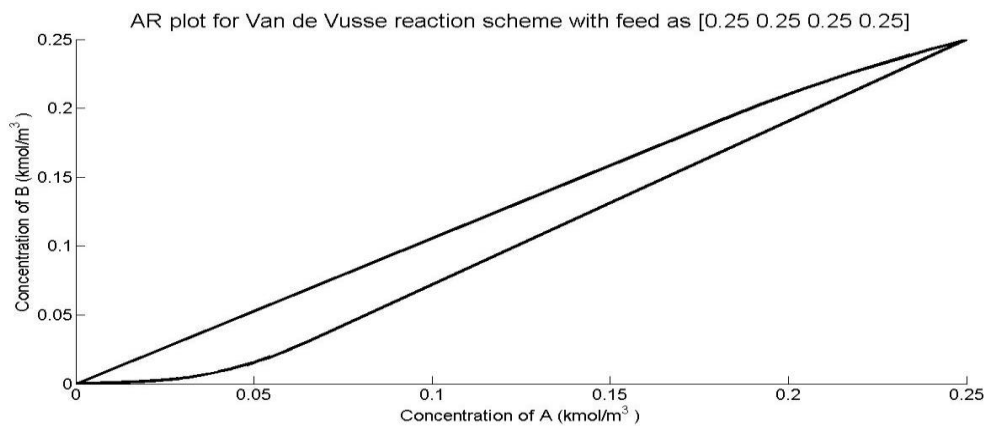


Fig. 3.16. AR plot for Van de Vusse reaction scheme with feed as [0.25 0.25 0.25 0.25]

### 3.3.8. Feed composition: [0 1 0 0]

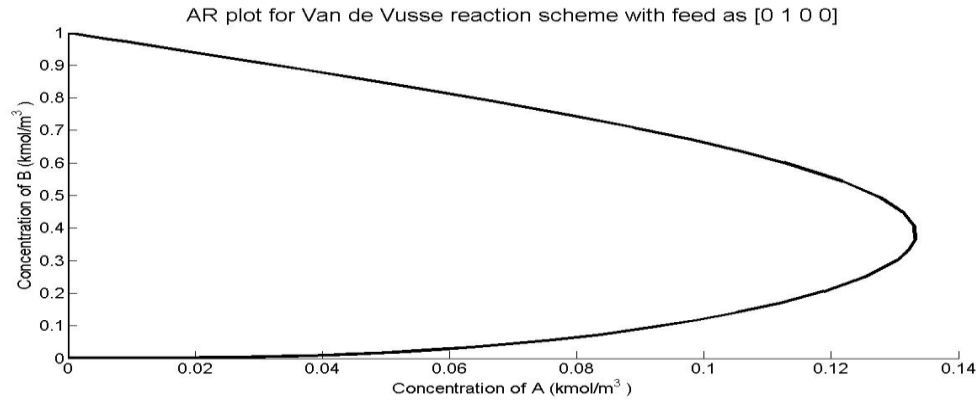


Fig. 3.17. AR plot for Van de Vusse reaction scheme with feed as [0 1 0 0]

### 3.3.9. Feed composition: [0 0.5 0.5 0]

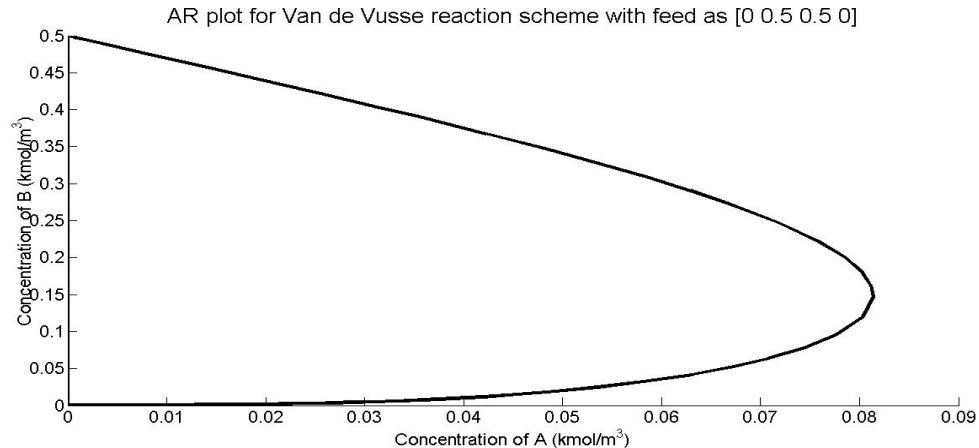


Fig. 3.18. AR plot for Van de Vusse reaction scheme with feed as [0 0.5 0.5 0]

### 3.3.10. Feed composition: [0 0.5 0 0.5]

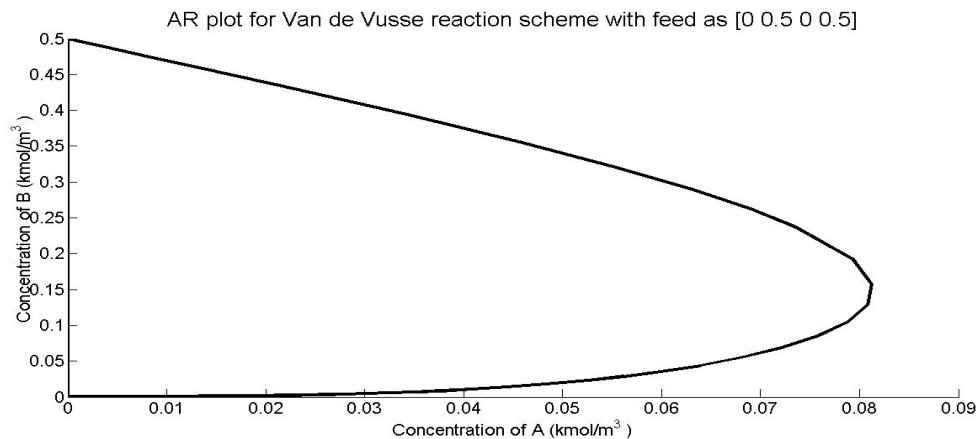
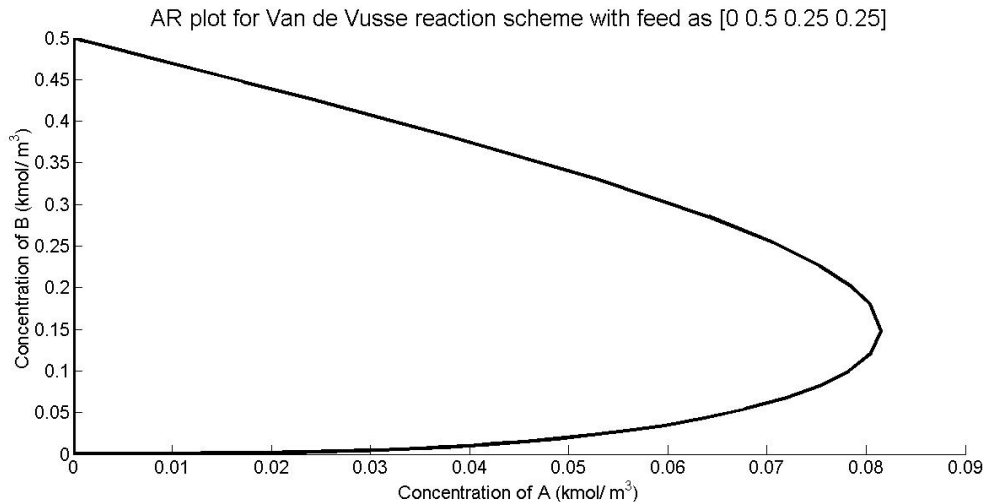


Fig. 3.19. AR plot for Van de Vusse reaction scheme with feed as [0 0.5 0 0.5]

### 3.3.11. Feed composition: [0 0.5 0.25 0.25]



*Fig. 3.20. AR plot for Van de Vusse reaction scheme with feed as [0 0.5 0.25 0.25]*

Thus, the figures 3.10 – 3.20 show the plots for AR in  $C_A$ - $C_B$  concentration space for different feed concentrations. The reason behind this study is to come out with the flexibility of the tool, which gives us the complete and correct AR no matter what inputs we enter.

## **3.4. Other reaction schemes: Trambouze and Denbigh**

Having looked at the Van de Vusse reaction scheme, we turn our attention to other reaction schemes, so as to validate the generic nature of our algorithm, i.e. to claim that our tool can work for any reaction scheme and kinetics that are thrown by the user. We look at Trambouze and Denbigh reaction schemes and construct the ARs for them.

### 3.4.1. Trambouze reaction scheme

Trambouze reaction scheme is an example of parallel series reactions, where a component,  $A$ , gives three products,  $B$ ,  $C$ , and  $D$  via three different parallel reactions.



$k_1$  = rate constant for the reaction of A going to B = 0.025 kmol m<sup>-3</sup>s<sup>-1</sup>

$k_2$  = rate constant for the reaction from A to C = 0.2 s<sup>-1</sup>

$k_3$  = rate constant for the reaction A to D = 0.4 m<sup>3</sup> kmol<sup>-1</sup>s<sup>-1</sup>

Feed Concentration:  $C_{AO} = 1$  kmol m<sup>-3</sup>;  $C_{BO} = C_{CO} = C_{DO} = 0$ , where  $C_{io}$  represents the initial concentration of the species  $i$ .

The PFR rate law equations are given by:

$$\frac{dC_A}{d\tau} = -k_1 - k_2 C_A - k_3 C_A^2 \quad (3.28)$$

$$\frac{dC_B}{d\tau} = k_1 \quad (3.29)$$

$$\frac{dC_C}{d\tau} = k_2 C_A \quad (3.30)$$

$$\frac{dC_D}{d\tau} = k_3 C_A^2 \quad (3.31)$$

The CSTR rate law equations are:

$$C_A - C_A^0 = \tau(-k_1 - k_2 C_A - k_3 C_A^2) \quad (3.32)$$

$$C_B - C_B^0 = \tau(k_1) \quad (3.33)$$

$$C_C - C_C^0 = \tau(k_2 C_A) \quad (3.34)$$

$$C_D - C_D^0 = \tau(k_3 C_A^2) \quad (3.35)$$

We proceed in accord to our proposed method and find the Attainable Region in the  $C_A$ - $C_C$  concentration space.

Fig. 3.21 shows the normal PFR trajectory (in blue) and its convexified region (in dashed black) as a result of Stage 1 calculations.

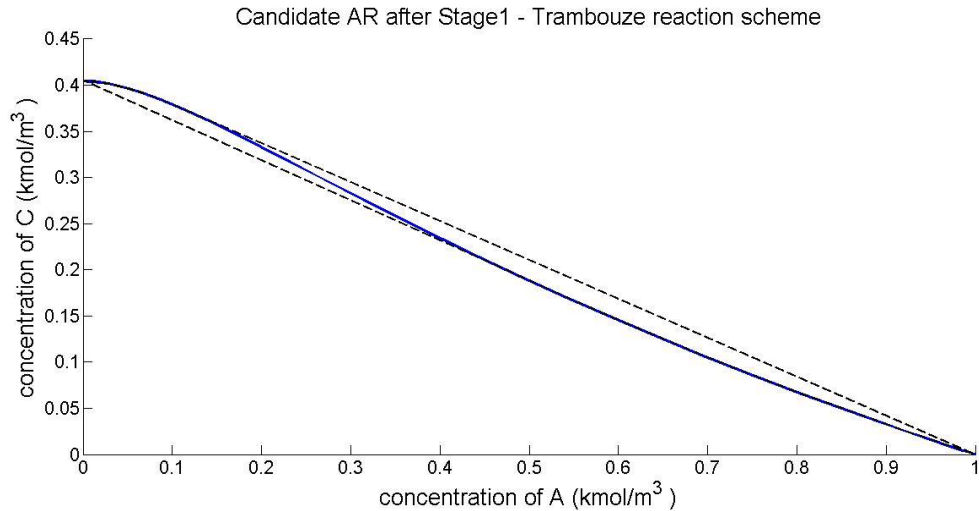


Fig. 3.21. Candidate AR plot for Trambouze reaction scheme – Stage 1

Proceeding, we look whether CSTR trajectories drawn from the points on the boundary in the non-convex region can extend the region. Fig. 3.22 shows the normal CSTR trajectory from the available feed point (in green). The dashed black region is the candidate AR at this stage.

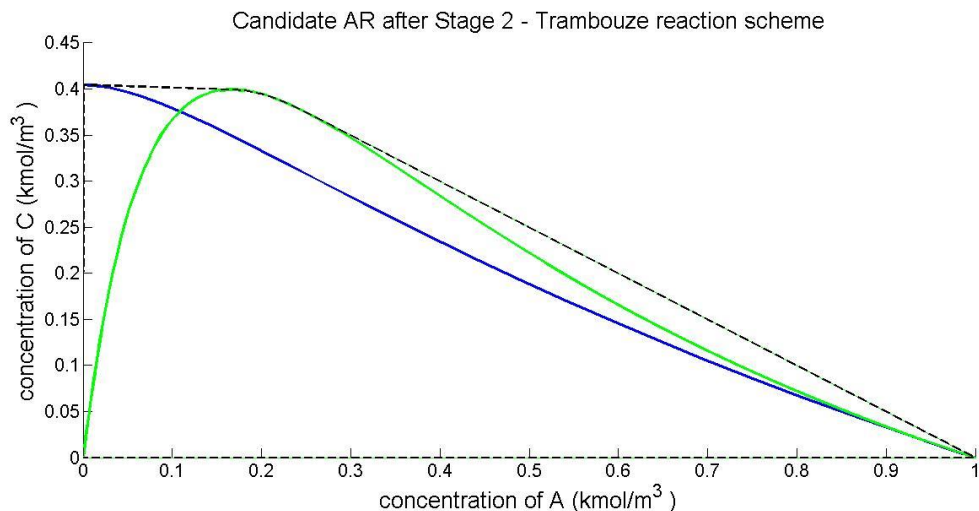


Fig. 3.22. Candidate AR plot for Trambouze reaction scheme – Stage 2

Further, Fig. 3.23 shows that the candidate AR obtained after Stage 2 is extended by a PFR trajectory, as shown by curve PQR. Again, the dashed black region represents the candidate AR after this stage.

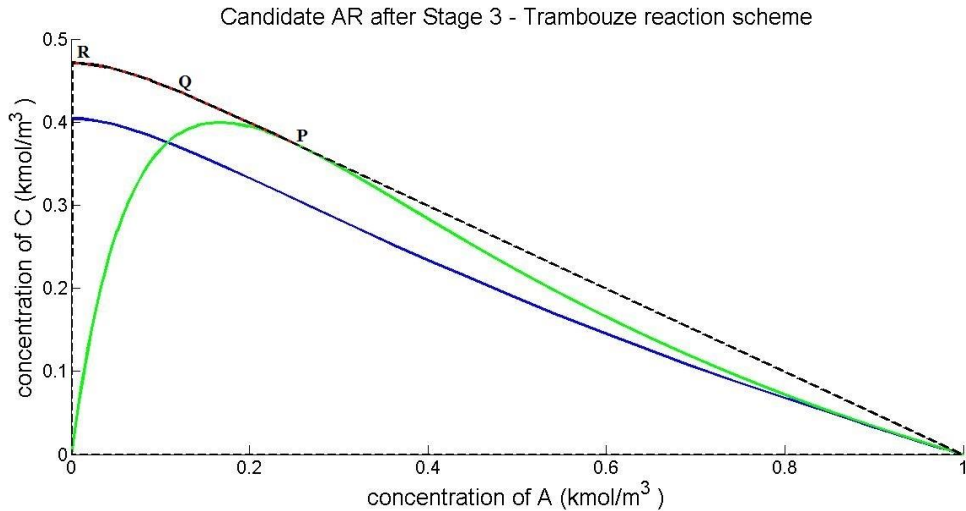


Fig. 3.23. AR plot for Trambouze reaction scheme – Stage 3

In our simulations, we saw that Stage 4 and Stage 5 did not extend the candidate AR obtained after Stage 3 and thus three stages are enough to get the complete AR. Thus, the final AR is shown by the dashed black region in Fig. 3.23. Construction of AR for the same reaction kinetics was done by (Wang, et. al., 2006), and their result is shown in Fig. 3.24.

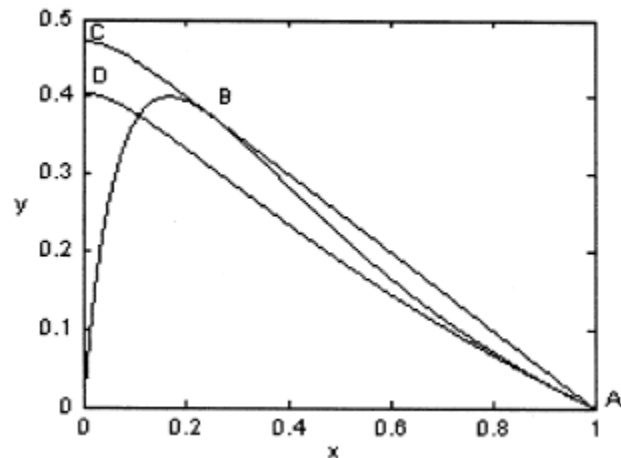
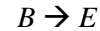
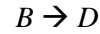
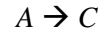


Fig. 3.24. AR plot for Trambouze reaction scheme – from literature (Wang et. al., 2002)

We compare the two results and find that they are same, both qualitatively and quantitatively.

### 3.4.2. Denbigh Kinetics

The Denbigh reaction scheme is given as follows



$k_1$  = rate constant for the reaction of  $A$  going to  $B$  =  $1 \text{ m}^3 \text{ kmol}^{-1} \text{s}^{-1}$

$k_2$  = rate constant for the reaction from  $A$  to  $C$  =  $0.1 \text{ s}^{-1}$

$k_3$  = rate constant for the reaction  $B$  to  $D$  =  $0.1 \text{ s}^{-1}$

$k_4$  = rate constant for the reaction  $B$  to  $E$  =  $0.1 \text{ m}^3 \text{ kmol}^{-1} \text{s}^{-1}$

Feed Concentration:  $C_{AO} = 1 \text{ kmol m}^{-3}$ ;  $C_{BO} = C_{CO} = C_{DO} = 0$ , where  $C_{io}$  represents the initial concentration of the species  $i$ .

We proceed with our algorithm and plot the AR as shown:

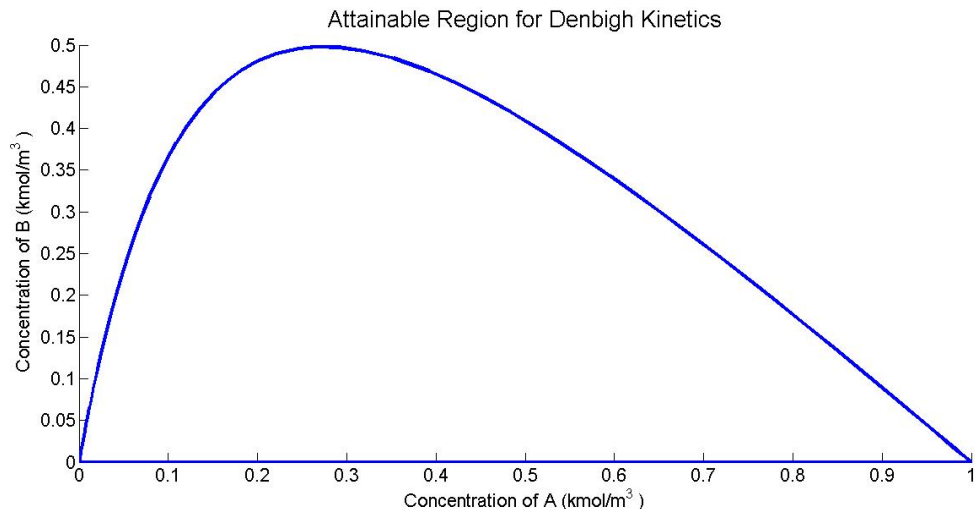


Fig. 3.25. AR plot for Denbigh reaction scheme

There is no two-dimensional AR plotted in literature for Denbigh Kinetics. But to validate our results, we compare the conversion obtained in the two sets of results. Previous work done (Hildebrandt and Glasser, 1990) obtained a maximum production of 3.541 moles of  $D$  for an input

feed of A of 6 moles. That amounts to 59.02% conversion of A. Our results gave 58.89% conversion which are close enough to the results in literature.

### **3.5. Attainable Regions under restrictions on feed availability and reactor volume**

In this section, we adopt simultaneous constraints of limitation of feed availability and limitation on reactor size and have a look at the ARs obtained and their nature. Such a study is important as it pertains to real-life situations wherein the feed is not available indefinitely and also the reactor size is limited due to cost and maintenance factors.

So, suppose we have been provided with a constraint on the availability of feed flow rate and also a constraint on the volume of the reactor to be used. Studies show that the convexity of AR as proposed by researchers is challenged here. The convexity of the AR was proposed by putting forward the argument that if the outputs of two reactors operating in parallel are mixed, any concentration on the straight line joining these two points can be achieved by adjusting the flow rates. Also, in case of a single reactor, the feed can be bypassed and any concentration on the straight line joining the output concentration and feed concentration can be achieved by mixing in adjusted flow rates. Now, since there is only a single reactor with a fixed volume, the first argument cannot be availed. Also, since there is a limitation on the availability of feed, the second argument may also fail.

We have to emphasize that both the constraints are important. If there is a restriction only on feed availability and not on reactor volume, the residence time still can be varied from zero to infinity by maneuvering the volume of the reactor from a very small-sized reactor to a very large one. Similarly, if there is a restriction on only the reactor size and not the feed availability, the residence time can again be varied from zero to infinity by setting the flow rate very high or very low respectively. Thus, when both the constraints are present simultaneously, only then, there is an actual constraint on the residence time.

We take the Van de Vusse reaction scheme and kinetics, as given in Section 3.1 and try to capture the ARs for a single reactor system, where the availability of feed is restricted to a maximum of 1

$\text{m}^3/\text{s}$  and only one CSTR of volume  $1 \text{ m}^3$  is available. We take a generic model wherein the feed is both fed to the reactor and also bypassed. Also, all the feed need not necessarily go to the reactor or bypass, i.e., some of it may go unused. The model is shown in Fig. 3.26.

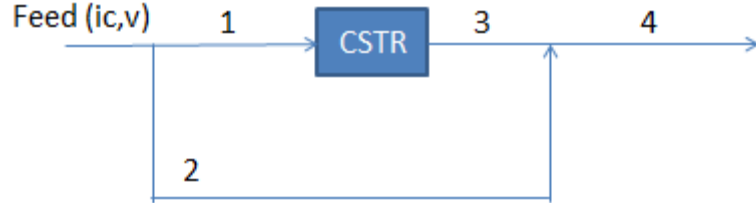


Fig. 3.26. The model for a single CSTR

The feed available is characterized by  $ic$ , the concentration of the feed ( $[1 \ 0 \ 0 \ 0]$ ), and  $v$ , the flow rate of the feed. The following equations govern the working of the model.  $v_i$  denotes the flow rate of  $i^{\text{th}}$  stream.  $\text{frac}_1$  denotes the fraction of the available feed that enters the reactor and can be any number from 0 to 1.  $C_{ij}$  denotes the concentration of  $j^{\text{th}}$  specie in the  $i^{\text{th}}$  stream.  $\bar{C}_i$  is the concentration vector in the  $i^{\text{th}}$  stream.

$$\bar{C}_i = [C_{iA} \ C_{iB} \ C_{iC} \ C_{iD}] \quad (3.36)$$

Equations for the one reactor model:

$$v_1 = v * \text{frac}_1 \quad (3.37)$$

$$v_2 = v * (1 - \text{frac}_1) \quad (3.38)$$

$$v_3 = v_1 \quad (3.39)$$

$$v_4 = v_2 + v_3 \quad (3.40)$$

$$\bar{C}_1 = ic \quad (3.41)$$

$$\bar{C}_2 = ic \quad (3.42)$$

$$C_{3A} = C_{1A} + \tau * (-k_1 C_{1A} + k_2 C_{1B} - k_4 C_{1A}^2) \quad (3.43)$$

$$C_{3B} = C_{1B} + \tau * (k_1 C_{1A} - k_2 C_{1B} - k_3 C_{1B}) \quad (3.44)$$

$$C_{3C} = C_{1C} + \tau * (k_3 C_{1B}) \quad (3.45)$$

$$C_{3D} = C_{1D} + \tau * (k_4 C_{1A}^2) \quad (3.46)$$

$$\bar{C}_4 = \frac{\bar{C}_2 * v_2 + \bar{C}_3 * v_3}{(v_2 + v_3)} \quad (3.47)$$

In our simulations, we increase the value of  $frac_1$  from 0 to 1 in a certain step size as the amount of the feed that goes inside the system can vary from a very little amount to a maximum of 1. The equations are solved for all values of  $frac_1$ .

The minimum residence time that would be achievable is when all the feed goes in the reactor. Since the volume of the reactor is  $1 \text{ m}^3$  and the maximum feed available is  $1 \text{ m}^3/\text{s}$ , this value turns out to be 1 s. Thus, residence times between 0 and 1 s (1 not included) are not feasible.

Now, if we run the reactor at this residence time (1 s), all the feed goes in the reactor and nothing is bypassed. So, there is only one attainable point for this residence time, which is found out to be  $(0.0919, 0.0057, 0.0574, 0.8449)$ , shown by point P, in Fig. 3.27.

Now, we consider a residence time of 2 seconds. The flow rate thus should be reactor volume divided by 2, i.e.,  $0.5 \text{ m}^3/\text{s}$ . In our simulations, this corresponds to  $frac_1$  equal to 0.5. Thus, the feed going into the reactor is  $0.5 \text{ m}^3/\text{s}$  and that being bypassed is a maximum of  $0.5 \text{ m}^3/\text{s}$ . The concentration at the reactor exit,  $\bar{C}_3$  is found out to be  $(0.0651, 0.0042, 0.0840, 0.8468)$ , shown by point Q. Thus, the mixed cup concentration is given by

$$\bar{C}_4 = \frac{0.5 * (0.0651, 0.0042, 0.0840, 0.8468) + 0.5 * (1, 0, 0, 0)}{1} \quad (3.48)$$

$$\bar{C}_4 = (0.5325, 0.0021, 0.042, 0.4234) \quad (3.49)$$

This is shown by the point R in the figure. Now, all the feed that goes in the bypass stream may not be actually bypassed but some of it may be left unused. This is because it is not necessary to use all the available feed. So, the line joining the points Q and R shows points that can be attained by choosing to bypass suitable quantities between 0 and  $0.5 \text{ m}^3/\text{s}$ . The difference between  $0.5 \text{ m}^3/\text{s}$  and what bypass is chosen, is said to be left unused.

Similarly, we consider the case of residence time being 4. The flow rate thus should be reactor volume divided by 4, i.e.,  $0.25 \text{ m}^3/\text{s}$ . In our simulations, this corresponds to  $frac_1$  equal to 0.25. Thus, the feed going into the reactor is  $0.25 \text{ m}^3/\text{s}$  and that being bypassed is a maximum of  $0.75 \text{ m}^3/\text{s}$ . The concentration at the reactor end,  $\bar{C}_3$  is found out to be  $(0.0456, 0.003, 0.1196, 0.8318)$ , shown by point S. Thus, the mixed cup concentration is

$$\bar{C}_4 = \frac{(0.25) * (0.0456, 0.003, 0.1196, 0.8318) + (0.75) * (1, 0, 0, 0)}{1}, \quad (3.50)$$

$$\bar{C}_4 = (0.7614, 0.000750.0299, 0.208) \quad (3.51)$$

It is shown by the point T in the figure. Again, the line joining the points S and T shows points that can be attained by choosing to bypass suitable quantities between 0 and 0.75 m<sup>3</sup>/s. The rest of the bypass is said to be left unused. Similar analysis can be done by carrying the residence time in steps up to a large number.

The attainable region is enclosed between the blue trajectories, as shown in Fig. 3.27.

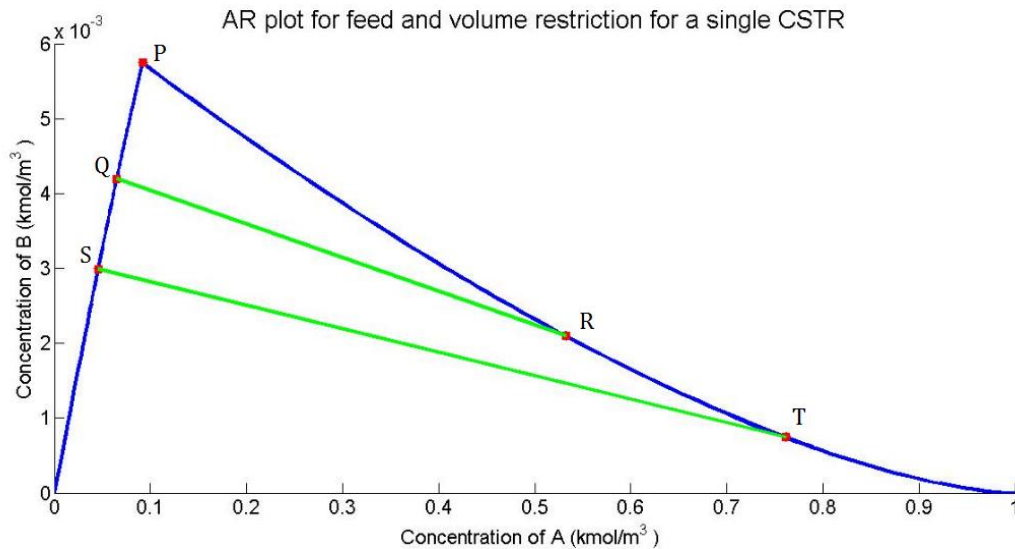


Fig. 3.27. AR plot for a single CSTR of volume 1 m<sup>3</sup> and maximum feed available of 1m<sup>3</sup>/s (Van de Vusse reaction scheme)

We observe that the plot obtained is non-convex. The non-convexity can be observed along PRT. The concentration corresponding to point P cannot be simply mixed with the feed, because all the feed that was available has already been consumed to attain P. Similarly, all points in the concave region cannot be obtained by mixing because there isn't simply enough feed to achieve those points and given there is only one reactor available of fixed size.

We see that the boundary along PQS in Fig. 3.27 is a part of the CSTR region we obtained in Section 3.1, i.e. under no feed and volume restriction. The CSTR region with no constraints is given by region ABCDA and that with the feed and volume constraints is given by region AECDA in Fig. 3.28. The boundary of the CSTR region with no constraints that is not included in the region with the feed & volume constraints corresponds to when the residence time is between 0 and 1 s. Had there been enough feed, or had we been able to adjust the volume of the CSTR somehow, then we would have been able to traverse the remaining portion as well.

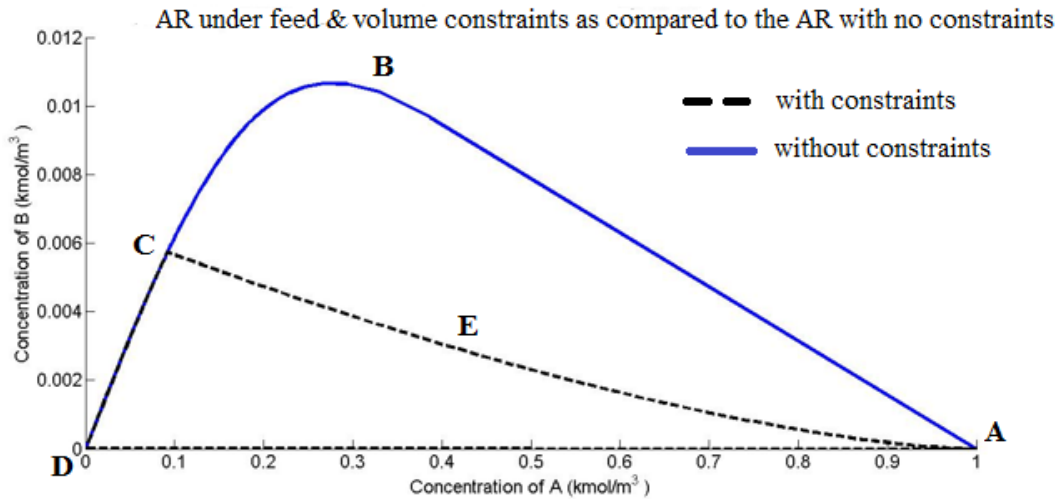


Fig. 3.28. Comparison of ARs with and without feed & volume constraints

Similarly, the AR plots when the CSTR volume, or in more general terms, the residence time is limited to 0.5, 0.1 and 0.05 s, are shown in the plots Fig. 3.29 – 3.31 respectively.

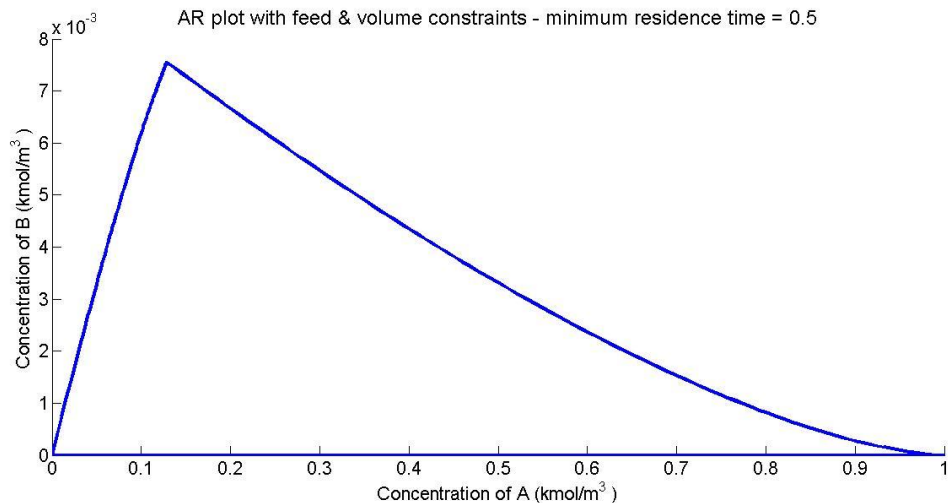


Fig. 3.29. AR plot for a single CSTR of volume 0.5 m<sup>3</sup> and maximum feed available of 1m<sup>3</sup>/s(Van de Vusse reaction scheme)

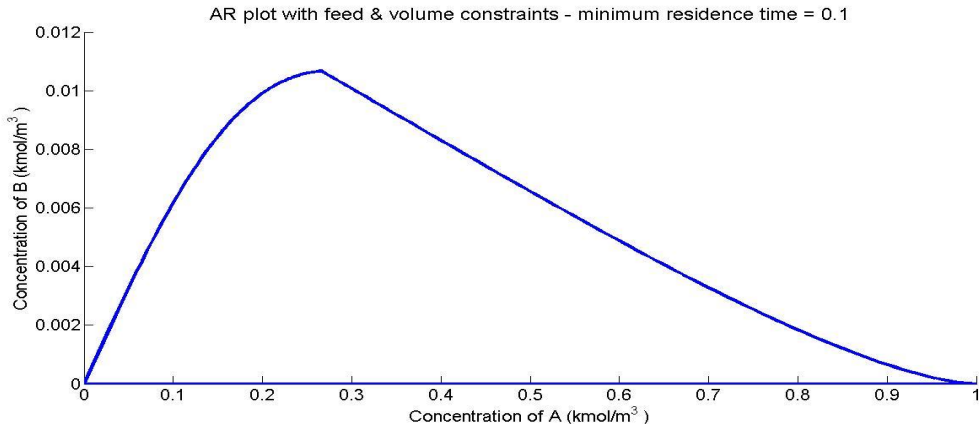


Fig. 3.30. AR plot for a single CSTR of volume  $0.1 \text{ m}^3$  and maximum feed of  $1 \text{ m}^3/\text{s}$  (VdV reaction scheme)

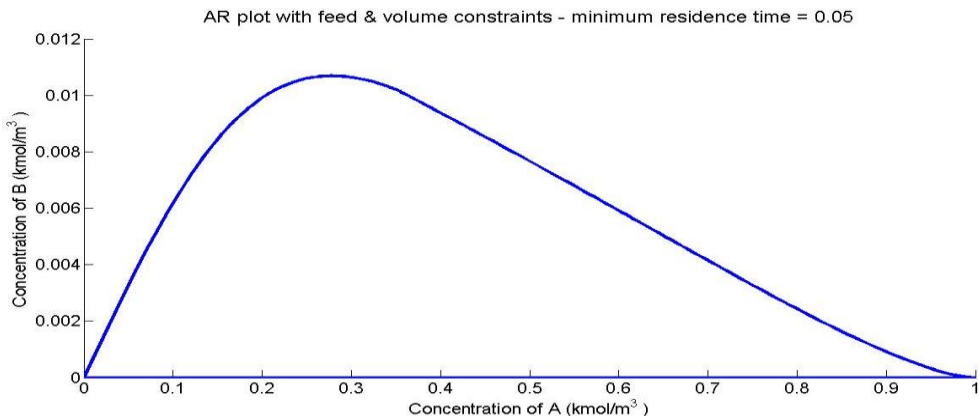


Fig. 3.31. AR plot for a single CSTR of volume  $0.05 \text{ m}^3$  and maximum feed of  $1 \text{ m}^3/\text{s}$  (VdV reaction scheme)

As can be seen from the above figures, all the regions in Figs. 3.29-3.31 are still a part of the AR under no constraints. Lowering the minimum residence time allows us to attain more and more area of the AR obtained under no constraints.

Similarly, the AR for a single PFR with fixed volumes of 1, 0.5, 0.1 and  $0.05 \text{ m}^3$  respectively are shown in Fig. 3.32 – 3.35. The reactor model remains the same. CSTR equations given in Eqns. 3.43-3.46 are replaced by the corresponding PFR equations.

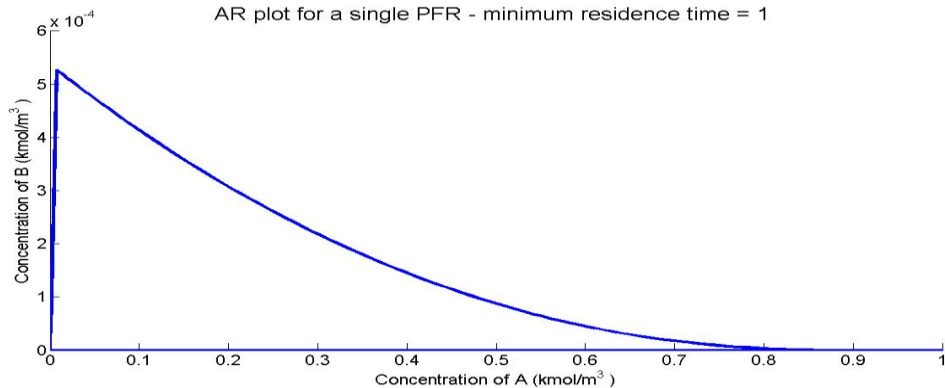


Fig. 3.32. AR plot for a single PFR of volume 1 m<sup>3</sup> and maximum feed available of 1 m<sup>3</sup>/s (Van de Vusse reaction scheme)

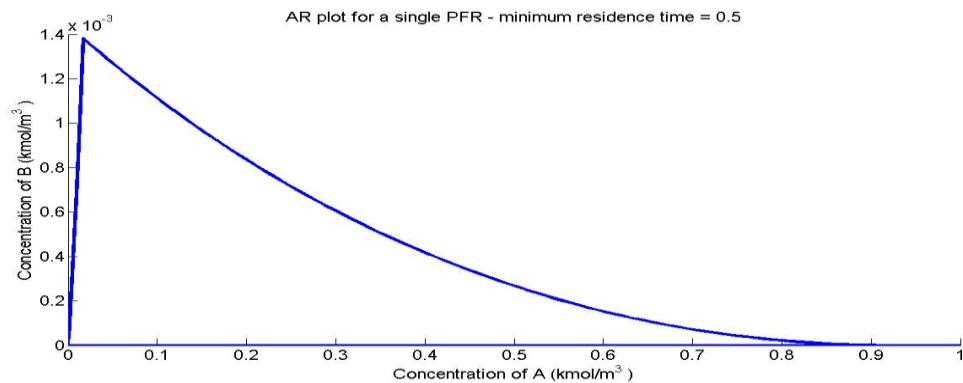


Fig. 3.33. AR plot for a single PFR of volume 0.5 m<sup>3</sup> and maximum feed of 1 m<sup>3</sup>/s (VdV reaction scheme)

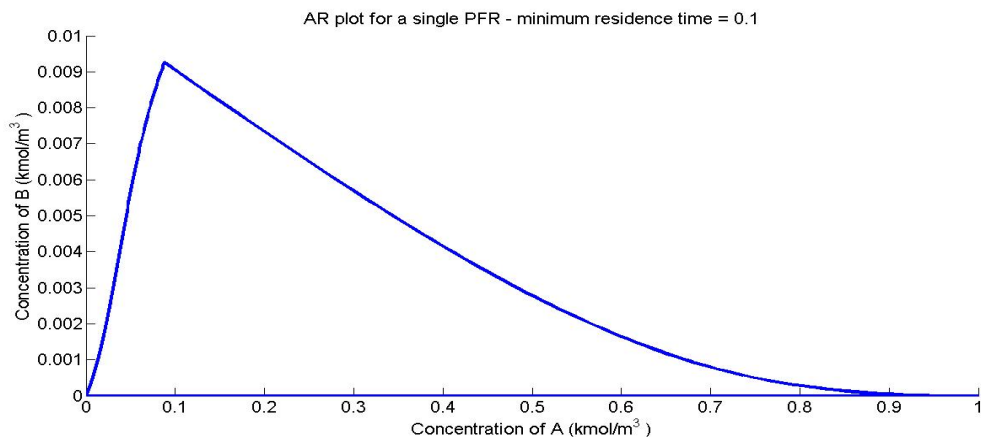


Fig. 3.34. AR plot for a single PFR of volume 0.1 m<sup>3</sup> and maximum feed of 1 m<sup>3</sup>/s (VdV reaction scheme)

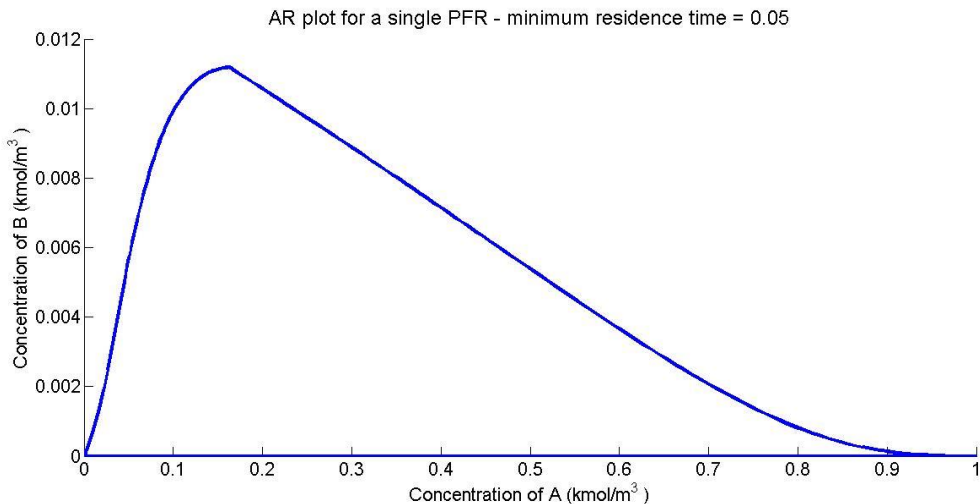


Fig. 3.35. AR plot for a single PFR of volume  $0.05 \text{ m}^3$  and maximum feed of  $1 \text{ m}^3/\text{s}$  (VdV reaction scheme)

Again, it goes without mentioning that these regions are a part of the PFR region that was obtained under no restrictions, and include more and more of its area as we decrease the minimum residence time.

We know that AR is a collection of all points that can be obtained by using any type and arrangement of reactor(s). Thus, for the constraints of one single reactor of fixed volume of  $1 \text{ m}^3$  and feed availability of  $1 \text{ m}^3/\text{s}$ , the complete AR will be the combination of points obtained from the CSTR as well as PFR. Fig. 3.36 shows both the CSTR (solid green) and PFR (dashed blue) curves. As we see, the PFR region is included in that of the PFR region and thus, the AR in this case is given by the green region.

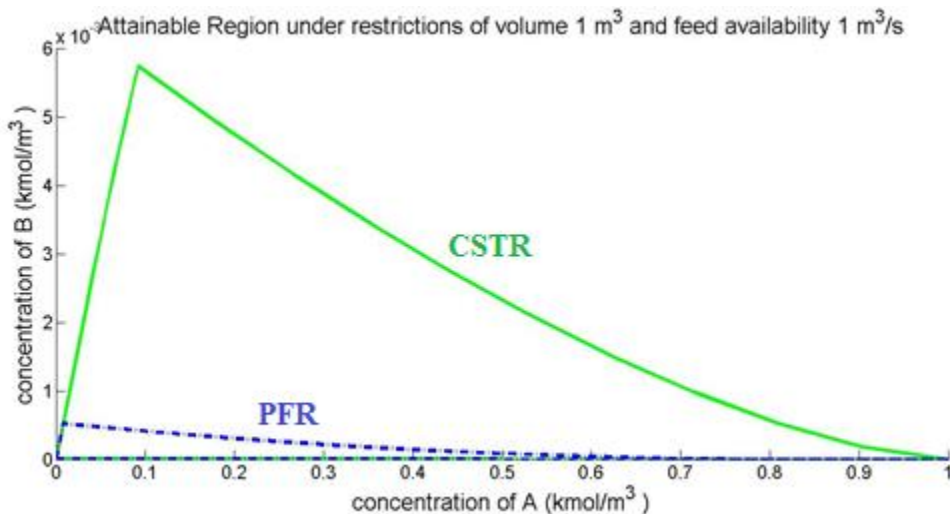


Fig. 3.36. PFR and CSTR plots for the AR under feed availability and reactor volume restrictions

Now, we extend this concept to two reactor systems. The restriction on the feed availability remains the same. Both the reactors now have volumes of  $1 \text{ m}^3$  each. The reason that we take the same volume,  $1 \text{ m}^3$  for both the reactors, is that, in industries, there must be a minimum size of the reactor. We have taken this minimum size as  $1 \text{ m}^3$  in our example. Any value could have been used and we have taken the mentioned value of  $1 \text{ m}^3$ , just for the sake of an example. Obviously, the methodology presented is not limited to this value but can be used for any value.

Similarly, we can extend this concept to three reactors, four reactors and so on. Literature has shown that very often, no more than three reactors were required in a process. Thus, we extend the concept of construction of AR under restrictions of volume and feed availability till three reactor systems.

For two reactor systems, there are two arrangements possible: series or parallel. We explain the model of the series arrangement.  $R_1$  and  $R_2$  are the two reactors. In the series arrangement, we have 4 possible combinations for  $\{R_1, R_2\}$ , those being,  $\{\text{CSTR}, \text{CSTR}\}$ ,  $\{\text{PFR}, \text{CSTR}\}$ ,  $\{\text{CSTR}, \text{PFR}\}$  and  $\{\text{PFR}, \text{PFR}\}$

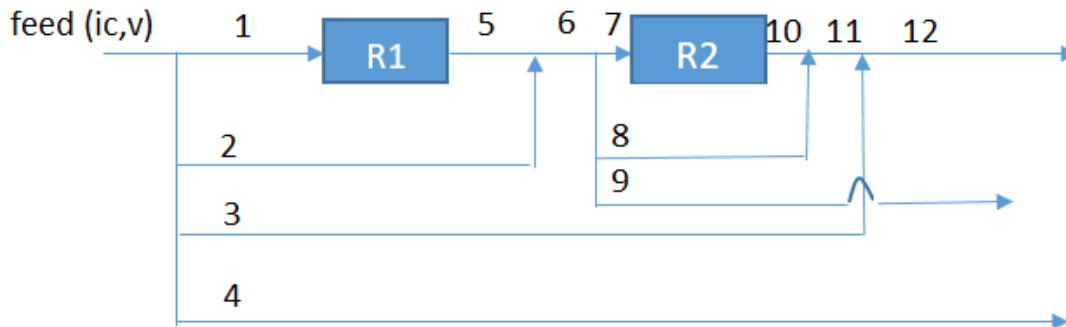


Fig. 3.37. Two reactor series model

As in the one reactor model, the feed is characterized by  $ic$  ( $[1 \ 0 \ 0 \ 0]$ ), the feed concentration, and  $v$ , the flow rate. In the equations,  $v_i$  denotes the flow rate of  $i^{th}$  stream.  $frac$  denotes a fraction and can be any number from 0 and 1.  $\bar{C}_i$  denotes the concentration vector of the  $i^{th}$  stream. *rate\_equations* represent the rate law equations and these depend on the type of reactor, i.e. whether  $R_1$  or  $R_2$  is a PFR or a CSTR. Also, they are a function of the concentration entering the reactor.

$$v_1 = v * frac_1 \quad (3.52)$$

$$v_2 = v * (1 - frac_1) * frac_2 \quad (3.53)$$

$$v_3 = v * (1 - frac_1) * (1 - frac_2) * frac_3 \quad (3.54)$$

$$v_4 = v * (1 - frac_1) * (1 - frac_2) * (1 - frac_3) \quad (3.55)$$

$$\overline{C}_1 = \overline{C}_2 = \overline{C}_3 = \overline{C}_4 = ic \quad (3.56)$$

$$v_5 = v_1 \quad (3.57)$$

$$\overline{C}_5 = rate\_equations(\overline{C}_1) \quad (3.58)$$

$$v_6 = v_5 + v_2 \quad (3.59)$$

$$\overline{C}_6 = \frac{\overline{C}_2 * v_2 + \overline{C}_5 * v_5}{(v_2 + v_5)} \quad (3.60)$$

$$v_7 = v_6 * frac_4 \quad (3.61)$$

$$v_8 = v_6 * (1 - frac_4) * frac_5 \quad (3.62)$$

$$v_9 = v_6 * (1 - frac_4) * (1 - frac_5) \quad (3.63)$$

$$\overline{C}_7 = \overline{C}_8 = \overline{C}_9 = \overline{C}_6 \quad (3.64)$$

$$v_{10} = v_7 \quad (3.65)$$

$$\overline{C}_{10} = rate\_equations(\overline{C}_7) \quad (3.66)$$

$$v_{11} = v_8 + v_{10} \quad (3.67)$$

$$\overline{C}_{11} = \frac{\overline{C}_8 * v_8 + \overline{C}_{10} * v_{10}}{v_8 + v_{10}} \quad (3.68)$$

$$v_{12} = v_3 + v_{11} \quad (3.69)$$

$$\overline{C}_{12} = \frac{\overline{C}_3 * v_3 + \overline{C}_{11} * v_{11}}{v_3 + v_{11}} \quad (3.70)$$

The feed is divided in four parts: Stream 1 enters the reactor  $R_1$ . Stream 2 is bypassed to the exit of  $R_1$ . Stream 3 is bypassed to the exit of  $R_2$ . Stream 4 is left unused. Stream 5 is obtained at the output of reactor  $R_1$ . The flow rate of Stream 6 is the sum of Stream 2 and Stream 5 and its concentration is the mixed cup concentration of Streams 2 and 5. Now, Stream 6 is divided in to three other streams. Stream 7 goes to reactor  $R_2$ . Stream 8 is bypassed to the output of reactor  $R_2$ . Stream 9 is left unused. Stream 10 is obtained at the output of reactor  $R_2$ . The flow rate of Stream 11 is the sum of Stream 8 and Stream 10 and its concentration is the mixed cup concentration. The flow rate of Stream 12, which is the overall output stream is the sum of Stream 3 and Stream 11 and its concentration is the mixed cup concentration.

Thus, by changing the values of  $frac_1$ ,  $frac_2$  and  $frac_3$ , from 0 to 1, we get all the possible combinations. The union of all such points obtained at the output in these combinations is our AR for that particular combination of  $R_1$  and  $R_2$ . The ARs for the four combinations are shown below:

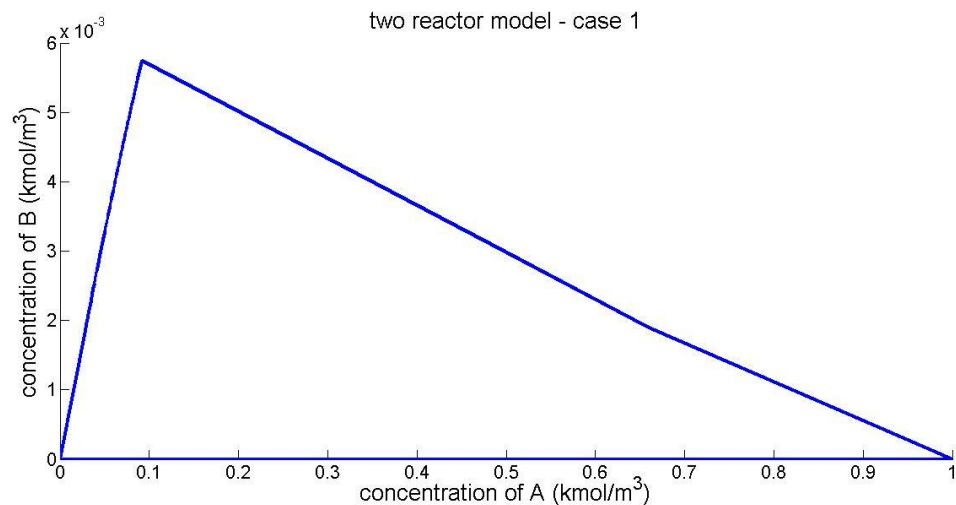


Fig. 3.38. AR for two reactor model under feed and volume constraints for VdV reaction scheme – case 1

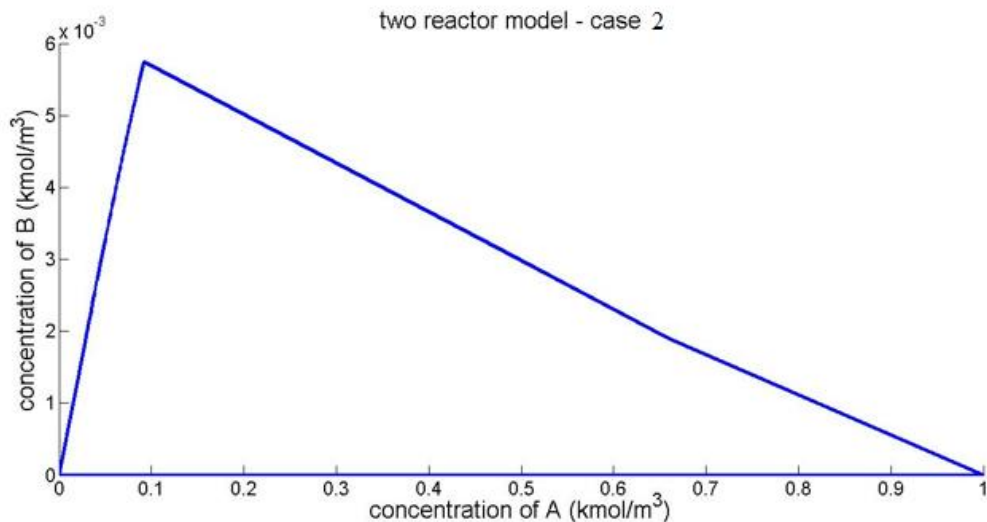


Fig. 3.39. AR for two reactor model under feed and volume constraints for VdV reaction scheme – case 2

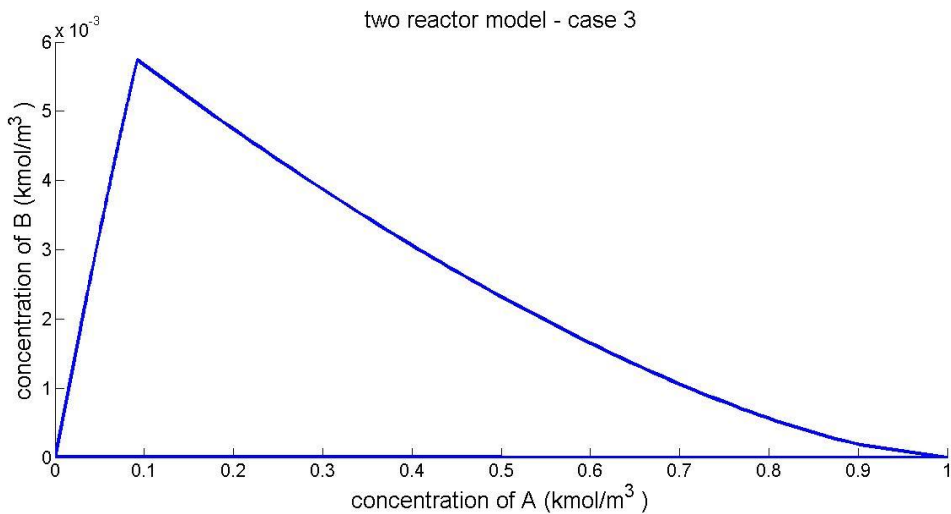


Fig. 3.40. AR for two reactor model under feed and volume constraints for VdV reaction scheme – case 3

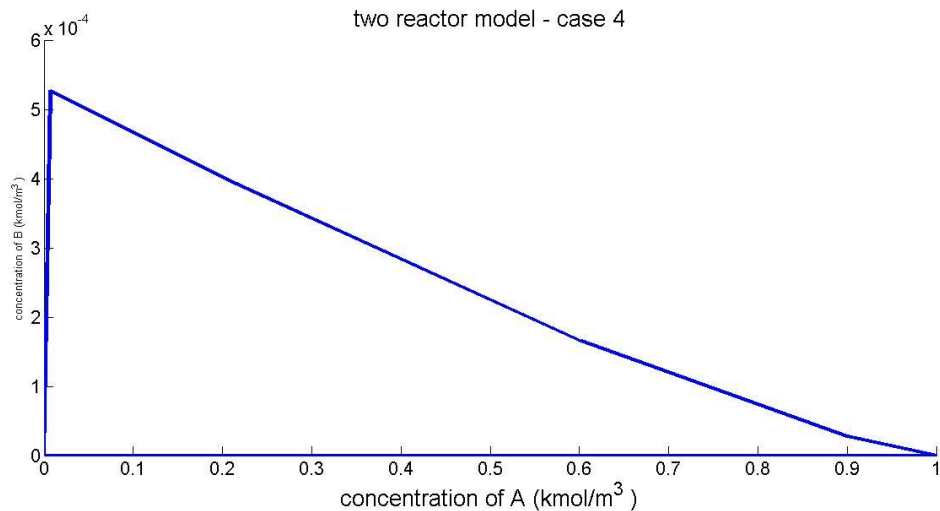


Fig. 3.41. AR for two reactor model under feed and volume constraints for VdV reaction scheme – case 4

Similarly, we solve the equations for the parallel arrangement. In the parallel arrangement, we have 3 possible combinations for  $\{R_1, R_2\}$ , those being {CSTR,CSTR}, {CSTR,PFR} and {PFR,PFR}. The equations for this arrangement are not shown here.

The model for the parallel arrangement of the two reactors is shown in Fig. 3.42 followed by the ARs for the three combinations in Fig. 3.43 - 3.45.

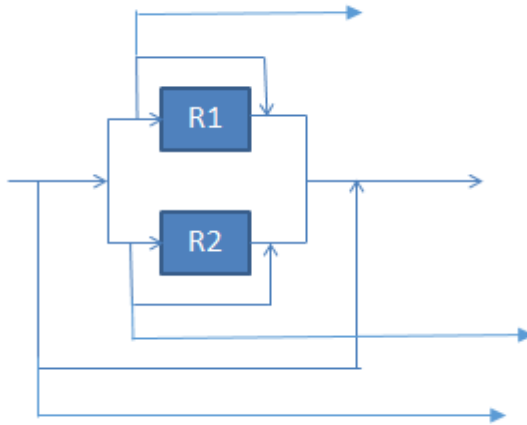


Fig.3.42. Two reactor parallel model

The AR plots for the three combinations are as shown below:

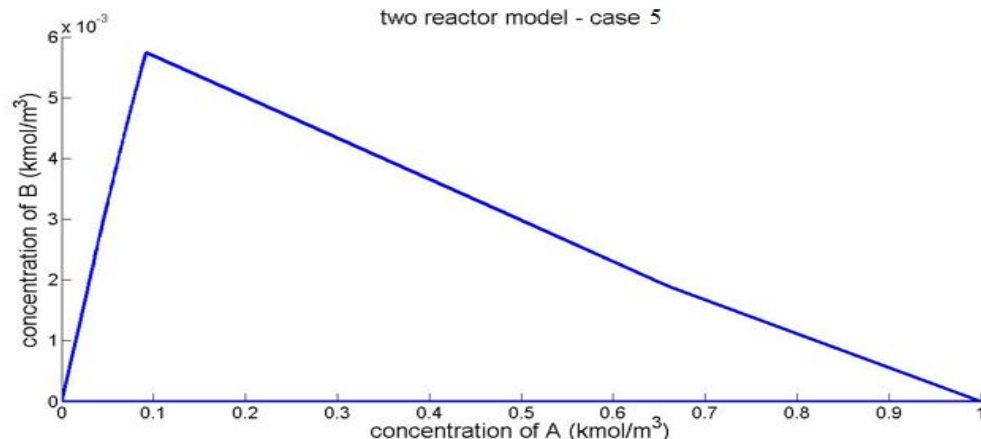


Fig. 3.43. AR for two reactor model under feed and volume constraints for VdV reaction scheme – case 5

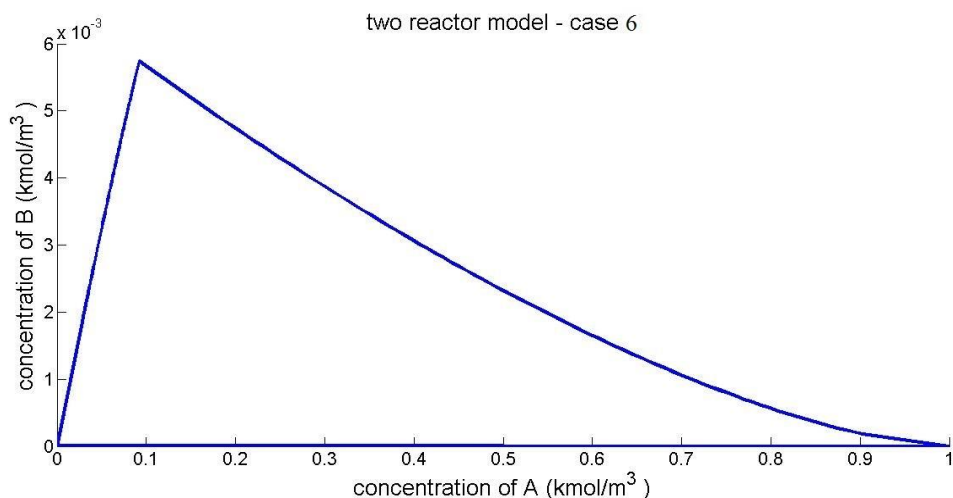


Fig. 3.44. AR for two reactor model under feed and volume constraints for VdV reaction scheme – case 6

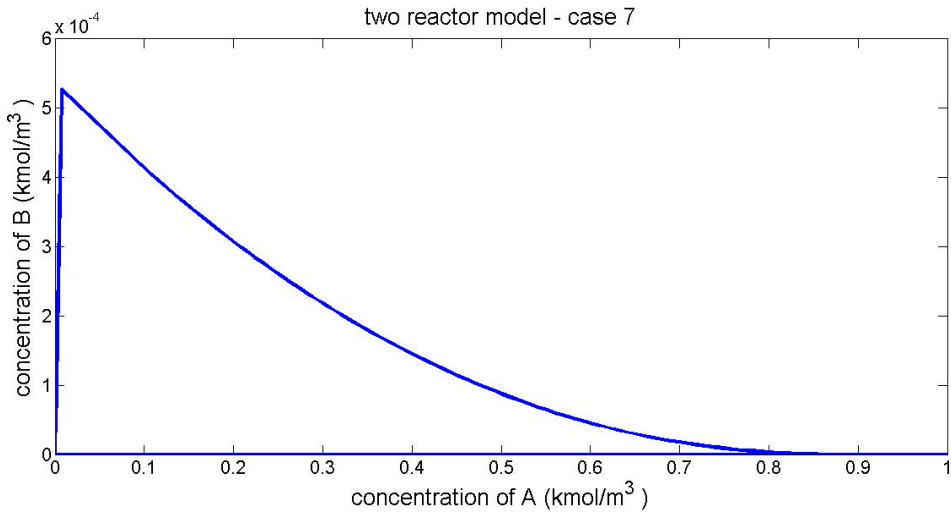


Fig. 3.45. AR for two reactor model under feed and volume constraints for VdV reaction scheme – case 7

Further, reiterating the fact that AR is a collection of all points that can be obtained using any type and arrangement of reactors, we take the union of ARs of all the seven cases above and present the final AR for a two reactor model for the Van de Vusse (VdV) reaction scheme under the restrictions of fixed volume of  $1 \text{ m}^3$  for both the reactors and maximum feed availability of  $1 \text{ m}^3/\text{s}$ . We observe that this AR is also not convex.

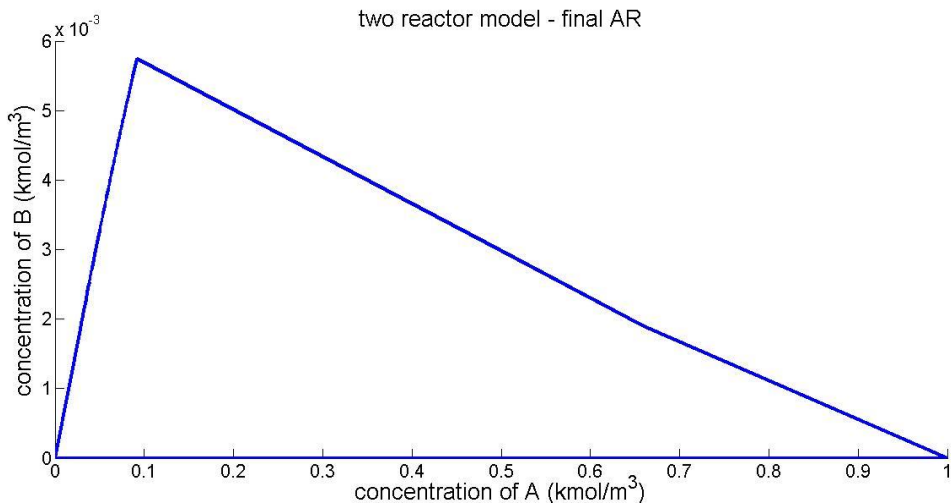


Fig. 3.46. Final AR for two reactor model under feed and volume constraints for VdV reaction scheme

We compare this against the AR obtained for the one reactor model and find that the AR is enlarged. As we recall, we had mentioned in the beginning of this section that the first premise for arguing the convexity of the AR was that two reactors could operate in parallel and the when their outputs are mixed, we get concentrations corresponding to all points lying on the line joining the points

corresponding to these outputs. For a single reactor model, this argument failed. However, with the addition of another reactor in this model, the AR has become less constrained as can be seen from Fig. 3.47. Nevertheless, the constraints are not completely relaxed and the AR is still non-convex.

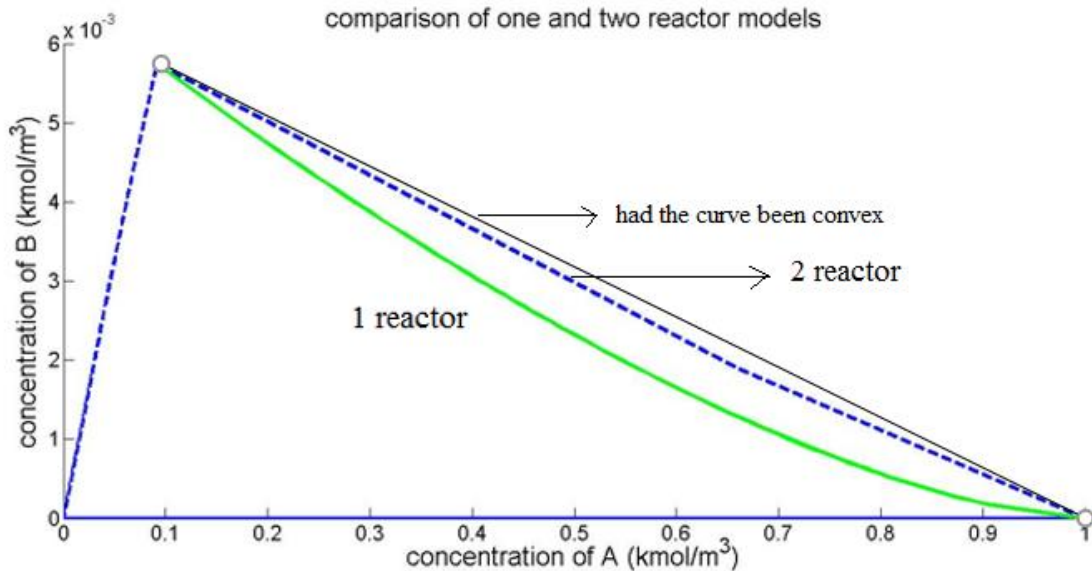


Fig. 3.47. Comparison of the ARs for one and two reactor models under restrictions of feed and volume

Proceeding similarly as in previous cases, we present the arrangements and combinations for three reactor systems. We have four arrangements for three reactor systems as shown in Figs.3.48 - 3.51. Again, we do not show the equations for these models but the same methodology is applied here as well. The four arrangements are followed by the ARs for all the combinations of the respective arrangement, as shown in Fig. 3.52 - 3.55.

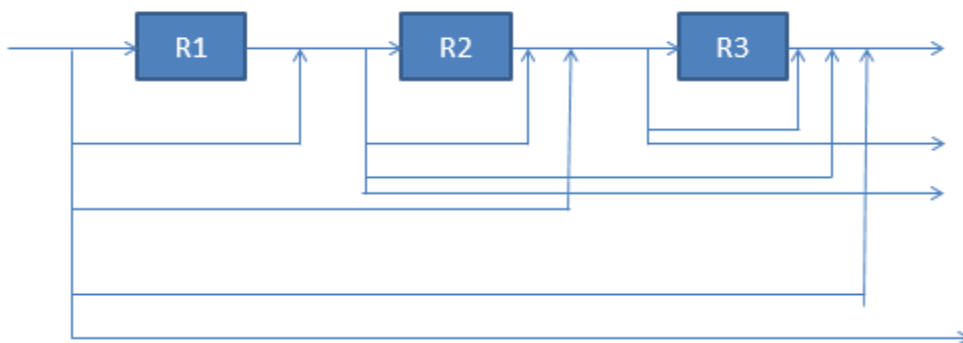


Fig. 3.48. Three reactor model – Arrangement I

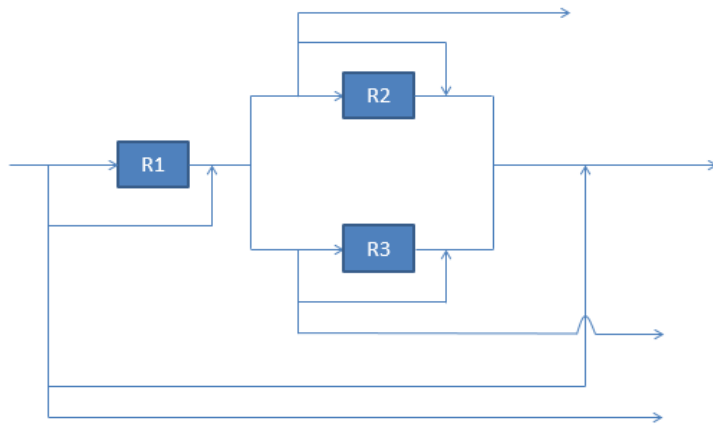


Fig. 3.49. Three reactor model – Arrangement 2

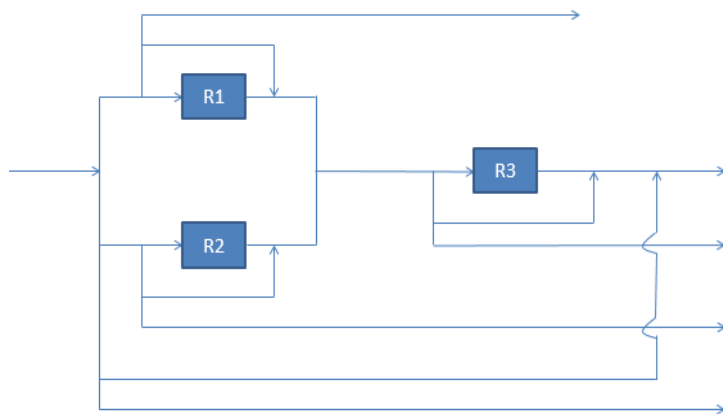


Fig. 3.50. Three reactor model – Arrangement 3

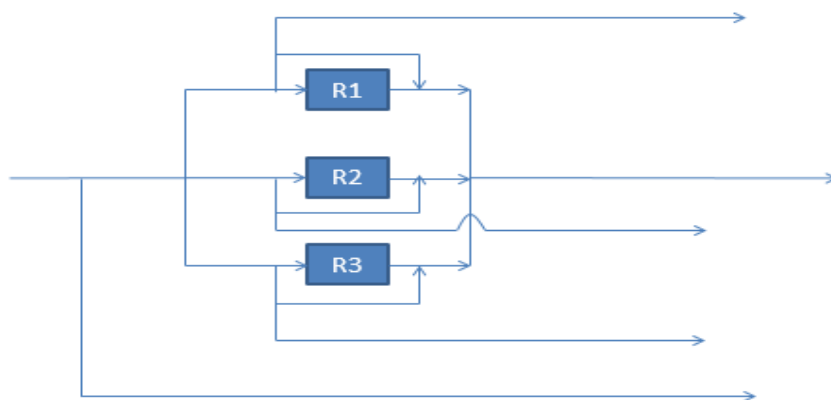


Fig. 3.51. Three reactor model – Arrangement 4

ARs for Arrangement 1:

Combinations for  $\{R_1, R_2\}$  are:

$\{P,P,P\}, \{P,P,C\}, \{P,C,P\}, \{P,C,C\}, \{C,P,P\}, \{C,P,C\}, \{C,C,P\}, \{C,C,C\}$

where P denotes PFR and C denotes CSTR.

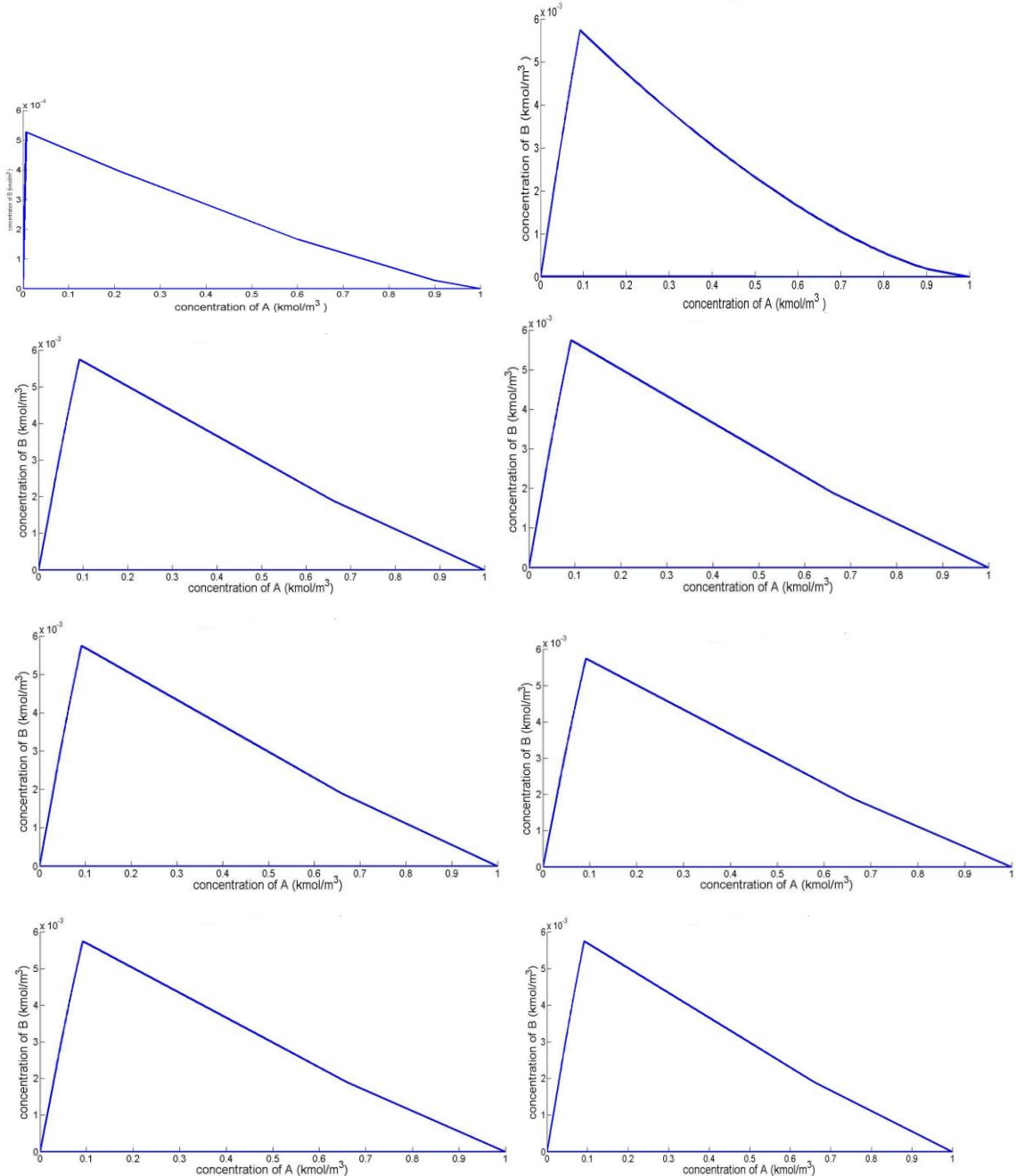


Fig. 3.52. ARs for all combinations of  $R_1$  and  $R_2$  in Arrangement 1 of three reactor model

ARs for Arrangement 2:

Combinations for  $\{R_1, R_2\}$  are: {P,P,P}, {P,P,C}, {P,C,C}, {C,P,P}, {C,P,C}, {C,C,C}

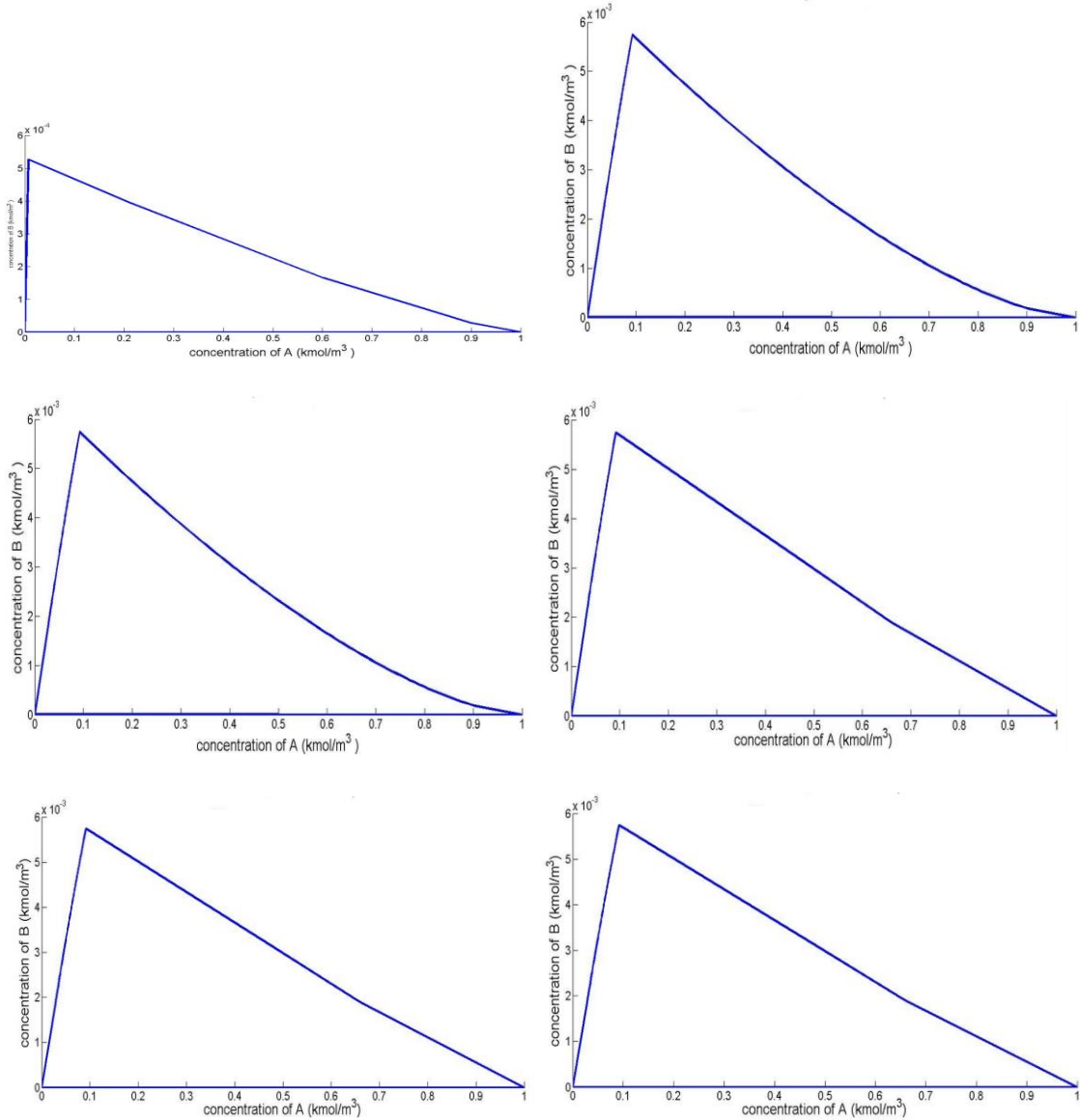


Fig. 3.53. ARs for all combinations of  $R_1$  and  $R_2$  in Arrangement 2 of three reactor model

ARs for Arrangement 3:

Combinations: {P,P,P}, {P,P,C}, {P,C,C}, {C,P,P}, {C,C,P}, {C,C,C}

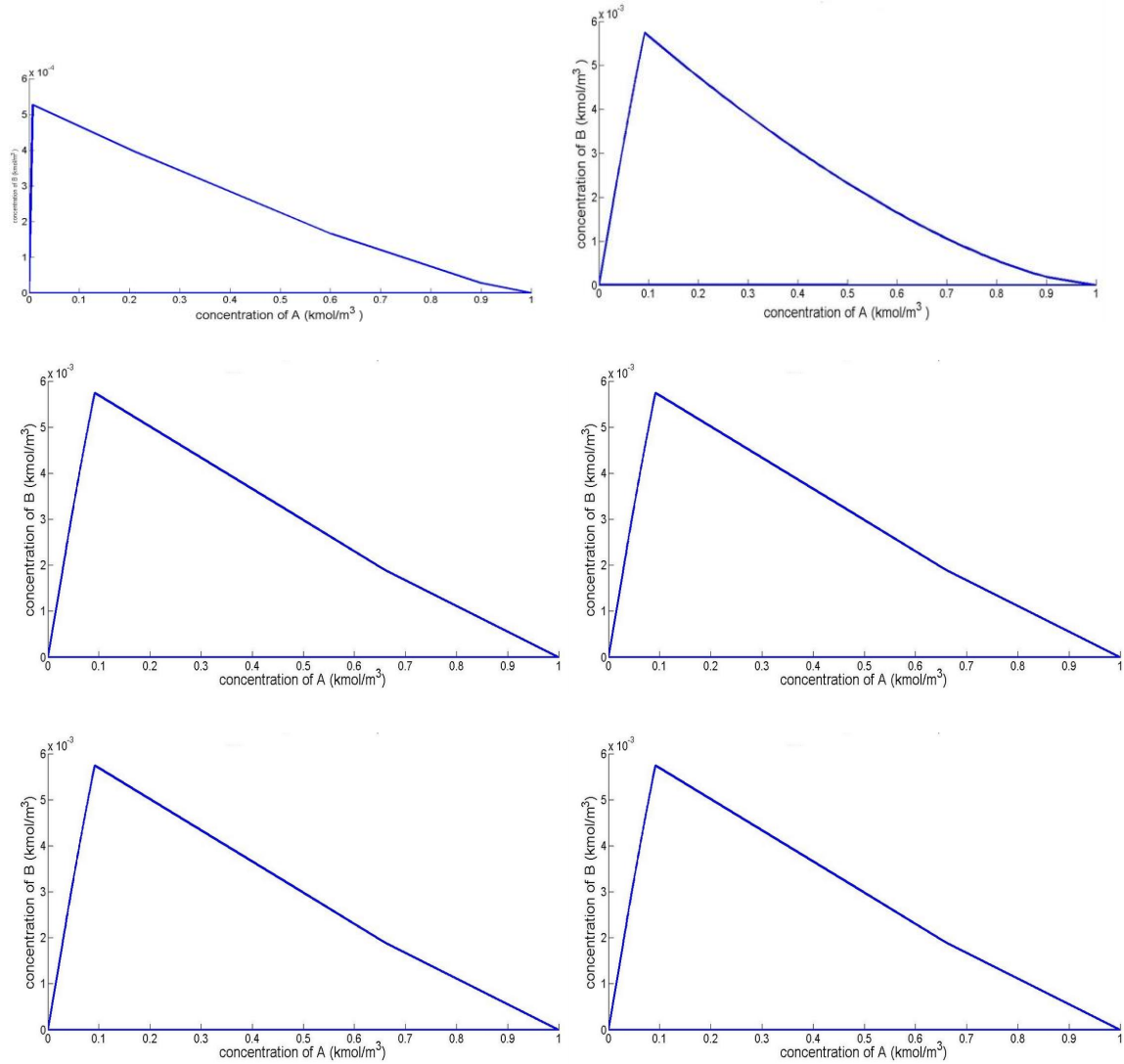


Fig. 3.54. ARs for all combinations of  $R_1$  and  $R_2$  in Arrangement 3 of three reactor model

ARs for Arrangement 4:

Combinations: {PFR,PFR,PFR}, {PFR,PFR,CSTR}, {PFR,CSTR,CSTR}, {CSTR,CSTR,CSTR}

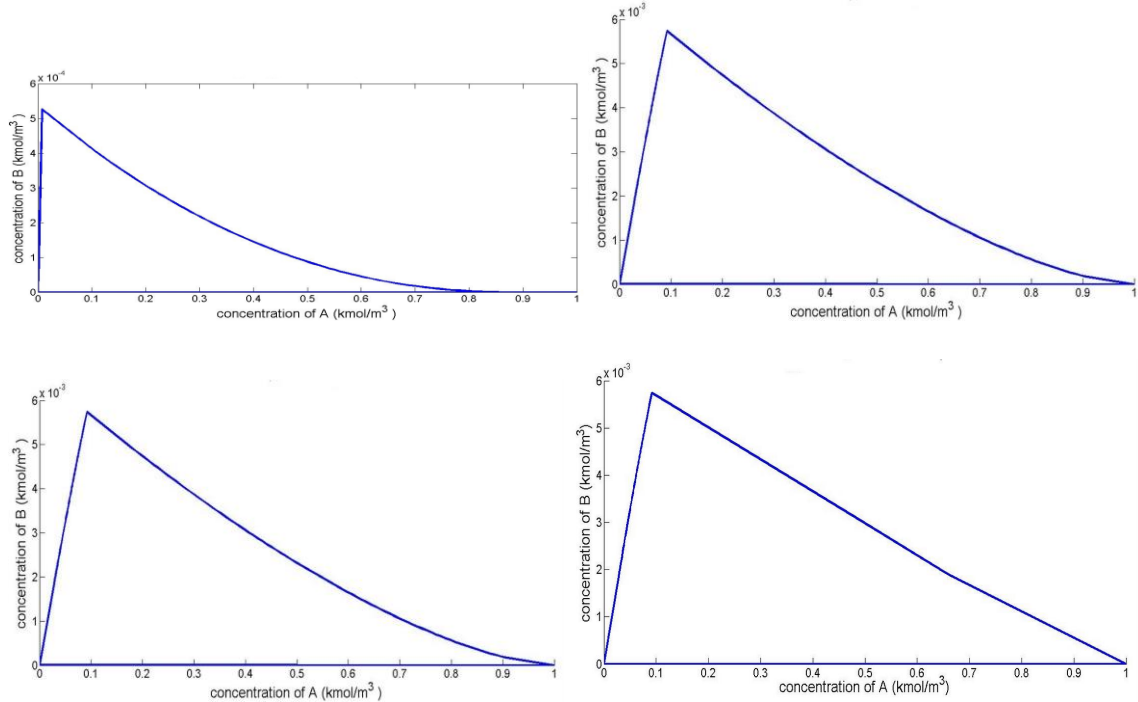


Fig. 3.55. ARs for all combinations of  $R_1$  and  $R_2$  in Arrangement 4 of three reactor model

Proceeding as we did for two reactor model, we plot the final AR which is the union of all points from all the cases.

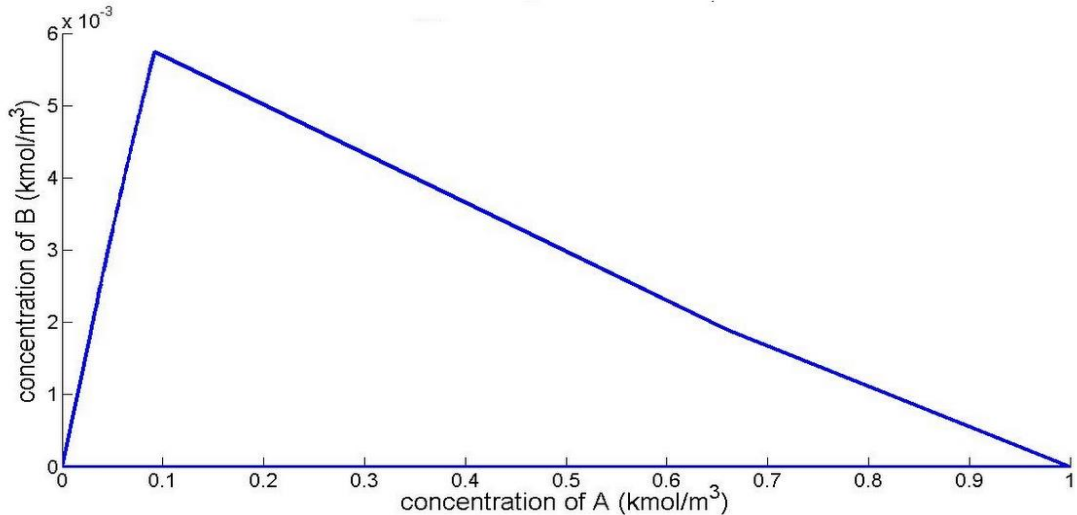


Fig. 3.56. Final AR for three reactor model under feed and volume constraints for VdV reaction scheme

We find that this plot is exactly the same as the final AR for two reactor model. Thus, the addition of the third reactor has not extended the AR further. The reason that two reactor systems extended the AR region when compared to one reactor system was that the first argument of convexity failed in one reactor systems but worked in two reactor systems. This argument being, two reactors can operate in parallel and have their outputs mixed and thus, we can attain all the concentrations corresponding to all the points lying on the line segment joining the points corresponding to these outputs. Now when we compare two and three reactor systems, there is no further relaxation in the constraints and thus, no further extension of the AR. One must however note that extension of AR by incorporating the second reactor but no extension of the AR by incorporating a third reactor is only a result of the example presented. This may not apply to each and every case.

The same methodology applies to any reaction scheme and its kinetics that we wish to investigate. Also, it is flexible enough to incorporate any values of the maximum feed availability and the volume of reactor(s).

In this chapter, we looked at the step by step construction of the AR using the rate vector method. These steps included constructing reaction lines, mixing lines and convexification. There is no instance where the working of the tool is specific to any single reaction scheme or kinetics and is thus generic in nature. We confirmed the generic nature and the accuracy of our results of the AR plots for Van de Vusse, Trambouze and Denbigh reaction schemes by comparing our results against the ones in literature. Though not shown in the study, the tool works for all other reaction schemes and the associated kinetics (order and rate constants of reactions) that are thrown by the user and gives correct results. We showed that the tool is flexible enough to plot the AR in any two dimensions that one wishes for. Also, the tool works correctly for any feed composition that is being fed. Lastly, we saw the construction of AR under restrictions of feed availability and reactor volume for the Van de Vusse reaction scheme. We looked at the construction of such ARs for one, two and three reactor systems. We found that the two reactor model extended the area under the AR as compared to the one reactor model for this reaction scheme and its associated kinetics. Again, the methodology is flexible enough so as to produce results for any reaction scheme and kinetics defined by the user. Thus, we have presented methodologies for the construction of ARs for any reaction scheme, kinetics, feed composition and constraints of feed availability and reactor size. We are now in a position to derive the reactor network design using the AR, as we will see in Chapter 4. This is one of the most important reasons why ARs are studied.

## CHAPTER 4

# OPTIMAL REACTOR NETWORK DESIGN USING ATTAINABLE REGION

We have so far developed an algorithm for construction of the Attainable Region and validated its generality by plotting it for various reaction schemes and comparing it against previous works. We also saw that the algorithm works for any feed composition. We thus have an AR generator now which can give us the correct AR in any two dimensions for any user given reaction scheme and kinetics and the feed condition. We now extend the concept of AR to solve real life problems. In the next section, we find whether a given concentration can be obtained at the output and if yes, we present a way to devise the strategy to attain that point in the section after it. The reactor network(s) obtained are then worked for optimality. In the subsequent section, we look at optimization of a user-defined objective function with the domain being the AR and locate the point that gives us this optimized objective function. We then look at how to attain this point.

### **4.1. To know whether the required point can be attained or not?**

Suppose we are given a reaction scheme and its kinetics. Also, suppose that we are given a concentration that is required to be achieved at the output. We need to find whether the point corresponding to this required concentration is attainable, i.e. whether it lies inside/on the AR, and if it does, what is the best strategy to attain it.

Say, we have a user-defined point that needs to be checked for whether it lies inside or on or outside the AR. Suppose there are four species ( $A, B, C, D$ ) involved in the reaction scheme given. Now, suppose the point is  $\bar{p}$  and its coordinates are defined as  $[p_1 \ p_2 \ p_3 \ p_4]$ . As we recall, the AR that we plotted was in two dimensions. So, we first plot the 2-D projection in  $[C_A \ C_B]$  concentration space. Now, we check whether  $[p_1 \ p_2]$  lies inside or on the AR in this space. For this, we make use of the *inpolygon* command in *MATLAB*, which tells us the whether the point lies inside or on the boundary or outside the region. The input arguments of this function are the coordinates of the

point, and the data points of the curve that we want to check against. The output arguments of the function are *in* and *on* in the form [*in*, *on*]. If the point lies inside the boundary of the region, *in* returns 1 while *on* returns 0. If the point lies on the boundary of the region, both *in* and *on* return 1. If the point lies outside the region, both *in* and *on* return 0. Thus, if the output argument is [1,0] or [1,1], we can say that the point is attainable with respect to the concentration space  $[C_A \ C_B]$ .

We repeat the procedure for the other five combinations of point coordinates, namely, [*p1 p3*], [*p1 p4*], [*p2 p3*], [*p2 p4*] and [*p3 p4*] and check where they lie with respect to  $[C_A \ C_C]$ ,  $[C_A \ C_D]$ ,  $[C_B \ C_C]$ ,  $[C_B \ C_D]$  and  $[C_C \ C_D]$  concentration spaces respectively. If the coordinates lie inside or on the region for all the six concentration spaces, i.e., if the *inpolygon* function returns [1,1] or [1,0] for all the six cases, then we conclude that the point can be attainable. Even if one of the cases do not satisfy this condition, then the point does not lie inside/on the AR region.

If the user is not interested in the concentrations of all the species, then we need not look into all the dimensions of the AR. For example, the user just wants the certain concentrations of two species,  $C_A$  and  $C_B$ . In such a case, we need to apply the *inpolygon* command to only the concentration space  $[C_A \ C_B]$ . If the *inpolygon* function returns [1,1] or [1,0], then we say the required point is attainable.

Similarly, if the user just wants that the concentration of one species, say  $B$ , to be some defined value,  $C_{B,required}$ , then we can just look at any 2D space containing  $C_B$ , say the  $[C_A \ C_B]$  space and look whether there is any point on the line  $y = C_{B,required}$  that lies inside/on the AR in  $[C_A \ C_B]$  space.

If the point does not lie inside/on the AR, then it cannot be attained by any possible reactor network and thus there is no point in looking at the strategy to attain it. However, once we know that the point lies inside/on the attainable region, we then move on to find the strategy to attain it.

The strategy to obtain the reactor network design for such a point is presented in the next section. This is followed by looking at alternate strategies and formulating the cost optimization functions to arrive at the optimal design.

## 4.2. Reactor Network Design to attain the desired point

We recall that while constructing AR, we had stored all the points for both normal trajectories, and their respective convexified regions, for all the stages. Also, we had stored the points for the boundary of the final AR. So, looking at the AR, it is a collection of the stored data points, connected by straight lines so that the obtained region is convex. In this section, we look at the various regions in which the required point may lie, and present the methods to achieve such points.

A required point is said to belong to a particular stage if:

- i) the point lies on one of the normal trajectories.
- ii) the point lies on one of the convexified regions.
- iii) the point lies inside one of the normal regions.
- iv) the point lies between one of the normal trajectories and its convexified region.

Thus, if any of the four cases is true for a particular stage, the point is said to belong to that stage and thus, the point can be attained using regions from that stage. We illustrate the four possible cases now.

Illustration 4.2.1 (a): The required point lies on the normal trajectory.

Let us take an example where the required point is  $(0.4576, 0.0070, 0.005, 0.5349)$ . The point lies on the normal PFR trajectory obtained from Stage 1. As discussed earlier, the *inpolygon* command allows us to know whether the point inside or on or outside a region. We use the *inpolygon* function to confirm whether the point lies on the normal Stage 1 PFR trajectory. The output argument, [in, on] is obtained as [1,1] and we can thus confirm that the point lies on the boundary of the normal PFR trajectory, as shown in Fig. 4.1, where the required point is in red.

So now, we compare our required point with the matrix  $X_1$ , by running a *for* loop. As we recall,  $X_1$  is the matrix containing the data points lying on the normal PFR trajectory. Now, if there is a match, we note the feed point (which is  $[1 \ 0 \ 0 \ 0]$  in this case) and the residence time that was required to achieve this point. We had used the *ode15s* solver to compute the concentration at the exit of the PFR. The output arguments of this command are the concentrations and the residence time. So, if there is a match between the required point and the points in the matrix,  $X_1$ , then we find the index

of the match in the matrix, and then find the value stored in that index in the residence time matrix,  $T_1$ . This will be the required residence time.

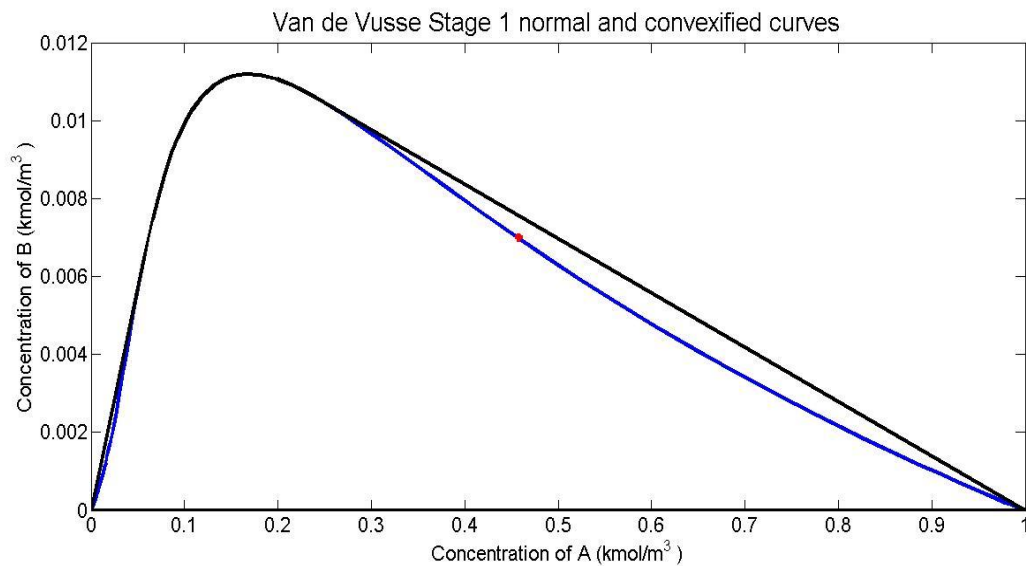


Fig. 4.1. Stage 1 region for VdV reaction scheme showing the point required (red) - Illustration 4.2.1(a)

We know that there is only feed point possible in this case, which is [1 0 0 0]. Now, we run a *for* loop starting from 1 to the size of the  $X_1$  matrix and compare whether the point matches with any of the data points stored in  $X_1$ . We see that the point indeed matches with one of the stored values and the index of the *for* loop where the match occurs is 22. So, we see the value of the 22<sup>nd</sup> cell in the matrix  $T_1$ , which happens to be 0.0117. So, operating a PFR from the available feed [1 0 0 0] for a residence time of 0.0117 s gives us our required point. The reactor network is shown in Fig. 4.2.

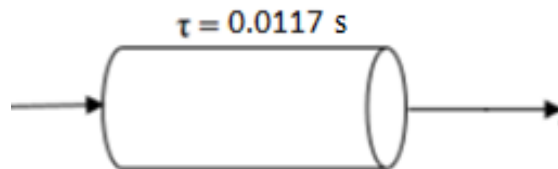


Fig. 4.2. The reactor network to obtain the point desired in Illustration 4.2.1(a)

We consider another situation where the required point lies on the normal trajectory.

Illustration 4.2.1(b): The required point is (0.5403, 0.0057)

As we discussed earlier, the user may be interested in concentrations of only two components. Using the function *inpolygon*, we see that the point lies on the Stage 1 normal PFR trajectory as the output argument is [1,1].

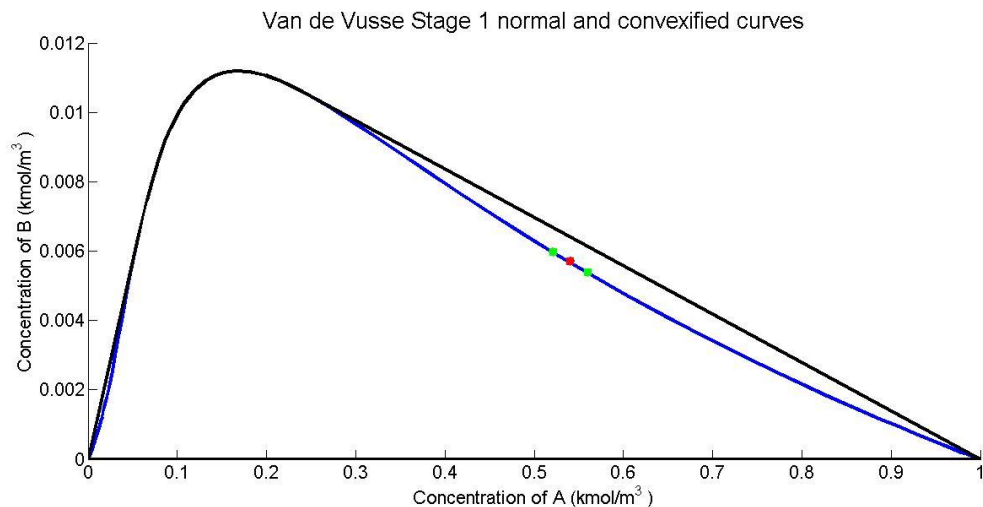


Fig. 4.3. Stage 1 region for VdV reaction scheme showing the point required (red) - Illustration 4.2.1(b)

Now, proceeding similarly as in the previous example, we run a *for* loop starting from 1 to the size of the  $X_1$  matrix and compare whether the point matches with any of the data points stored in  $X_1$ . We find that there is no such match.

Now, if we know that the required point lies on the boundary (using *inpolygon*) but it does not match with the stored points, then it means that the point lies on the straight line joining two certain adjacent points on the boundary. So, we find the two adjacent points between which our required point lies. This is done by running a *for* loop from 1 to the size of the matrix  $X_1$  minus one, and checking the required point against each one in the matrix such that the coordinates of the required point must be between any two adjacent points in the matrix.

Once these two points are found, we find the residence times to attain the two points and thus estimate the residence time required to attain the required point by taking a weighted average. The feed point here is again [1 0 0 0].

We find that the required point lies on the straight line joining the 19<sup>th</sup> [(0.5596, 0.0054)] and 20<sup>th</sup> [(0.5210, 0.0060)] rows in the matrix  $X_1$ . The points are shown in green in Fig. 4.3. The residence

times corresponding to the 19<sup>th</sup> and 20<sup>th</sup> cells are 0.0078 s and 0.0091 s. These are found in the same way as the previous illustration. Now, we see how far the required point is away from the 19<sup>th</sup> point towards the 20<sup>th</sup> point. We see that the required point is at the center of the line segment joining the 19<sup>th</sup> and 20<sup>th</sup> points. Thus, we estimate the residence time required to attain the required point as  $(0.0078 + 0.0091)/2 = 0.00845$  s.

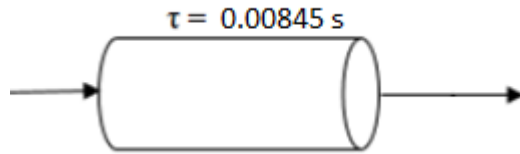


Fig. 4.4. The reactor network to attain the point desired in Illustration 4.2.1(b)

Illustration 4.2.2: The point lies not on the normal trajectory, but its convexified region.

The required concentration of A and B respectively is 0.6999 and 0.0042 kmol/m<sup>3</sup> respectively.

We implement the *inpolygon* command and see that for the Stage 1 normal trajectory, the [in, on] output is [0,0] and for its convexified curve, it is [1,1]. Thus, the point lies outside the normal PFR trajectory and on the convexified region, as can be confirmed from Fig. 4.5.

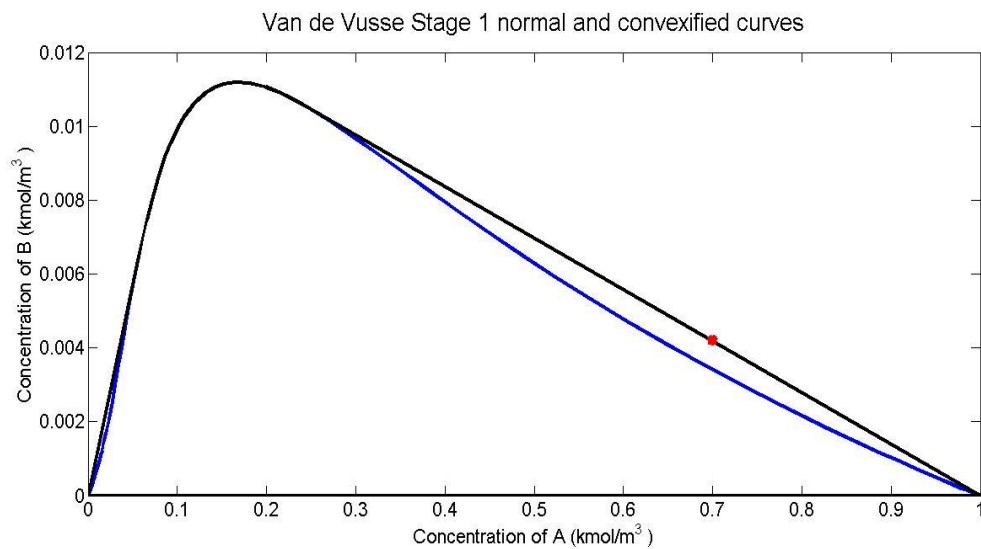


Fig. 4.5. Stage 1 region for VdV reaction scheme showing the point required (red) in Illustration 4.2.2

We now run a *for* loop from 1 to the size of the  $Y_1$  matrix minus 1, and check if the coordinates of the required point lie numerically between those of some point in the matrix and that of its adjacent point.

We find that the required point lies on the straight line joining the points (0.2498,0.0105) and (1,0). Thus, if the concentrations corresponding to these points are mixed in a certain proportion, we can attain the required point. The proportion can be determined by the exact location of the required point, i.e. how far it is from the two points. The mixing rule that was mentioned in Chapter 1 is used to find the numerical value of this proportion.

The second point, as we know is the feed point. So, bypassing the feed to the PFR exit is the network that will allow us to attain the required point. If the second point was not the feed point but some other point on the normal trajectory, we would have to operate two PFRs in parallel such that their outputs are mixed, as was seen in Chapter 1.

The point (0.2498,0.0105) was the 29<sup>th</sup> cell in the matrix  $X_1$ . The corresponding value in the matrix  $T_1$  was 0.0294. So, to attain the required point, we must run a PFR for a residence time of 0.0294 s and bypass the feed. The fraction of feed entering the reactor,  $a$  can be found using the formula:

$$C_{mixedcup} = aC_{PFRexit} + (1 - a)C_{feed} \quad (4.1)$$

where,  $C_{mixedcup}$  is the required concentration,  $C_{PFRexit}$  is the concentration at the exit of the PFR and  $C_{feed}$  is the feed concentration. The value of  $a$  can thus be found.

$$\begin{aligned} (0.6999, 0.0042) &= a * (0.2498, 0.0105) + (1 - a) * (1, 0) \\ (0.6999 - 1, 0.0042 - 0) &= a(0.2498 - 1, 0.0105 - 0) \\ a &= 0.4 \end{aligned}$$

Thus, the value of  $a$  is 0.4. Thus finally, the complete reactor network design to attain this point is to operate a PFR at a residence time of 0.0294 s, such that 40% of the available feed only enters the reactor and the rest of it is bypassed.

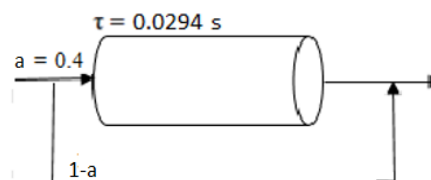


Fig. 4.6. The reactor network required to attain the point desired in Illustration 4.2.2

Illustration 4.2.3: The point lies inside the normal trajectory.

We again use *inpolygon* to check whether the required point lies inside the Stage 1 normal trajectory and not on the boundary. Once this is confirmed, we construct a line segment from the feed point of this stage (which is [1 0 0 0]) towards the required point and extend it to meet the boundary of normal trajectory. To facilitate this in our simulations, we create a function named *intersection* to find the point where the line intersects the boundary of the normal trajectory.

If this point matches with one of the stored points while constructing the AR, then we can find the residence time and the feed point, proceeding similarly as in Illustration 4.2.1(a). If not, we find the two points in the matrix,  $X_1$ , between which the intersection point lies and their respective residence times. The exact residence time can then be estimated, as was seen in Illustration 4.2.1(b).

Now, to achieve the required point, we have to mix the feed point and this intersection point in a certain proportion. This is found using the mixing rule. Thus, in this case, we need to operate a PFR for a certain residence time and mix the output with the bypassed feed in a certain ratio to achieve the required point.

This is illustrated using an example. Suppose we want to achieve point P, as shown in Fig. 4.7. The coordinates of the point P are (0.3,0.006). We use the *inpolygon* command to find whether the point lies within the normal Stage 1 trajectory and find that the [*in*, *on*] output arguments are [1,0]. So, the point lies inside the Stage 1 normal PFR trajectory.

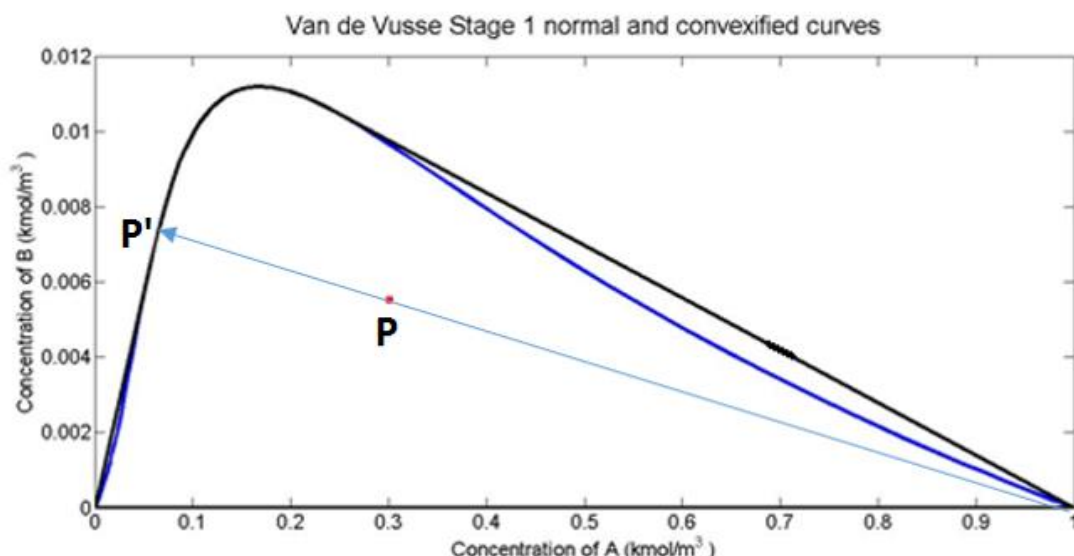


Fig. 4.7. AR plot for VdV Vusse reaction scheme showing the point required (P) in Illustration 4.2.3

Now, we draw a line from the feed point  $(1,0)$  towards the point  $P$  and extend to intersect at the PFR trajectory at  $P'$ , as shown by the cyan colored line. Using the *intersection* function, we find the concentration of the point of intersection of the line and curve,  $P'$ . Proceeding similarly as in the previous examples, we then find the residence time to achieve the intersection point, which is found to be  $0.1258$  s, and the fraction of feed sent to the reactor is found to be  $0.7533$ . We present the complete reactor network as follows:

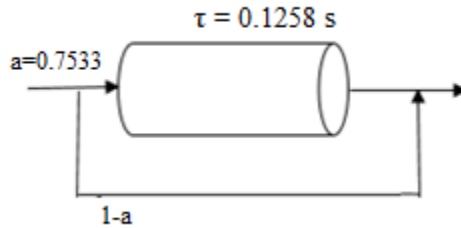


Fig. 4.8. The reactor network required to attain the point desired in Illustration 4.2.3

Illustration 4.2.4: Finally, we look at the case when the point lies between the normal and convexified regions. We use the *inpolygon* command to compare our required point with the normal region and its respective convexified region. If the *[in, on]* outputs are  $[0,0]$  and  $[1,0]$  respectively, then we conclude that the point lies outside the normal trajectory and inside the convexified region and thus lies between the normal and its respective convexified region for that particular stage and feed point. We construct a line joining the feed point and the required point and extrapolate it to intersect the normal trajectory. We find the point of intersection and then estimate the residence time and its feed point and present the reactor configuration. This is illustrated using an example.

The required point is  $(0.6, 0.005)$ , such that this corresponds to the point R in Fig. 4.9, which lies between the normal and its convexified trajectory (between the blue and black trajectories in the figure). We use *inpolygon* and see that the point lies between the Stage 1 normal trajectory and its respective convexified region. We construct a line joining the feed point  $(1,0)$  and the point R and extrapolate it to intersect the normal trajectory. We find the coordinates of the intersection point, and the residence time required to achieve that point similarly as in previous examples. Also, we find that the fraction of the feed needs to be bypassed. The reactor network design is shown in Fig. 4.10.

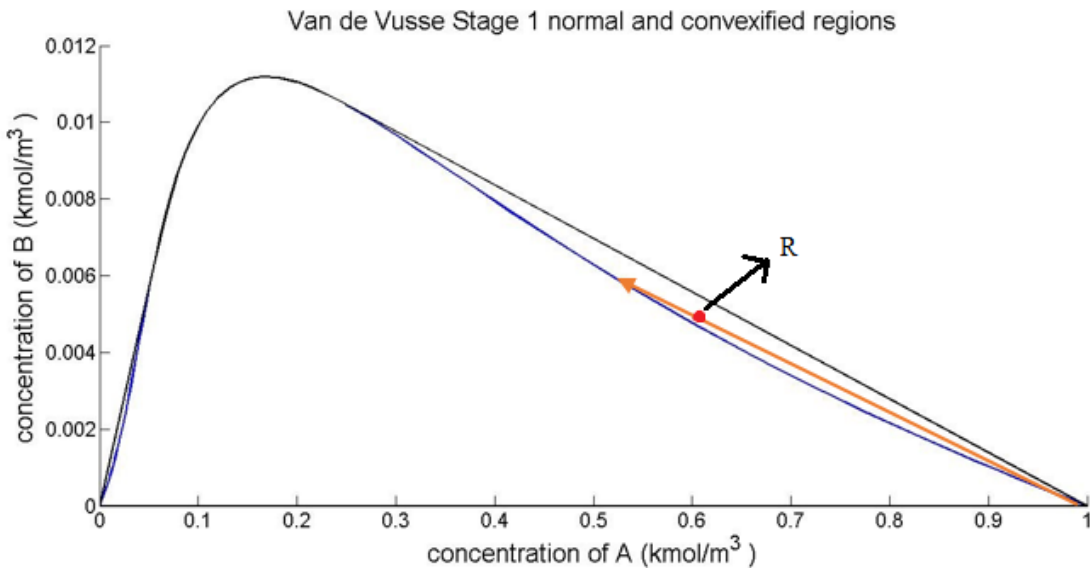


Fig. 4.9. AR plot for VdV Vusse reaction scheme showing the point required (R) in Illustration 4.2.4

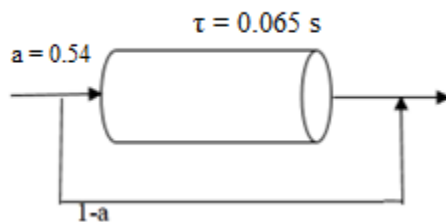


Fig. 4.10. The reactor network required to attain the point desired in Illustration 4.2.4

One must note that if the required point lies between the normal and convexified regions such that the feed point is not included in this concavity, the reactor network changes. For such a point, we locate two points on the normal trajectory such that the required point lies on the line segment joining these two points. When these two points are mixed in a certain ratio, we get the required point. The reactor network for attaining such a point is operating two reactors in parallel such that their outputs are mixed. This will be discussed in detail in Section 4.3.

So far, we have seen the four possible cases pertaining to Stage 1 only. What if the required point does not come into any of these cases for Stage 1? When this happens, we move on to the next stage, and see whether the required point can be classified in any of the four cases pertaining to this stage now. This is repeated. We present another two examples to explain.

Illustration 4.2.5: The required concentration of B is  $0.0122 \text{ kmol/m}^3$ .

The required point is shown in red in Fig. 4.11. Here, the user is worried only about the concentration of B. We start our algorithm by checking whether the required point belongs to Stage 1 curves. The answer is negative. As a result of the Stage 1 calculations, we find some feed points which are capable of extending the AR. We check whether the normal and convexified regions obtained from all such feed points have the required point inside or on them. The answer is again negative for all such regions in Stage 2. We repeat the same with Stage 3 trajectories and find that the required point lies on one of the normal trajectories. We compare the required point with the Stage 3 data point matrix  $X_{3i}$  and find that there is a match.

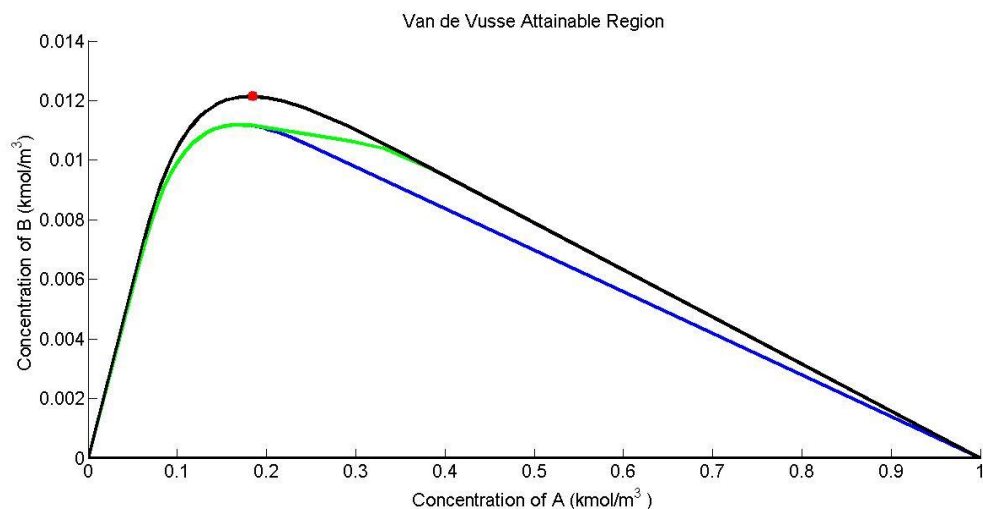


Fig. 4.11. AR plot for Van de Vusse reaction scheme showing the point required (red) in Illustration 4.2.5

We find that the feed to be given to the PFR is  $(0.3871, 0.0097)$  and that the PFR should be operated for a residence time of  $0.0275 \text{ s}$ . But, we only have a feed of  $(1,0)$  available with us. So, we look at how the point  $(0.3871, 0.0097)$  can be attained. We repeat the same procedure and see that this point lies on the normal Stage 2 CSTR trajectory. There is a match while comparing this point with the data point matrix,  $X_{2i}$  and to attain this point, a CSTR must be operated from the available feed point  $(1,0)$  for a residence time of  $0.04 \text{ s}$ .

Thus, the strategy to attain the required point is to first operate a CSTR for a residence time of  $0.04 \text{ s}$ . The output of this CSTR is to be fed to a PFR which is to be operated for a residence time of  $0.0275 \text{ s}$ .

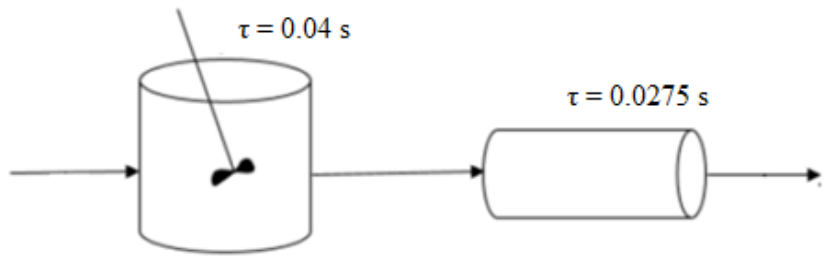


Fig. 4.12. The reactor network required to attain the point desired in Illustration 4.2.5

Illustration 4.2.6: Suppose we want point Q (0.2,0.0115) in Fig. 4.13.

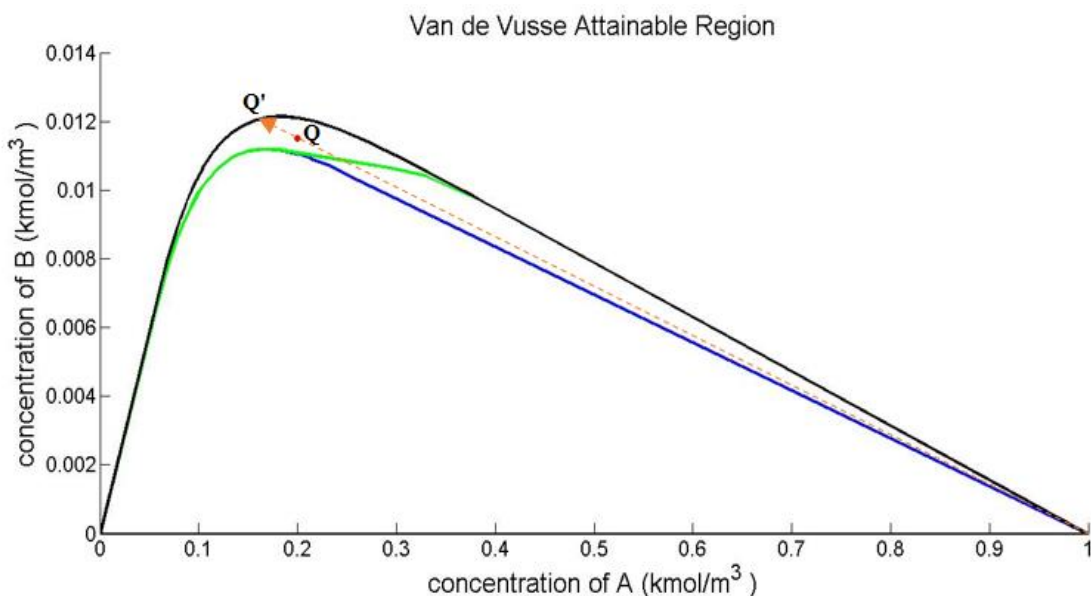


Fig. 4.13. AR plot for Van de Vusse reaction scheme showing the point required (red) in Illustration 4.2.6

We start our algorithm by checking whether the required point belongs to the Stage 1 regions. The answer is negative. As a result of the Stage 1 calculations, we find some feed points which are capable of extending the AR. We check whether the normal and convexified regions drawn from all such feed points has the required point inside or on the them. The answer is again negative for all such regions in Stage 2. We repeat the same with Stage 3 regions and find that the required point lies inside one of the normal trajectories. We find the point on the Stage 3 normal curve at which the line joining the feed point (1,0) and the point Q, when extrapolated, intersects at, and is given by point Q'. To attain Q', we see that a PFR would be required to operate at a residence time of

0.0354 s from the feed (0.3871, 0.0097). But, we only have a feed of (1,0) available with us. So, we look at how the point (0.3871, 0.0097) can be attained. We repeat the same procedure and see that this point lies on one of the normal Stage 2 CSTR trajectory. There is a match while comparing this point with the data point matrix,  $X_{2i}$  and to attain this point a CSTR must be operated from the available feed point (1,0) for a residence time of 0.04 s. The available feed is to be bypassed at the PFR exit. The fraction bypassed comes out to be 0.0468 and that sent to the reactor comes out to be 0.9532.

Thus, the strategy to attain this point is to first have a CSTR for a residence time of 0.04 s. The output of this CSTR is to be sent to a PFR which has to be operated for a residence time of 0.0354 s. The available feed is bypassed to the exit of the PFR. The fraction of feed entering the reactor is 0.9532.

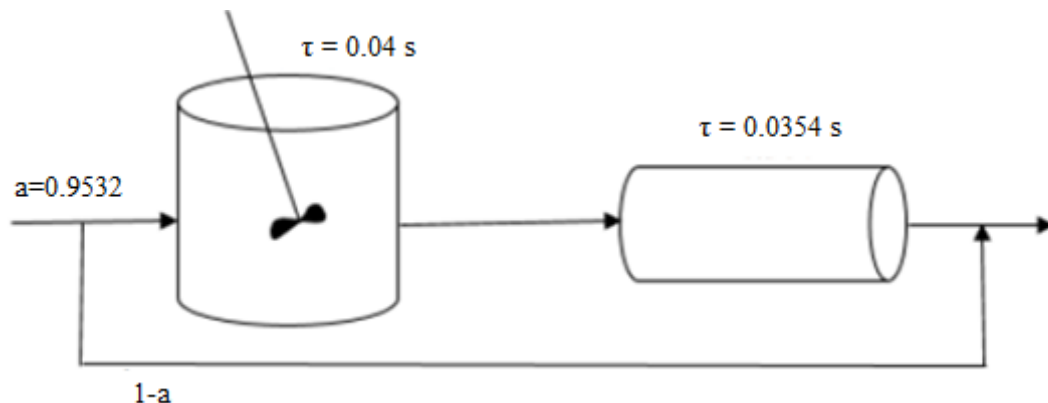


Fig. 4.14. The reactor network required to attain the point desired in Illustration 4.2.6

### 4.3. Optimal Reactor Network

In the previous section, we presented algorithms for the basic four positions where the required point may lie pertaining to a particular stage. However, the reactor networks suggested may not be optimal. As we will see below, the reactor networks suggested in the previous section were one of the many possible network designs possible.

Illustration 4.3.1: Let us revisit Illustration 4.2.1. The point lies on the normal PFR trajectory obtained from Stage 1 and thus, operating a PFR at a residence time which was found to be 0.0117 s allowed us to attain it.

However, this may not be the optimal reactor network. We recall that while constructing the AR, the points in the concave region of Stage 1 were taken as feed points for constructing Stage 2 CSTR trajectories. If one of these feed points is the same as the one used in Stage 1, i.e. [1 0 0 0], then the CSTR trajectory drawn from here can also be of interest. As we see from Fig. 4.15, a line from the available feed to the required point, when extrapolated, meets the CSTR trajectory drawn from the available feed at a certain point. Thus, a CSTR with bypass is also a possible reactor network.

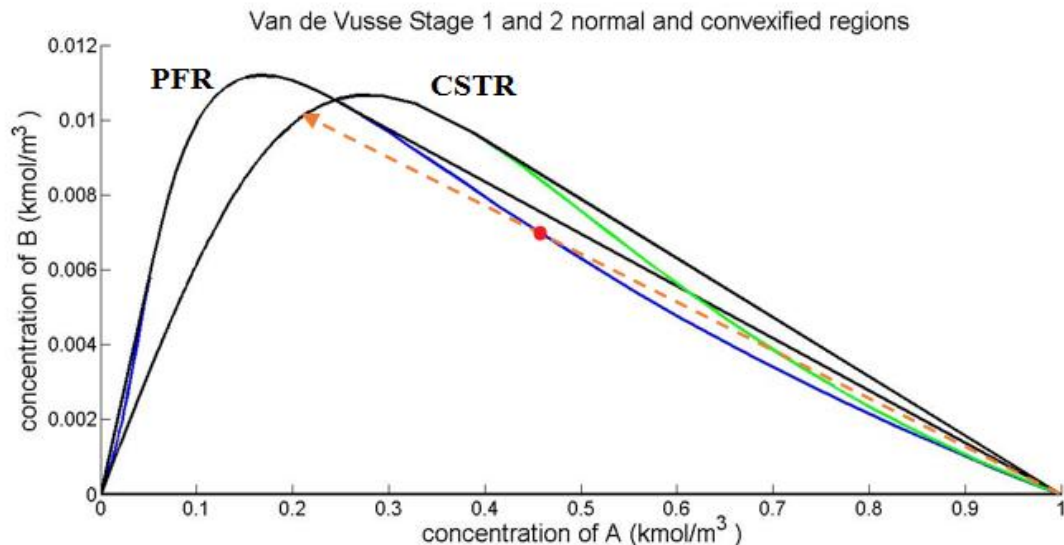


Fig. 4.15. Alternate strategy to attain the required point(red) – Illustration 4.3.1

So now, we use the *inpolygon* command to confirm whether the required point lies inside the normal CSTR region from the available feed point, and find that the [*in*, *on*] output arguments are [1,0]. We draw a line (dashed orange) from the available feed point [1 0 0 0] towards the required point and extend it to intersect at the CSTR trajectory, as shown in Fig. 4.15. Using the *intersection* function, we find the coordinates of the point of intersection of the line and curve. To attain this point, we have to operate a CSTR at a residence time of 0.1684 s. The fraction of feed sent to the reactor is found to be 0.69 using the mixing rule, as mentioned in Illustration 4.2.2. Thus, the alternate reactor network is as shown below:

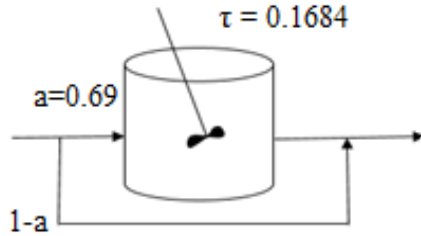


Fig. 4.16. Alternate reactor network to attain the example discussed in Illustration 4.2.1

One must note that CSTR trajectories originating from points other than the feed point used in Stage 1 ([1 0 0 0]) are not of interest, because to achieve a feed point other than this point, we would be required to operate the PFR for a certain residence time first. Thus, for attaining the required point, we would have to employ a PFR followed by a bypassed CSTR. In such a case, we see that two reactors are required. We abide by the thumb rule which states that, lesser the number of reactors in the network, more optimal is the design. Thus, all such designs requiring two reactors are discarded.

This can be generalized for any stage: If the required point belongs to Stage  $i$  i.e., it adheres to any one of the four attainable cases (mentioned in Section 4.2) for that stage, we find the feed point of the regions constructed that allowed us to attain the point. Now, we must check whether the point belongs to Stage  $i+1$  regions originating from the same feed point. If it does, then we have another possible solution in the  $i+1^{th}$  stage. However, any region originating from other feed points must strictly not be considered.

Further, we can draw any line segment connecting any points on the normal CSTR trajectory except the available feed, such that it passes through the required point. This is also a way to attain the required point. The physical significance is that we are operating two CSTRs in parallel and mixing their outputs. This is yet another possible configuration. In fact, there are many such line segments that we can draw passing through the required point and thus, there are many designs for this configuration, the difference between these being the residence times at which these reactors are operated and the mixing fraction. But, we see that here, we require two reactors instead of one. In such a case, we abide by the thumb rule that that lesser the number of reactors, better the design. Thus, this configuration is discarded.

Thus, we have two possibilities for the reactor network design, as are shown in Fig. 4.17.

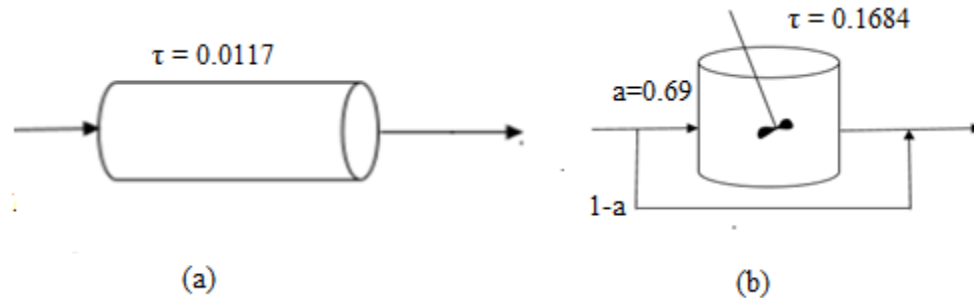


Fig. 4.17. Possible reactor networks to attain the point (0.4576,0.0070) in the VdV reaction scheme

The network incurring the lesser costs can be said to be the optimal one. Reactor costs include both the capital cost as well as the operating cost. The capital cost is a function of the reactor type and volume and the operating costs depend on the flow rate. Thus, these costs depend upon the type of reactor and the residence time for which that reactor is to be operated. It can be written as:

$$\beta_R = \beta_R(\text{reactor type}, \tau) \quad (4.2)$$

where  $\beta_R$  denotes the cost associated with the reactor. As can be seen, it depends on the reactor type, i.e. whether it is CSTR or PFR, and the residence time,  $\tau$  at which it is operated.

In the second configuration, there is an additional cost of mixing associated with bypassing the feed,  $\beta_M$ .

Thus, the cost associated with the first network, which was, operating a PFR can be written as

$$\beta_1 = \beta_R(\text{PFR}, 0.0117) \quad (4.3)$$

Similarly, the cost associated with the second network, which was to operate a CSTR with bypass is

$$\beta_2 = \beta_R(\text{CSTR}, 0.1684) + \beta_M \quad (4.4)$$

The cost functions associated with mixing and reactor operations are to be fed by the user. The design having the minimum cost out of the two can be said to be the optimal reactor network.

**Illustration 4.3.2:** Similarly, we revisit Illustration 4.2.2. The required point P (in Fig. 4.18) lies on the convexified PFR trajectory and thus, operating a PFR with bypass is a possible reactor network as seen in Illustration 4.2.2. Now, we look whether this required point lies inside/on the normal

trajectory from the available feed or its convexified region or between the two regions, in Stage 2. We find that it lies between the normal CSTR trajectory from the available feed point and its convexified region. We draw a line segment from the feed point through P, and it traverses along the convexified curve of the PFR. It intersects the CSTR trajectory at point P' (0.6115,0.0054). To attain the point P', we need to employ a CSTR for a residence time of 0.0102 s and the fraction of feed sent to the CSTR is 0.77.

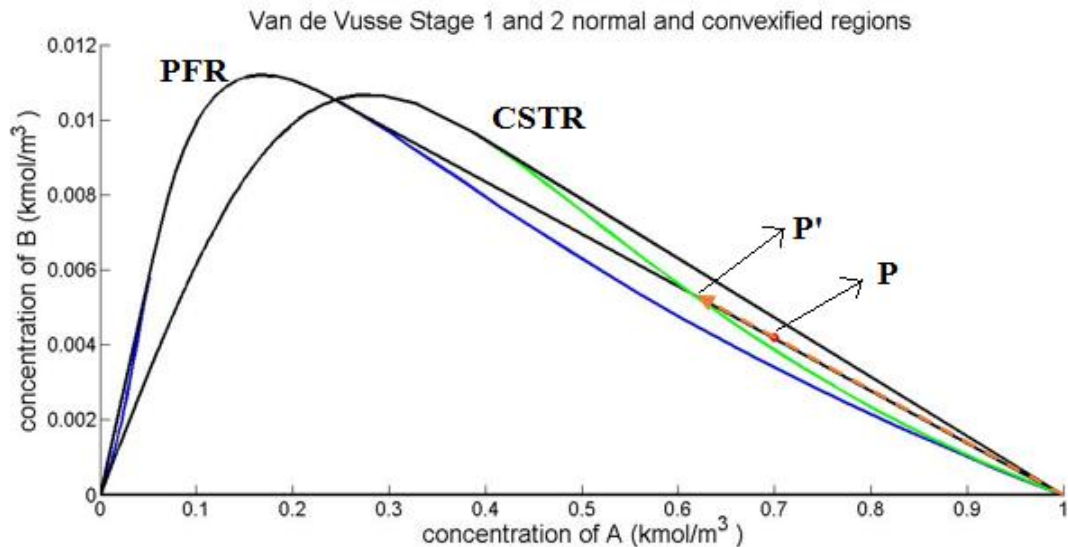


Fig. 4.18. Alternate strategy to attain the required point(red) – Illustration 4.3.2

Thus, operating a CSTR with bypass is a possible configuration. The network design is given as follows:

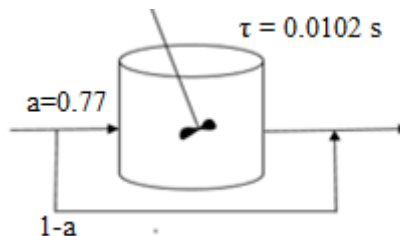


Fig. 4.19. Alternate reactor network to attain the example discussed in Illustration 4.2.2

Thus, the possible designs are:

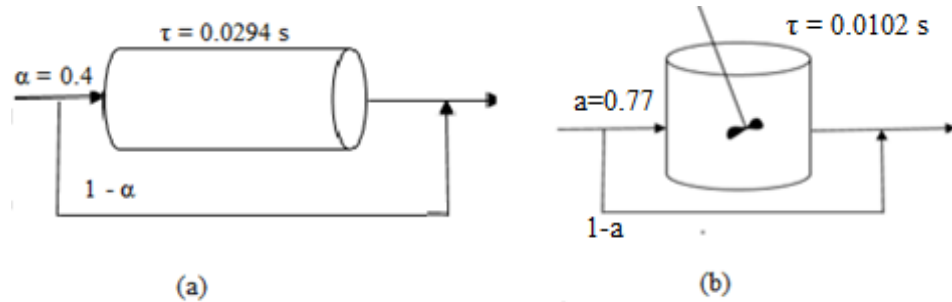


Fig. 4.20. Possible reactor networks to attain the point (0.6999,0.0042) in the VdV reaction scheme

The costs incurred in the two designs are

$$\beta_1 = \beta_R(PFR, 0.0294) + \beta_M \quad (4.5)$$

$$\beta_2 = \beta_R(CSTR, 0.0102) + \beta_M \quad (4.6)$$

The optimal reactor network is given by the one which gives the minimum cost and the cost associated with that design is given by

$$\min(\beta_1, \beta_2) \quad (4.7)$$

One must note that if the point lies on a convexified region not including the feed, the configuration to attain it would be the operation of two PFRs in parallel. Thus, we require two reactors here.

In such a case, we check if the point also lies

- i) on or inside the normal CSTR trajectory from the available feed point, or
- ii) between this normal trajectory and its convexified region, or
- iii) on its convexified region such that this convexified region includes the available feed point.

In these cases, only one reactor (CSTR) is required (with or without bypass). Thus, we discard the former case since it required two reactors.

This can off course be generalized on a stage by stage basis.

Similar analysis can be done for the required points in Illustration 4.2.3 and 4.2.4.

Illustration 4.3.3:

Now, we look at a situation when the required point does not belong to Stage 1 and lies on the normal Stage 2 trajectory. Operating a CSTR is a possible solution that comes to mind. The design can be found by working on the lines of Illustration 4.2.1, but for Stage 2. Now, for further possibilities, we have a look at Stage 3 regions originating from the same feed point that was used to construct the Stage 2 normal trajectory on which the required point lies.

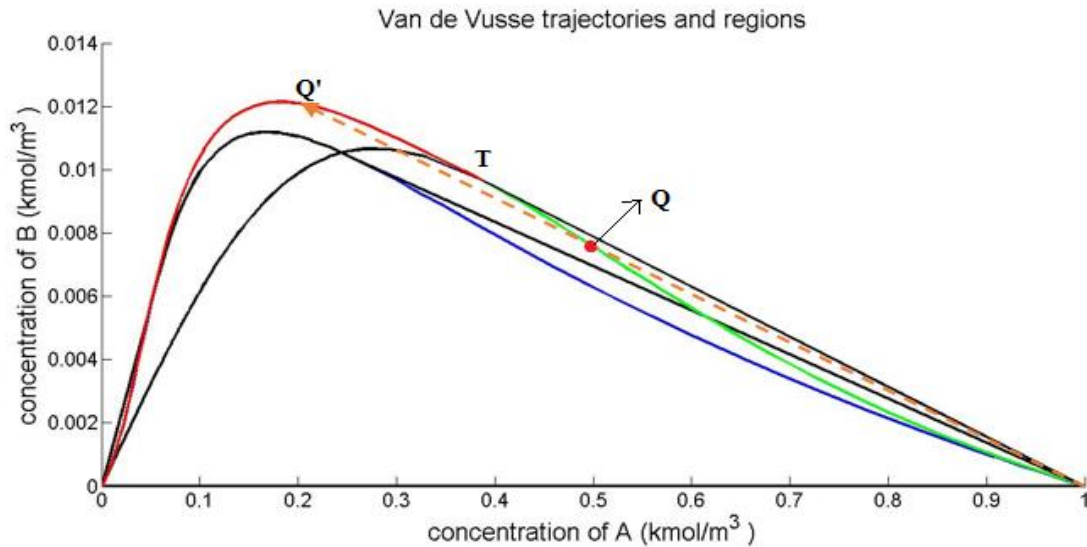


Fig. 4.21. Strategies to attain point Q – Illustration 4.3.3

We require the point Q, whose coordinates are (0.4969, 0.0076) as shown in Fig. 4.21. We check for Stage 1 and find that the point that does not come under any of the four categories mentioned at the beginning of Section 4.2. Thus, the point lies outside the Stage 1 regions. We move our attention to Stage 2 and find that the point lies on the normal CSTR trajectory originating from the available feed, which is ([1 0 0 0]). Thus, to attain the required point, we need to operate a CSTR. The residence time can be found using methods mentioned in the previous section and it comes out to be 0.02 s. Thus, the reactor network design required is:

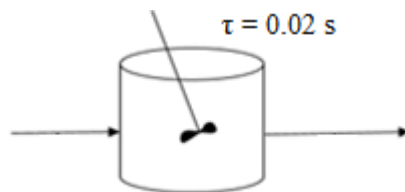
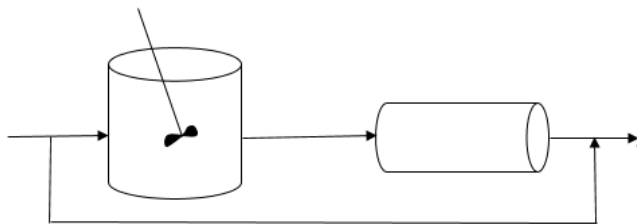


Fig. 4.22. Reactor network design to attain point Q in Illustration 4.3.3.

The required point adheres to one of the four cases for Stage 2 regions originating from the available feed point. Thus, we look whether there is any region in Stage 3 which originates from this same feed point and if it does, we look at which of the four cases the required point adheres to. We find that for this feed point, there is no Stage 3 region. Thus, we must stop and the design presented in Fig. 4.22 is optimal.

However, one may get tempted to draw a line from the feed point to Q and extrapolate it to meet the Stage 3 trajectory at Q'. In such a case, to attain Q', we need to attain point T first, and with this point as the feed, operate a PFR for a certain residence time. To attain point T, we require to operate a CSTR. Thus, the reactor network is shown in Fig. 4.23. Clearly, this is not an optimal network since it involves two reactors (and we already have a network having one reactor only).



*Fig. 4.23. Non-optimal reactor network to attain the point in Illustration 4.3.3*

Now, we look at another problem where the concept of cost reduction, or for that matter, the concept of finding the optimal reactor network design out of multiple possibilities comes into picture.

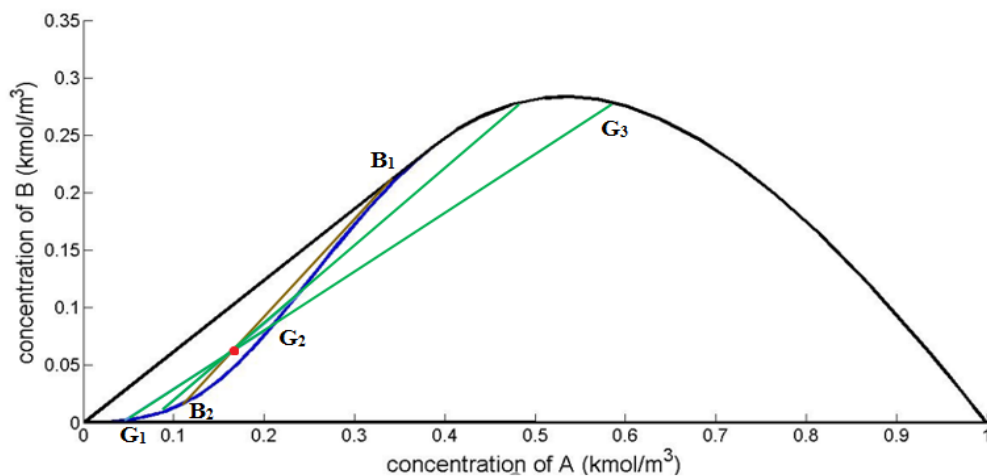
The required point lies in between the normal and convexified regions. We tend to look at a point lying between the bottom left concave region and its convexified region in the Van de Vusse AR. But since the concavity in that region is very small, it is difficult to work in the tight spaces there. Thus, we take another reaction scheme to understand this case. We have to note that changing the reaction scheme does not alter the concept behind finding how to attain such kind of points.

Illustration 4.3.4: We take the reaction scheme discussed earlier in Chapter 1, which is as follows:



The reactions are elementary and the rate constants of the two reactions are  $1 \text{ m}^3/\text{kmol/s}$  and  $1 \text{ s}^{-1}$ . The feed is pure A with its concentration being  $1 \text{ kmol/m}^3$ . The normal and convexified PFR

regions (Stage 1) are shown in Fig. 4.24. The red point is the required point, its coordinates being (0.16,0.06).



*Fig. 4.24. Stage 1 normal and convexified curves for the reaction scheme 2A->B->C showing the required point (red) and the multiple strategies that can be used to attain it (Illustration 4.3.4)*

It is easy to see that the point can be attained by mixing the points at the end of the brown line,  $B_1B_2$ . As can be seen,  $B_1$  is the point where the concavity in the normal trajectory begins and it lies on the normal trajectory and thus can be attained by operating a PFR at a certain residence time. Now, we construct a line segment from  $B_1$  passing through the required point and intersecting the curve at  $B_2$ . Again,  $B_2$  lies on the normal PFR trajectory and thus can be attained by employing another PFR for a certain residence time. Now, if we operate these two PFRs in parallel such that their outputs are mixed are in a certain proportion, we can attain our required point. The residence times required to attain the points  $B_1$  and  $B_2$ , are found to be 1.5726 s and 8.8092 s respectively. The fraction of output from the first PFR while mixing the two streams is found to be 0.2026.

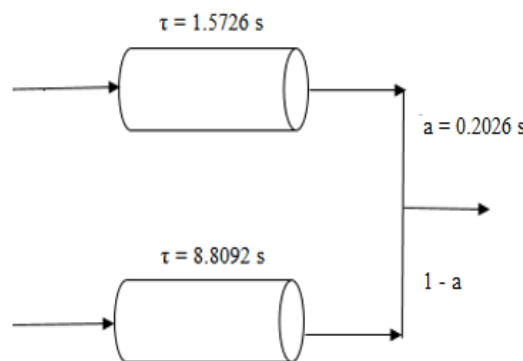


*Fig. 4.25. One possible reactor network design required to attain the point desired in Illustration 4.3.4*

We now see that the reactor network presented in Fig. 4.25 may not be the only possible reactor network. There are further possibilities, as shown by the green lines. We consider the line segment  $G_1G_2$ , which shows that the points  $G_1$  and  $G_2$ , which lie on the normal PFR trajectory can be mixed to obtain the required point. Similarly, concentrations corresponding to points  $G_1$  and  $G_3$  can be mixed to attain the required concentration.

Thus, we see that we can attain such a point if we can construct a line segment between any two points lying on the normal trajectory such that the line segment passes through the required point. Further, the pair of points need not be specific to the pair. For example,  $(G_1, G_2)$  and  $(G_1, G_3)$  are two pairs of points which can be used to attain the required point and the point  $G_1$  is common to both. Thus, it is possible that even one point such as  $G_1$  can be mixed with two different points to get the required point. Of course, the proportion in which they are mixed will differ.

The structure of the reactor network remains the same in all cases. It comprises of two PFRs in parallel such that their outputs are mixed. What is different between these multiple possibilities is the residence times of the two PFRs and the proportion in which the two outputs are mixed. Thus, to find an optimal solution, we have to obtain the network that minimizes the costs involved. The costs involved are the capital and operating costs of the PFRs at their respective residence times, and the cost of mixing.

Thus, to find the optimal reactor network for such a case, we find all points on the normal PFR trajectory from which line segments can be drawn to pass through the required point such that when these are extrapolated, they intersect the trajectory again. These points at which the line segments intersect are found using the *intersection* function stated earlier. If there is no possible intersection, the function gives empty value indicating that the line segment, when extrapolated does not intersect the trajectory again. Now, once all such pairs of points are determined, we make use of the  $X_1$  and  $T_1$  matrices to find the residence times, as was explained in Illustration 4.2.1. Further, the proportion in which they are mixed is found out using the mixing rule. Now, we ask the user to enter the expression for cost associated with the reactor, which would be a function of the type of reactor and its residence time and also the expression for the mixing cost. The minimum of the summation of the operating and mixing costs is then found and we have our optimal reactor network. The minimization function is formulated as follows:

$$\min \beta_i = \beta_R(PFR_1, \tau_{i1}) + \beta_R(PFR_2, \tau_{i2}) + \beta_M \quad (4.8)$$

$$i = 1, 2, 3, \dots, n \quad (4.9)$$

where  $i$  denotes all the points on the normal trajectory from which the line segments drawn to pass through the required point, are capable of intersecting at another point on the trajectory when extrapolated.

So, having known how to obtain the reactor network(s) to attain each point on and inside the AR, we look at how the whole boundary of the AR for the Van de Vusse reaction scheme can be traversed. To do this, we take each point on the boundary of the AR and one by one, look at the reactor network(s) needed to attain each of the points with the help of the same procedure we have discussed. Fig. 4.26 shows the coupled diagram of the Attainable Region and the reactor network required to achieve it.

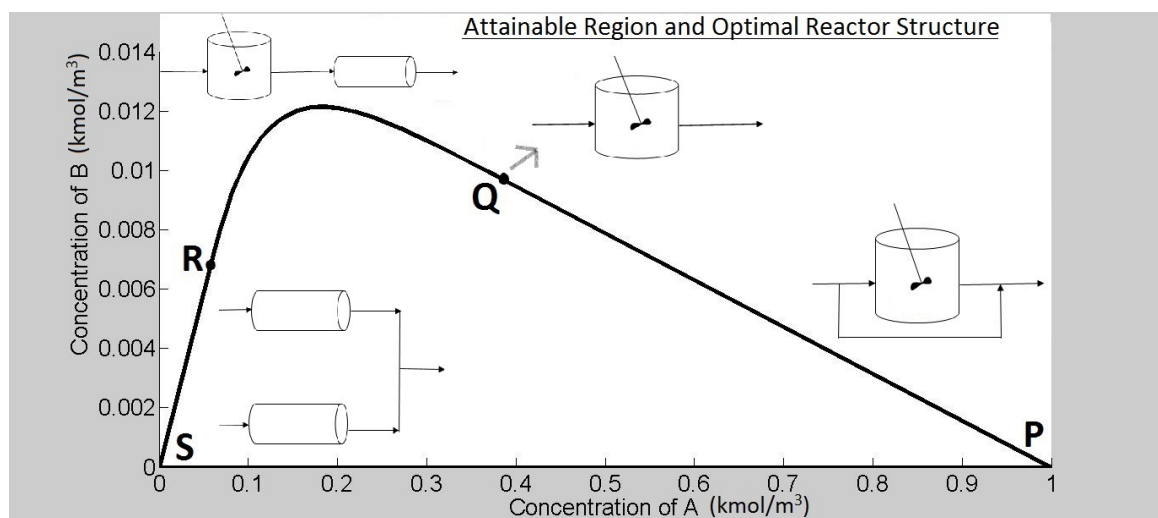
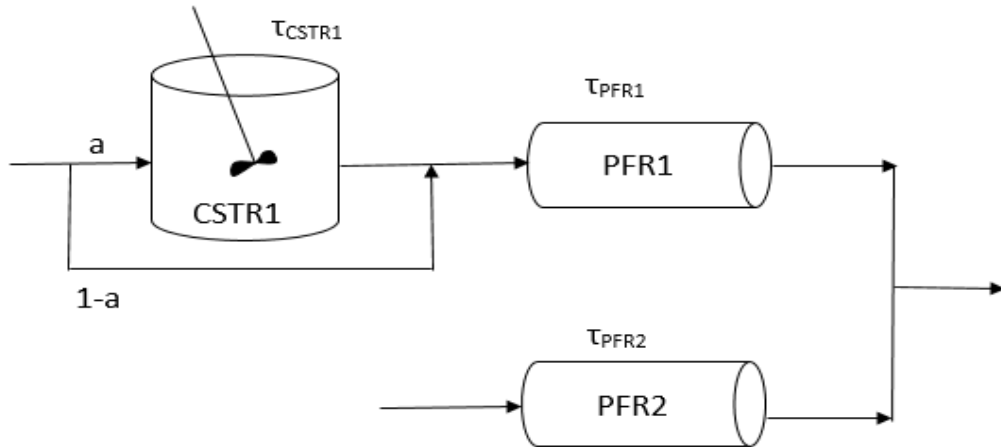


Fig. 4.26. Coupled Attainable Region plot and the optimal reactor network scheme to traverse the boundary for the Van de Vusse reaction scheme

We see that to traverse the boundary PQ, we need to operate a CSTR with the feed bypassed. The amount of feed bypassed to the CSTR exit determines how close or far the required point will be from P (or Q). For the point Q, we have to employ a CSTR with no bypass. Along the curve QR as shown in the figure, a CSTR followed by a PFR is the suitable reactor network and finally, to obtain the region RS, two PFRs have to be operated in parallel such that the output concentration of one of the PFR corresponds to R, and the other to S. We see that the point S is or tends to (0,0). That means complete conversion of A.

Thus, the final reactor network to traverse the boundary that we arrive at for the given reaction scheme is shown in Fig. 4.27.



*Fig. 4.27. Optimal Reactor Network for the Van de Vusse reaction scheme*

We now see how the reactor network generated above can be employed to achieve the AR boundary shown in Fig. 4.26. Note that the network shown above is a generalized one such that it accounts for the total AR. As we will see, for the attainment of any particular point, all the three reactors may not be required and only one or two reactors are sufficient.

By employing CSTR1 for a residence time of 0.04 s, we obtain the point Q. Also, by varying the feed bypassed, we obtain all the points on the black curve connecting P and Q. Next, to obtain the points on the black curve connecting Q and R, it is alright to not bypass any feed to the outlet as we are only interested in the point Q as our feed to PFR1. We employ PFR1 with its feed as the outlet of CSTR1 operated at residence time of 0.04 s (point Q). To attain the point R, the residence time for PFR1 is 0.1279 s. Thus, to attain the AR boundary along QR, we must employ a CSTR for a residence time of 0.04 s and follow it up in series with PFR1 for residence times between 0 and 0.1279 s. The black curve connecting R and S can be obtained by employing the two PFRs in parallel such that the exit of PFR1 corresponds to point R, and that of PFR2 corresponds to point S, which is obtained by operating the PFR2 at a very large residence time.

We observe that both PFR1 and PFR2 are left redundant when attainment of PQ (excluding point Q) is considered. PFR1, PFR2 and the bypass are left redundant when the attainment of point Q is considered. PFR2 is left redundant when attainment of QR is considered. CSTR1 is rendered redundant as far as attainment of the region RS is concerned. Thus, we see that the three reactors are not all required to attain any single point.

We compare our results with the work done by Metzger and Glasser. (Metzger and Glasser, 2007) Fig. 4.28 shows the comparison. Fig. 4.28(a) and 4.28(c) show the attainable region and the optimal reactor network obtained from the previous studies. Our respective results are demonstrated in Fig. 4.28(b) and 4.28(d).

As can be seen from Fig. 4.28, our results match exactly with those obtained by Metzger and Glasser, except the region RS in our work. Since their work was targeted at achieving maximum production of species  $B$ , they have left out the convexification at the region RS. Our result has been rigorously obtained to get maximum attainable region space. We saw in Section 3.2 while projecting the AR on  $(C_A, C_C)$  and  $(C_A, C_D)$  planes that this region can be crucial if the price function favors formation of species  $C$ .

The slight discrepancy in the reactor network obtained from our algorithm and from that obtained by Metzger and Glasser also arises because of the same reason.

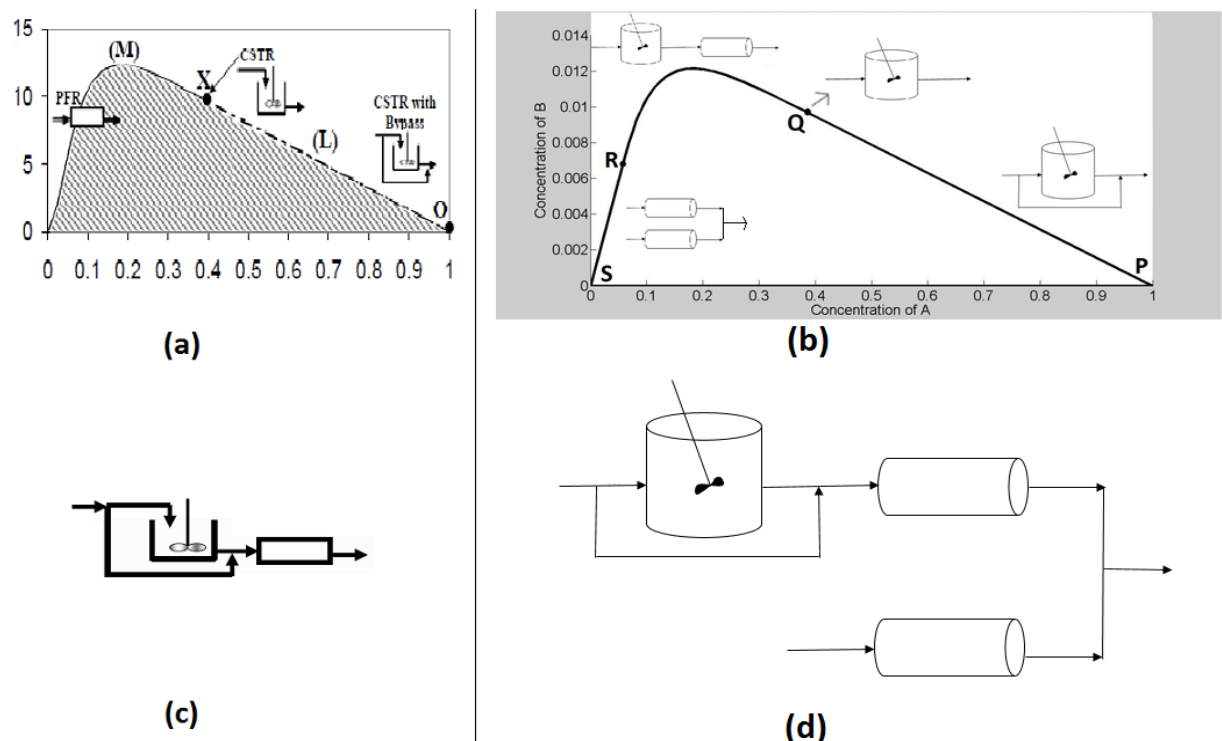


*Fig. 4.28. Comparison of our results with those of Metzger and Glasser. (a) Attainable region from previous study. (b) Attainable region from our results (c) Optimal Reactor Network from previous study (d) Optimal Reactor Network from our results. Figure 11(a) and 11(c) cited from ‘Teaching Reaction Engineering using the Attainable Region; Matthew J. Metzger, Benjamin J. Glasser’*

Now, we look at the reactor networks required to attain each point inside the AR. We combine this with the strategies to attain points on the boundary and present a table that provides us the complete guide towards the strategies to attain the required points. Fig. 4.29 shows the Attainable Region and the various regions we need to investigate. Table 4.1 shows the reactor networks for the various curves/regions.

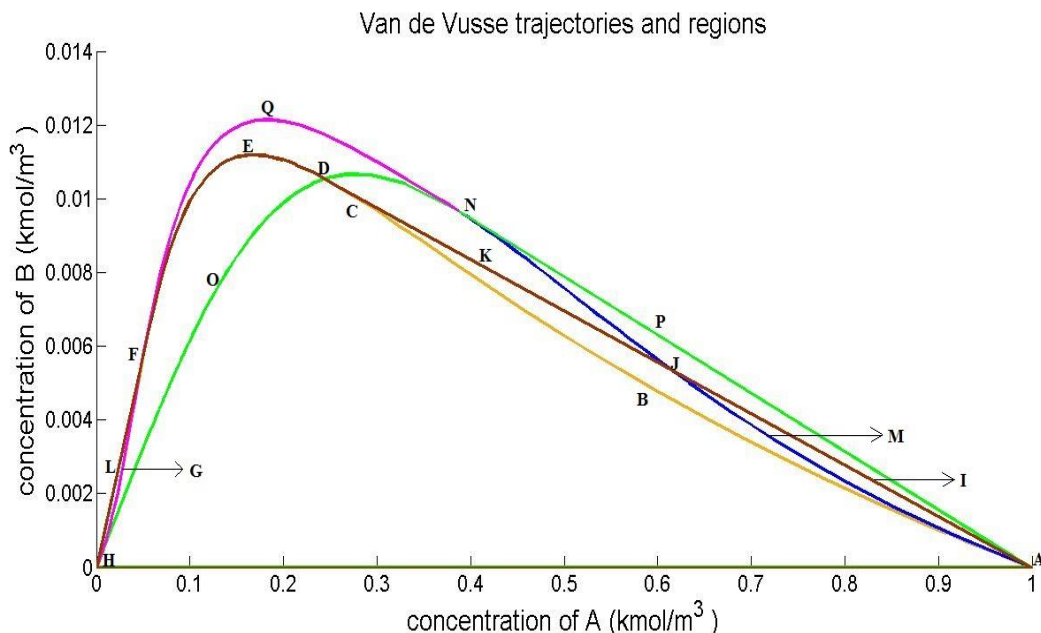
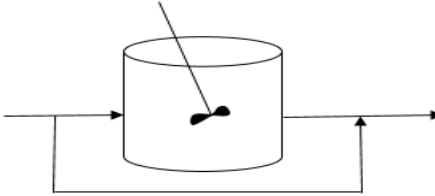
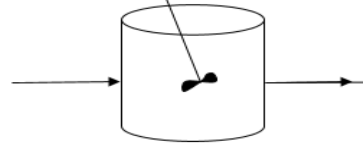
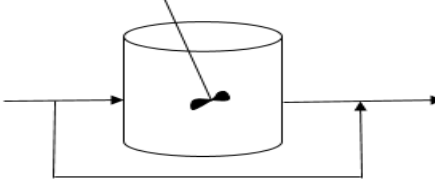
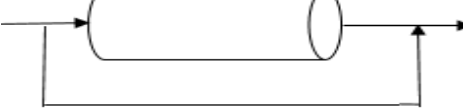
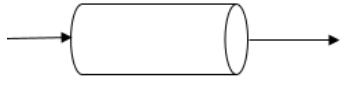
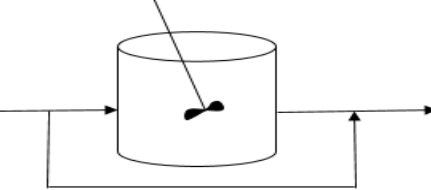
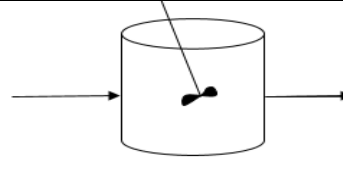
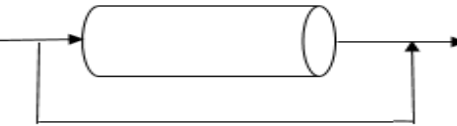
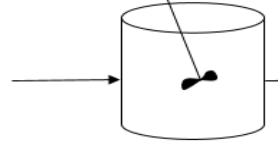
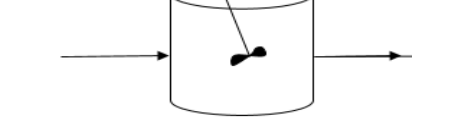
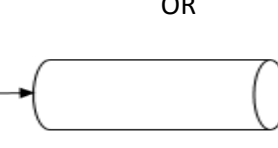
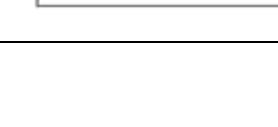


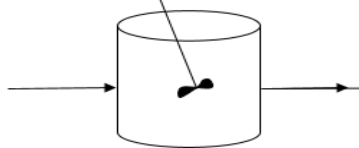
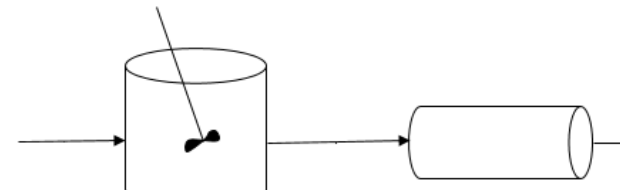
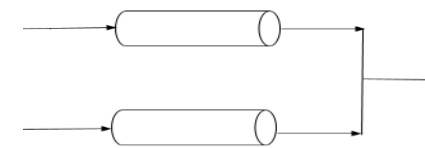
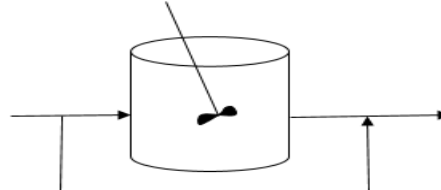
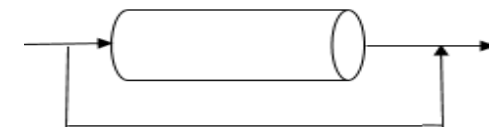
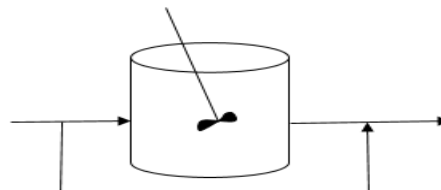
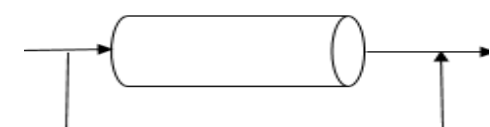
Fig. 4.29. AR plot for the Van de Vusse reaction scheme and its various trajectories and regions

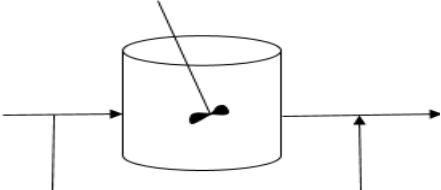
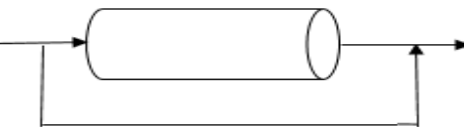
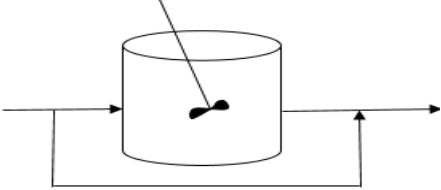
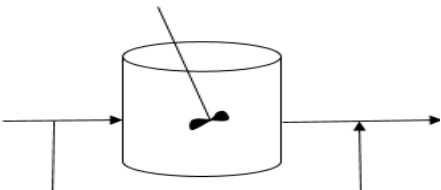
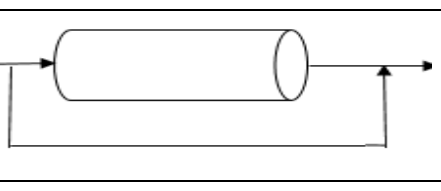
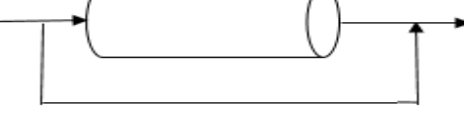
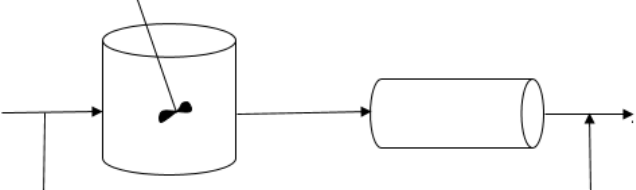
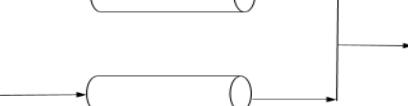
While presenting the reactor networks in Table 4.1., we have abided by the thumb rule that the reactor network with the least number of reactors is the optimal network. However, we see that in some cases, there is a possibility of more than one reactor network. For such cases, the decision as to which network to choose is based on the costs associated with the reactors and mixing.

Table. 4.1. The various regions on the AR and the respective reactor networks

1	Points on ABCD (except A and D)	 OR 
2	Point D	 OR 
3	Points on DEFGH (except D)	
4	Points on AIJKC (Except A and C)	 OR 

		 OR 
5	Point C	 OR 
6	Points on AMJ (except A)	 OR 
7	Points on JND (except J)	 OR 
8	Points on DOH (except D)	 OR 
9	Points on APN (except A and N)	

10	Point N	
11	Points on NQF (Except N)	
12	Points on FLH (except F)	
13	Points in the interior of ABCDOHA	 OR 
14	Points in the interior of AMJIA	 OR 

		 OR 
15	Points in the interior of ABCKJMA	
16	Points in the interior of AIJNPA	
17	Points in the interior of JKDNJ	
18	Points in the interior of DEFGHOD	
19	Points in the interior of NQFEDN	
20	Points in the interior of FLHGF	

## 4.4. Optimization of user-defined objective functions

We further extend our problem solving approach to another case. So far, we have looked at situations when the concentration corresponding to a point was given to us and we had to find the optimal reactor network. Now, we have a look at situations when we are provided with a price function (objective function) that we need to optimize and find the concentration that would enable us to achieve this optimized value.

Suppose we are given the reaction scheme and its kinetics and we also have the selectivity/price function that we need to maximize/minimize. We need to find which point inside or on the AR gives us the optimum value of such a function. Once this is done, we apply the algorithms discussed in the previous sections to find the strategy to attain it. We later demonstrate this using examples.

We use the *fmincon* tool in the *MATLAB Optimization Toolbox* to find the optimum value of the objective function. The input arguments to this solver are the objective function, the initial guess, the inequality constraints, the equality constraints and the upper and lower bounds. We formulate our problem as maximization or minimization of the specified objective function such that only the points inside or on the AR form the domain.

So, as we had mentioned earlier, the AR is a collection of points joined by straight lines such that the obtained region is convex. So, we find the equations of the straight lines between each of the two successive points by finding the slopes and intercepts.

$$\text{slope}_i = m_i = \frac{y_i - y_{i+1}}{x_i - x_{i+1}} \quad (4.10)$$

$$\text{intercept}_i = k_i = y_i - m * x_i \quad (4.11)$$

where,  $y$  and  $x$  are the ordinates and abscissae of the  $i^{th}$  point on the AR.  $y = mx + k$  is the equation form. Now, we need to find whether the value of each expression, i.e.,  $y - mx - k$  is positive or negative for any point inside the AR. For this, we first have to find a point that will surely lie inside the AR. Thus, we find the range of the x-coordinate and the y-coordinate, i.e., the maximum and minimum of the x and y coordinates. Now, we find the mid-point of the x and y coordinates. This point will surely lie inside the AR as it is a closed convex region. The point need not be the midpoint of the range of the x and y coordinates but any point which we are sure of lying inside the AR.

Now, we evaluate and thus find the sign of each of the expressions  $y - mx - k$  with respect to this point. This is done because the *fmincon* solver accepts the inequality constraints only in the form

$$M \cdot t \leq d \quad (4.12)$$

where,  $M$  denotes the vector form of the coefficients of  $x$  and  $y$  in the equations, and  $d$  is the column vector of the constant terms in the equations.  $t$  is the variable in terms of which the objective function is described. In our case, the variables,  $x$  and  $y$  represent the concentration of the two species which we plot the AR in. Also, lower bounds of zero are set on the concentration of all species.

The default type of optimization in *fmincon* is minimization. So, in case we need to have a maximization objective function, we put a negative sign in front of the objective function.

The output arguments of the solver are the values of the variables that lead to the optimization of the objective function, and also the evaluated objective function at those points. So, we formulate the problem as

$$\min -f(C_j) \quad (4.13)$$

such that,

$$\pm y_i \mp m_i x_i \mp k_i \leq 0 \quad (4.14)$$

$$C_j \geq 0 \quad (4.15)$$

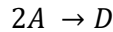
$$i = 1, 2, 3, \dots, n \quad (4.16)$$

$$j = 1, 2, 3, 4 \quad (4.17)$$

where  $n$  denotes the number of total equations formed from the  $n+1$  points on the AR, and  $j$  denotes the species in the reaction scheme. The sign in the constraint (4.14) depends on whether the evaluation of those equations with respect to the point inside the bounded region is negative or positive.

We apply our proposed approach to some examples of isothermal reaction mechanisms.

Example 4.4.1: Van de Vusse (irreversible) kinetics



We note that the reaction  $A \rightarrow B$  is irreversible unlike the reaction used in Section 3.1.

$k_1$  = rate constant for the reaction of  $A \rightarrow B = 10 \text{ s}^{-1}$

$k_2$  = rate constant for the reaction  $B \rightarrow C = 1 \text{ s}^{-1}$

$k_3$  = rate constant for the reaction  $2A \rightarrow D = 0.29 \text{ m}^3 \text{ kmol}^{-1} \text{ s}^{-1}$

Feed Concentration:  $C_{AO} = 1 \text{ kmol m}^{-3}$ ;  $C_{BO} = C_{CO} = C_{DO} = 0$ , where  $C_{io}$  represents the initial concentration of the species  $i$ .

The rate expressions are

$$[-k_1C_A - k_3C_A^2 \quad k_1C_A \quad k_2C_B \quad k_3C_A^2] \quad (4.18)$$

The objective function was the maximization of concentration of specie  $B$ , i.e.,  $C_B$ . We first construct the AR for these kinetics. The AR is plotted as shown in Fig. 4.30.

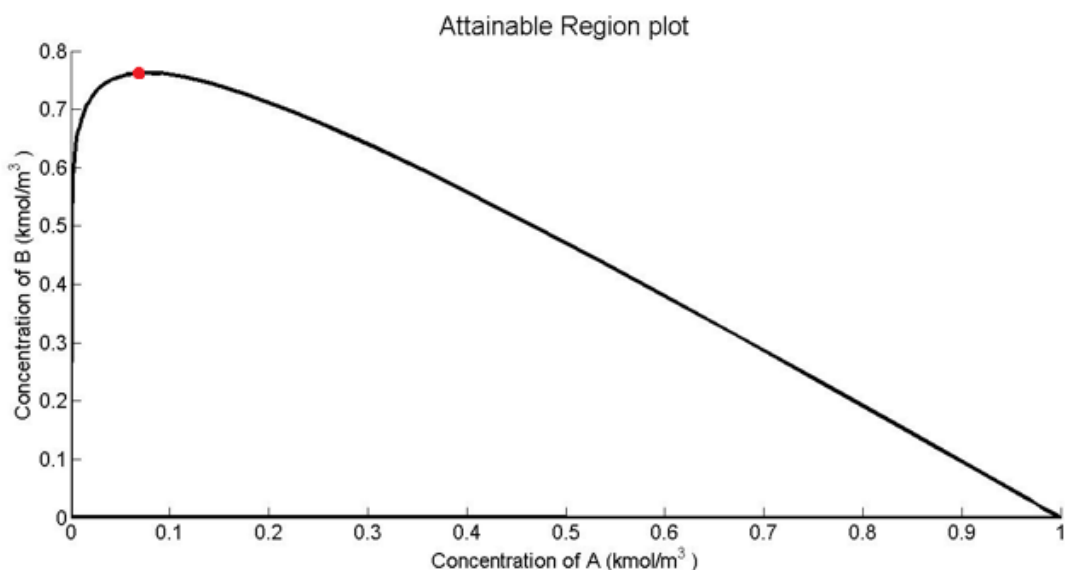
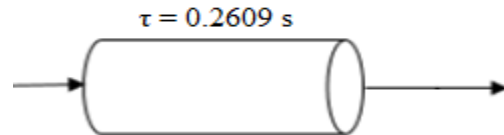


Fig. 4.30. The AR plot the Van de Vusse reaction scheme for the kinetics as given in Example 4.4.1

We then run the solver and get the maximum value to be 0.7634, and the point that allows us to get this maximum is (0.0718, 0.7634). This is shown by the red point in Fig. 4.30.

Now, having known the optimum value of the objective function and the point that enables us to obtain this value, we move on to find the strategy to attain this point. We use the procedure discussed in the previous section.

While constructing the AR, we found that only one stage was required in the construction of the complete AR. Here, a check on whether the point lies inside or on the AR is not required because we have already included these constraints in the optimization problem. So now, we use the algorithms used in Section 4.2. to find the reactor network to attain this point. We find that, the point lies on the normal PFR trajectory and thus, in order to attain the required point, we need to operate a PFR for a residence time of 0.2609 s. So addressing to the user's question, we can claim that to attain the maximum concentration of species B, he/she has to operate a PFR at a residence time of 0.2609 s. The reactor network is shown in Fig. 4.31.



*Fig. 4.31. Reactor network to attain the point desired in Example 4.4.1*

Similarly, we take another four cases and find the optimum value and the reactor network to attain the point enabling us to achieve this value, and compare them with previous studies. Each case involves a different set of rate constants and initial feed concentrations as shown in Table 4.2. For each case, the objective function is the same, i.e., the maximization of the species B.

Note that the rate expressions in each of these four cases are not simple. They are given as

$$[-k_1C_A - 2k_3C_A^2 \quad k_1C_A \quad k_2C_B \quad k_3C_A^2] \quad (4.19)$$

Note the first term here. In case of simple kinetics, it would have been  $-k_1C_A - k_3C_A^2$ . However, in the rate vector given, there is a factor of 2 in the second part of the first term.

For each case, we find the AR and apply the *fmincon* solver on the region obtained. We present the reactor network design for each case.

Table. 4.2. Parameters for Van de Vusse reaction scheme

Parameter	Case1	Case2	Case3	Case4
$k_1 (\text{s}^{-1})$	10	10	10	1
$k_2 (\text{s}^{-1})$	1	1	1	2
$k_3 (\text{m}^3 \text{ kmol}^{-1} \text{ s}^{-1})$	0.5	0.25	0.5	10
Feed concentration (pure A) ( $\text{kmol/m}^3$ )	0.58	0.58	5.8	1

For Case 1, the maximum  $C_B$  is found to be  $0.4368 \text{ kmol/m}^3$  and the reactor network is found to be a PFR operated for a residence time of 0.2635 s.

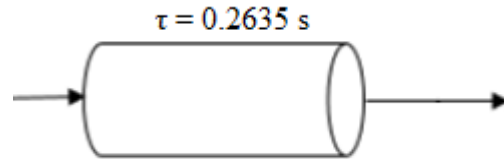


Fig. 4.32. The reactor network required to attain the point desired in Example 4.4.1 – Case 1

For Case 2, the maximum  $C_B$  is found to be  $0.4429 \text{ kmol/m}^3$  and the reactor network is found to be a PFR operated for a residence time of 0.2533 s.

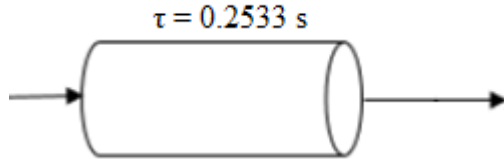
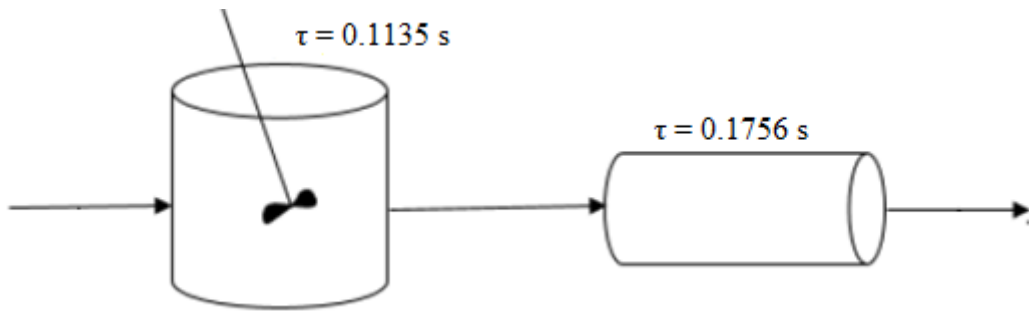


Fig. 4.33. The reactor network required to attain the point desired in Example 4.4.1 – Case 2

For Case 3, the maximum  $C_B$  is found to be  $3.6810 \text{ kmol/m}^3$  and the reactor network is found to be a CSTR operated for a residence time of 0.1135 s followed by a PFR operated for a residence time of 0.1756 s.



*Fig. 4.34. The reactor network required to attain the point desired in Example 4.4.1 – Case 3*

For Case 4, the maximum  $C_B$  is found to be  $0.0703 \text{ kmol/m}^3$ . The reactor network is a CSTR operated for a residence time of  $0.2952 \text{ s}$  followed by a PFR operated for a residence time of  $0.1552 \text{ s}$ .

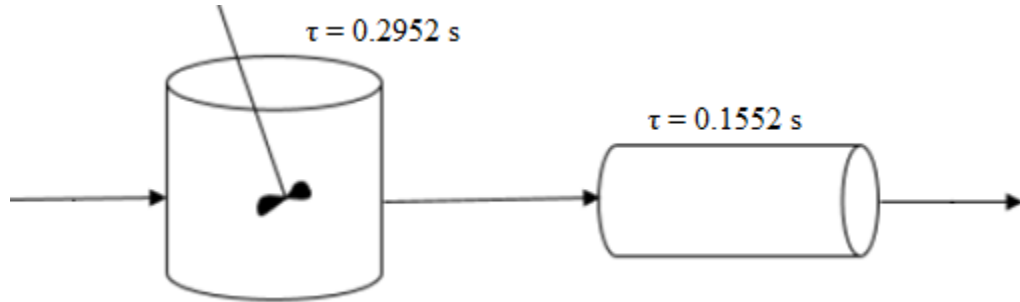


*Fig. 4.35. The reactor network required to attain the point desired in Example 4.4.1 – Case 4*

The results from our work are tabulated in Table 4.3. These are compared with the previous results given in literature.

*Table 4.3. Summary of the previous results as compared to this work for Van de Vusse reaction scheme – Example 4.4.1*

Reference	Objective	Reactor Network (residence time, in seconds)
<b>Case 1</b>		
This work	0.4368	PFR (0.2635)
Chitra and Govind <sup>a</sup>	0.4362	PFR
Achenie and Biegler <sup>b</sup>	0.4368	PFR (0.2965)
Kokossis and Floudas <sup>c</sup>	0.4364	PFR (0.25396)
Schweiger and Floudas <sup>d</sup>	0.43708	PFR (0.25335)
<b>Case 2</b>		
This work	0.4429	PFR (0.2533)
Achenie and Biegler <sup>e</sup>	0.4391	PFR (0.2370)
Balakrishna and Biegler <sup>f</sup>	0.4429	PFR (0.288)
Lakshmanan and Biegler <sup>g</sup>	0.4269	PFR (0.262)
Schweiger and Floudas <sup>d</sup>	0.44297	PFR (0.25458)
<b>Case 3</b>		
This work	3.6810	CSTR (0.1135) + PFR (0.1756)
Chitra and Govind <sup>a</sup>	3.6772	PFR
Kokossis and Floudas <sup>c</sup>	3.6796	CSTR (0.11382) + PFR (0.16989)
Schweiger and Floudas <sup>d</sup>	3.6819	CSTR (0.1135) + PFR (0.16984)
<b>Case 4</b>		
This work	0.0703	CSTR (0.2952) + PFR (0.1552)
Lakshmanan and Biegler <sup>g</sup>	0.0703	CSTR (0.302) + PFR (0.161)
Schweiger and Floudas <sup>d</sup>	0.070267	CSTR (0.29552) + PFR (0.15758)

<sup>a</sup> – (Chitra and Govind, 1981), <sup>b</sup> – (Achenie and Biegler, 1986), <sup>c</sup> – (Kokossis and Floudas, 1990),

<sup>d</sup> – (Schweiger and Floudas, 1999), <sup>e</sup> – (Achenie and Biegler, 1988), <sup>f</sup> – (Balakrishna and Biegler, 1992), <sup>g</sup> – (Lakshmanan and Biegler, 1996)

Example 4.4.2: Trambouze kinetics



$k_1$  = rate constant for the reaction of  $A$  going to  $B$  =  $0.025 \text{ kmol/m}^3/\text{s}^{-1}$

$k_2$  = rate constant for the reaction from  $A$  to  $C$  =  $0.2 \text{ s}^{-1}$

$k_3$  = rate constant for the reaction  $A$  to  $D$  =  $0.4 \text{ m}^3/\text{kmol/s}^{-1}$

The feed is pure  $A$ , its concentration being  $1 \text{ kmol/m}^3$ .

The rate expressions are

$$[-k_1C_A - k_2C_A - k_3C_A^2 \quad k_1C_A \quad k_2C_A \quad k_3C_A^2] \quad (4.20)$$

The objective was the maximization of the function  $C_C/(1 - C_A)$ . We first construct the AR for these kinetics. The AR is plotted in Fig. 4.36:

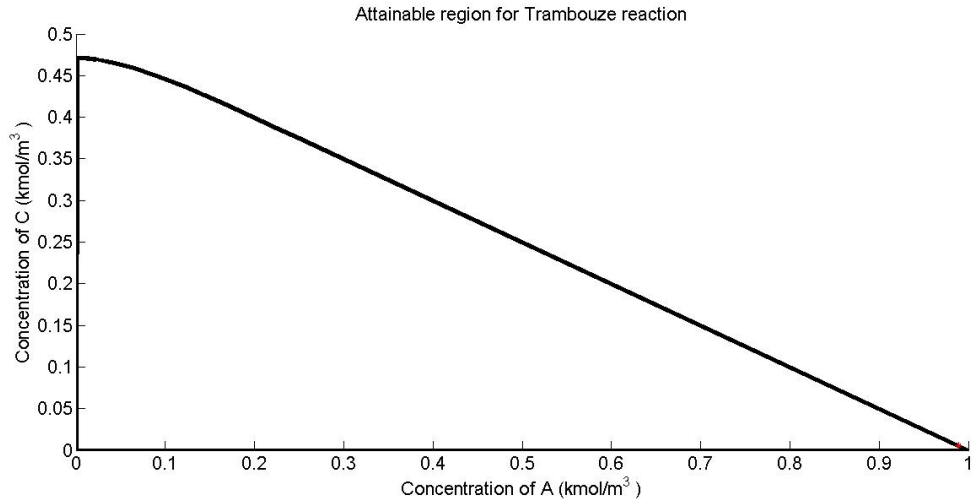
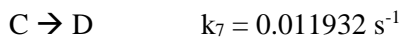
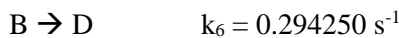
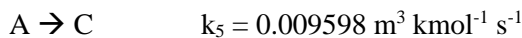
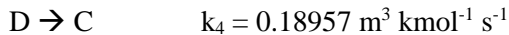
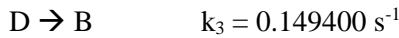
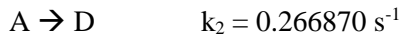
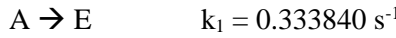


Fig. 4.36. The AR plot the Trambouze reaction scheme for the kinetics as given in Example 4.4.2

We run the solver and find that the maximum of the objective function occurs at multiple points with 0.5 at the maximum value, which matches with the work in previous works. (Schweiger and Floudas, 1999; Waghmare and Moharir, 2006).

### Example 4.4.3: $\alpha$ -Pinene reaction

The reaction mechanism for  $\alpha$ -Pinene reaction is shown below:



The rate expressions are not simple and are given by:

$$\begin{aligned} &[-k_1C_A - k_2C_A - 2k_5C_A^2 \quad k_3C_D - k_6C_B \quad k_5C_A^2 + k_4C_D^2 - k_7C_C \quad k_2C_A \\ &- k_3C_D - 2k_4C_D^2 + k_6C_B + 2k_7C_C \quad k_1C_A] \end{aligned} \quad (4.21)$$

The feed is pure A, its concentration being 1 kmol/m<sup>3</sup>.

The objective function is to maximize the selectivity of C with respect to D, i.e.,  $C_C/C_D$ . We constructed the AR in a  $C_C$  versus  $C_D$  plot as shown in Fig. 4.37. The blue line represents the normal PFR trajectory and the dashed black line represents its convexified curve.

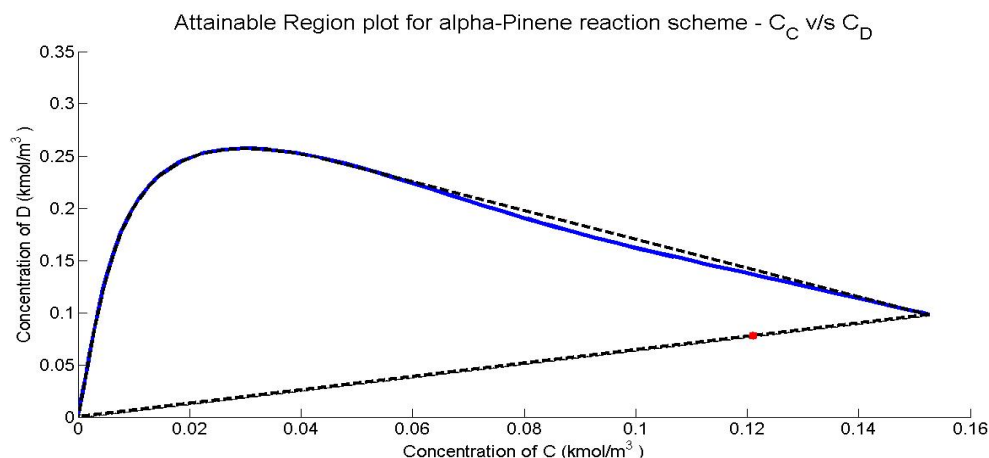


Fig. 4.37. The AR plot the alpha-Pinene reaction scheme for the kinetics as given in Example 4.4.3

The maximum selectivity is found to be 1.5573. (0.1221, 0.0784) is the point that allows us to achieve this maximum selectivity. This point is shown in red in the AR plot in Fig. 4.37.

As can be seen, the required point (shown in red) lies on the line joining feed and the end point of the normal trajectory. We confirm this using *inpolygon* function. The two points between which the convexification line has been joined are found to be (0.1526,0.098) and the feed point (0,0).

Now, we find  $a$ .

$$a * (0.1526,0.098) + (1 - a) * (0,0) = (0.1221,0.0784)$$

Thus,  $a$  is found to be 0.80.

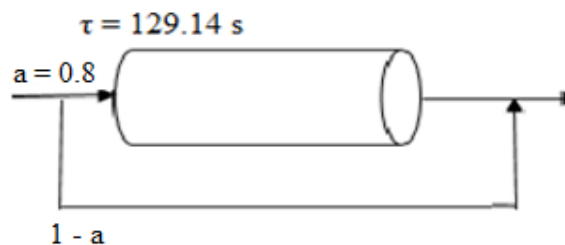


Fig. 4.38. The reactor network required to attain the point desired in Example 4.4.3

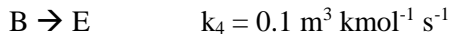
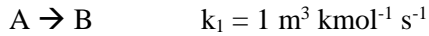
The following table shows the results from our work and those from previous works.

Table. 4.4. Summary of results for the alpha-Pinene reaction scheme (Example 4.4.3)

Reference	Maximum selectivity	Reactor Network (residence time, seconds)
This work	1.5573	PFR (129.14) + bypass ( $a=0.8$ )
Kokossis and Floudas <sup>c</sup>	1.402	-
Balakrishna and Biegler <sup>f</sup>	1.48	PFR (60)
Lakshmanan and Biegler <sup>g</sup>	1.48	PFR (60)
Schweiger and Floudas <sup>d</sup>	1.5570	PFR (586.97) + bypass

<sup>c</sup> – (Kokossis and Floudas, 1990), <sup>d</sup> – (Schweiger and Floudas, 1999), <sup>f</sup> – (Balakrishna and Biegler, 1992), <sup>g</sup> – (Lakshmanan and Biegler, 1996)

Example 4.4.4: Denbigh Kinetics



The rate vector is given by

$$[-k_1C_A^2 - k_3C_A \quad 0.5*k_1C_A^2 - k_2C_B - k_4C_B^2 \quad k_2C_B \quad k_3C_A \quad k_4C_B^2] \quad (4.22)$$

As we can see, the second term is not simple.

The feed is a mixture of *A* and *D*, their concentrations being 6 and 0.6 kmol/m<sup>3</sup> respectively.

The objective function is to maximize the selectivity of *B* with respect to *D*, i.e.,  $C_B/C_D$ . We constructed the AR in a  $C_B$  versus  $C_D$  plot as shown in Fig. 4.39.

The maximum selectivity is found to be 1.3210. (1.3904, 1.0526) is the point that allows us to achieve this maximum selectivity. The reactor network is shown in Fig. 4.40.

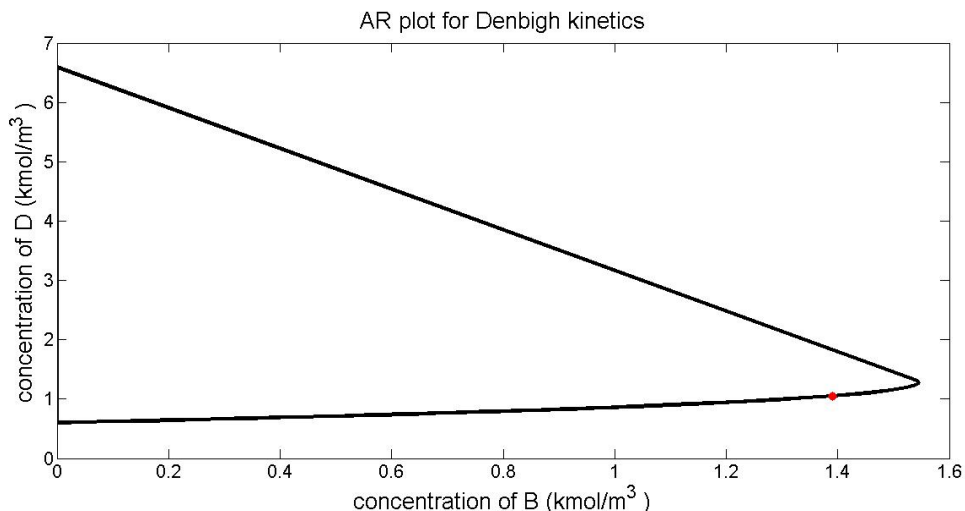
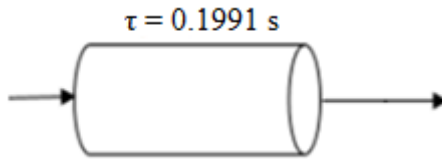


Fig. 4.39. The AR plot the Denbigh reaction scheme for the kinetics as given in Example 4.4.4



*Fig. 4.40. The reactor network required to attain the point desired in Example 4.4.4*

The table shows the results from our work as compared with previous studies.

*Table 4.5. Summary of results for the Denbigh reaction scheme (Example 4.4.4)*

Reference	Selectivity	Reactor Network (residence time, seconds)
This work	1.3210	PFR (0.1991)
Achenie and Biegler <sup>e</sup>	1.322	2 PFRs in series
Kokossis and Floudas <sup>c</sup>	1.319	PFR (0.207062)
Balakrishna and Biegler <sup>f</sup>	1.322	PFR (0.209)
Lakshmanan and Biegler <sup>g</sup>	1.322	PFR (0.209)
Schweiger and Floudas <sup>d</sup>	1.3218	PFR (0.2075)

<sup>c</sup> – (Kokossis and Floudas, 1990), <sup>d</sup> – (Schweiger and Floudas, 1999), <sup>e</sup> – (Achenie and Biegler, 1988), <sup>f</sup> – (Balakrishna and Biegler, 1992), <sup>g</sup> – (Lakshmanan and Biegler, 1996)

Thus, having studied extensively the construction of AR in Chapter 3, we use it to derive the reactor networks in this chapter. First of all, we saw whether a required concentration is attainable or not, i.e., whether the point corresponding to the required concentration lies inside/on the AR or outside. This is an important study because if the point is not attainable, then we do not move forward and we save ourselves efforts. If the point was found to be attainable, we found the possible reactor network(s). The reactor network(s) generated were then questioned for optimality. We found all the possible reactor network designs and formulated the cost optimization functions. These can be solved once we have input expressions for the various costs involved from the user. Finally, we looked at optimization of some of the user provided objective functions. These were taken from literature. Then, we found the reactor network design required to attain the points so as to bring the optimum value. We compared our results of optimum value and the reactor network design required to attain it against previous works and found that the sets of results match fairly. Thus, the whole purpose of finding a way to derive the optimal reactor network design and confirm its generic nature and accuracy was studied in this chapter.

## CHAPTER 5

### CONCLUSIONS

This study begins by introducing and understanding the concept of Attainable Region (AR). AR is the set of all possible concentrations that can be attained when any number and arrangement of reactors are operated for any set of parameters, such as residence time and bypass and for a given reaction scheme and its kinetics. It is usually represented in a two dimensional space with the two dimensions being concentration of any two species. By taking simple examples first, we saw that the AR can be zero dimensional, one dimensional and so on. The first property of AR is that the feed is always a part of the AR. The next property states that the concentration space corresponding to infinite reactor space time is also a point of the AR. The next property, and perhaps the most important one, is that AR is convex, i.e., if any two points in/on the region are attainable, then all the points on the line are also attainable. We also saw how the process of mixing can enable us to make the AR convex. The concavity that arises in the AR concentration space due to the process of reaction is taken care of by mixing.

We looked into the literature for methods to construct the AR. Three methods were seen, namely the Rate Vector method, linear programming method and the Infinite DimEnsionAl State-space (IDEAS) method. The rate vector method is governed by the PFR and CSTR rate vectors. We first draw a PFR trajectory from the feed point. By a PFR trajectory, we mean the trajectory obtained after solving the PFR rate equations. The rate vector for a PFR trajectory is the tangent to it at every point and must point outside, i.e. when extended, the vector should not touch the PFR trajectory again. We look for points where this does not happen. The region where we would find such rate vectors are concave and we convexify such regions. This convex region is a candidate AR. With these points in the concave regions as feed, we construct CSTR trajectories. Now, we see whether the CSTR trajectories and their convexified regions extend the candidate AR obtained earlier. This step is repeated until there is no further extension of the AR. This method was chosen over the linear programming and IDEAS methods because the latter two solved a set of equations for a particular reactor or a reactor network and found the AR with respect to that network. Several simulations would thus have to be carried out to get and guarantee the obtaining of the complete

AR. The rate vector method is computationally more efficient and also, it allows for easy visualization of the effect of the choice of reactors and mixing in the AR.

We incorporated the steps of the rate vector method in our tool. Our aim was to make the tool accurate and generic in nature. The tool is such that we just have to input the reaction scheme and its kinetics and the feed concentration, and we get the complete AR. The idea was to make it work for any number of reactions, any type of reactions (series or parallel; reversible or irreversible), any order of reactions and any value of the rate constants. To make sure of the generic nature, we constructed ARs for Van de Vusse, Trambouze and Denbigh kinetics. To make sure of the accuracy, we compared our results to previous works and found that the results match. Also, the tool is very flexible in the sense that it works for any feed composition and reaction scheme and its kinetics we enter as input, and can present the AR in any two dimensional space that the user may want.

A practical constraint in real life is that the feed is not infinitely available and also, we are given a single reactor of a fixed size. So, we investigated the construction of ARs under these restrictions. We saw that the convexity of the AR was challenged once we had such restrictions. Initially, the convexity of the AR was proposed by putting forward the argument that if the outputs of two reactors operating in parallel are mixed, any concentration on the straight line joining these two points can be achieved by adjusting the flow rates. Also, in case of a single reactor, the feed can be bypassed and all concentrations corresponding to points on the straight line joining the points represented by output concentration and feed concentration can be achieved by mixing in adjusted flow rates. Now, since there is only a single reactor with a fixed volume, the first argument cannot be availed. Also, since there is a limitation on the availability of feed, the second argument may also fail. We also extended this concept to two reactor systems and found that it extended the area under the AR for one reactor system. We also constructed ARs for three reactor systems under these conditions but found that there was no further extension.

Further, a reactor network generator was developed that makes use of the reactor trajectories and mixing lines used in the construction of the AR to find the reactor network design to achieve a required concentration, if this concentration is attainable. In other words, we answered the question: Will we be able to achieve this particular concentration? If yes, tell what is the reactor network and parameters to do that. We first illustrated cases on how to proceed and find a possible reactor network design when the required point (concentration) lied in one of four regions pertaining to a particular stage. Then, we found more possible networks by investigating the regions from the next stage. The thumb rule that the network with the least number of reactors is the most

optimal one, was used to eliminate all networks having more number of reactors. Once we had possibilities for the optimal network having the same number of minimum reactors, we formulated cost minimization functions, so as to get the best reactor network design.

Further, having a closed convex attainable region, we were able to optimize specified objective functions within this bounded region and find the concentration which would enable us to obtain this optimized value. Again, using the reactor network generator, we were able to arrive at the best reactor network design to do this. Thus, we answered the question: How can we maximize our earnings (optimize my objective function) and which concentration will enable us to do that? Also, what is the best reactor network design where the least cost will be incurred, that will enable us to achieve this concentration? Again, comparing against previous works, we validated the accuracy and generic nature of our results.

Thus, as a result of this study, we have a tool that can generate the Attainable Region (AR) for any feed composition, reaction scheme and kinetics that are considered, i.e. for any number of reactions, any combination of reactions (series/parallel; reversible/irreversible), any order of reactions, and any value of rate constants. Also, for a required point, either directly given to us by the user, or found out by solving optimization functions, we can tell whether it is attainable or not. If yes, we are in a position to derive possible reactor network designs. Knowledge of the cost functions associated with the operation of these networks can further enable us to find out the optimal reactor network design.

Fig. 5.1. shows the flowchart highlighting the key aspects of this study.

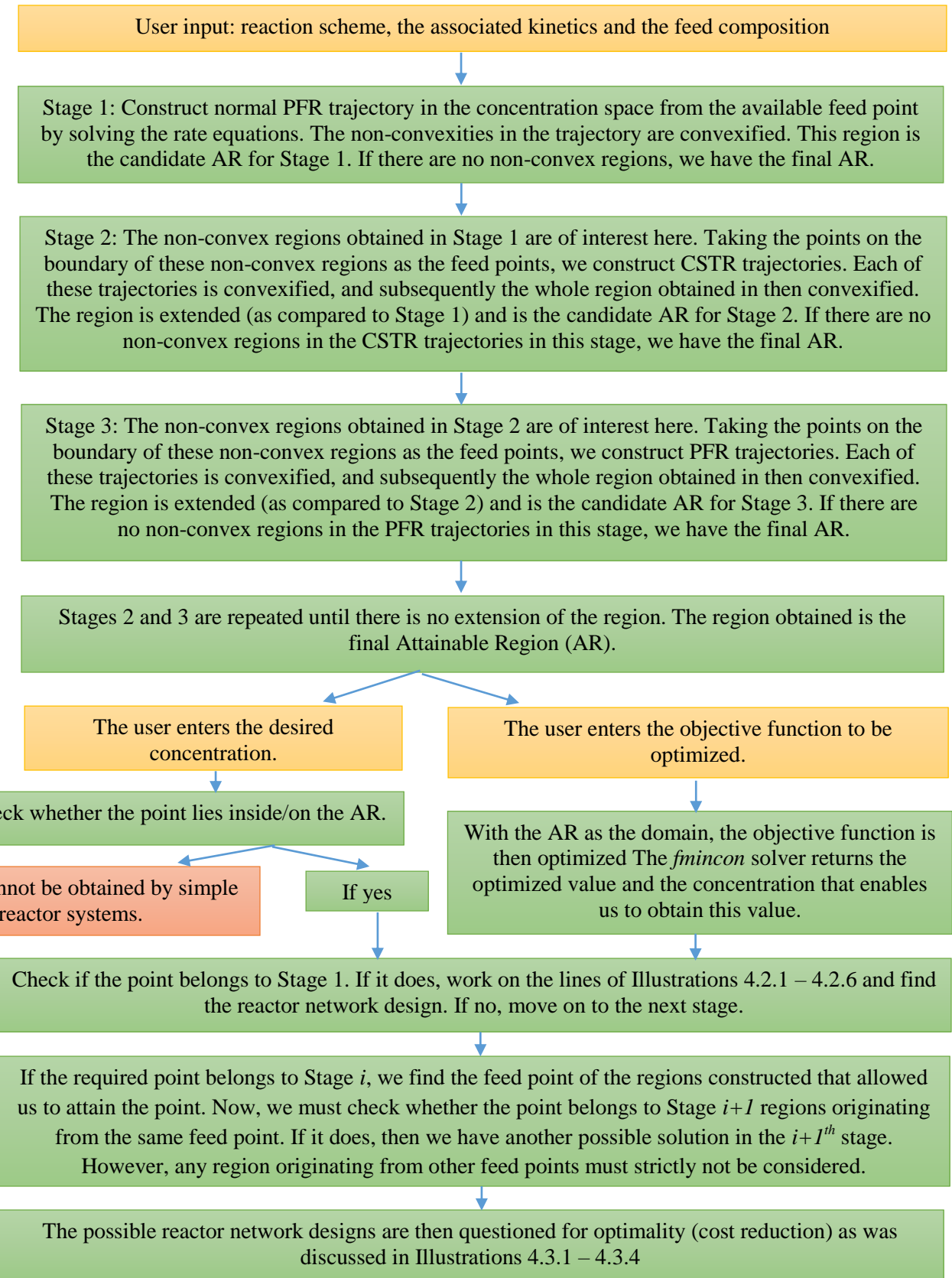


Fig. 5.1. Summary of the study

**References:**

- Achenie, L.K.E., Biegler, L.T., 1986, "Algorithmic Synthesis of Chemical Reactor Networks Using Mathematical Programming", *Industrial and Engineering Chemistry Fundamentals* 25, 621-627
- Achenie, L.K.E., Biegler, L.T., 1988, "Developing Targets for the Performance Index of a Chemical Reactor Network", *Industrial and Engineering Chemistry Research*, 27, 1811-1821
- Agarwal, V., Thotla. S., Kaur, R., Mahajani, S., 2008a, "Attainable regions of reactive distillation. Part II: Single reactant azeotropic systems", *Chemical Engineering Science* 63, 2928-2945.
- Agarwal, V., Thotla. S., Mahajani, S., 2008b, "Attainable regions of reactive distillation—Part I. Single reactant non-azeotropic systems", *Chemical Engineering Science* 63, 2946-2965.
- Amte, V., Gaikwad, R., Malik, R., Mahajani, S., 2012, "Attainable region of reactive distillation—Part IV: Inclusion of multistage units for complex reaction schemes", *Chemical Engineering Science* 68, 166-183.
- Amte, V., Nistala, S., Malik, R., Mahajani, S., 2011, "Attainable regions of reactive distillation—Part III. Complex reaction scheme: Van de Vusse reaction", *Chemical Engineering Science* 66, 2285-2297.
- Balakrishna, S., Biegler, L.T., 1992, "Constructive Targeting Approaches for the Synthesis of Chemical Reactor Networks", *Industrial and Engineering Chemistry Research* 31, 300-312
- Burri, J.F., Wilson, S.D., Manousiouthakis, V.I., 2002, "Infinite Dimensional State-space approach to reactor network synthesis: application to attainable region construction", *Computers & Chemical Engineering* 26, 849-862.
- Chitra, S.P., Govind, R., 1981, "Yield Optimization for Complex Reactor Systems", *Chemical Engineering Science* 36, 1219-1225

Danha, G., Hildebrandt, D., Glasser, D., Bhondayi, C., 2015, "A laboratory scale application of the attainable region technique on a platinum ore", Powder Technology 274, 14-19.

Feinberg, M., 1999, "Recent results in optimal reactor synthesis via attainable region theory", Chemical Engineering Science 54, 2535-2543.

Feinberg, M., 2000, "Optimal reactor design from a geometric viewpoint. Part II. Critical sidestream reactors", Chemical Engineering Science 55, 2455-2479.

Glasser, D., Hildebrandt, D., 1987, "A geometric approach to steady flow reactors: the attainable region and optimization in concentration space", Industrial & Engineering Chemistry Research 26, 1803-1810.

Glasser, D., Hildebrandt, D., 1997, "Reactor and process synthesis", Computers & Chemical Engineering 21, Supplement, S775-S783.

Glasser, D., Hildebrandt, D., Godorr, S., 1994, "The Attainable Region for Segregated, Maximum Mixed, and Other Reactor Models", Industrial & Engineering Chemistry Research 33, 1136-1144.

Godorr, S., Hildebrandt, D., Glasser, D., 1999, "Choosing Optimal Control Policies Using the Attainable Region Approach", Industrial & Engineering Chemistry Research 38, 639-651.

Godorr, S.A., Hildebrandt, D., Glasser, D., 1994, "The attainable region for systems with mixing and multiple-rate processes: finding optimal reactor structures", The Chemical Engineering Journal and the Biochemical Engineering Journal 54, 175-186.

Hildebrandt, D., Glasser, D., 1990, "The attainable region and optimal reactor structures", Chemical Engineering Science 45, 2161-2168.

Hildebrandt, D., Glasser, D., Crowe, C.M., 1990, "Geometry of the attainable region generated by reaction and mixing: with and without constraints", Industrial & Engineering Chemistry Research 29, 49-58.

Hopley, F., Glasser, D., Hildebrandt, D., 1996, "Optimal reactor structures for exothermic reversible reactions with complex kinetics", Chemical Engineering Science 51, 2399-2407.

Kauchali, S., Hausberger, B., Hildebrandt, D., Glasser, D., Biegler, L.T., 2004, "Automating reactor network synthesis: finding a candidate attainable region for the water–gas shift (WGS) reaction", Computers & Chemical Engineering 28, 149-160.

Kauchali, S., McGregor, C., Hildebrandt, D., 2000, "Binary distillation re-visited using the attainable region theory", Computers & Chemical Engineering 24, 231-237.

Kauchali, S., Rooney, W.C., Biegler, L.T., Glasser, D., Hildebrandt, D., 2002, "Linear programming formulations for attainable region analysis", Chemical Engineering Science 57, 2015-2028.

Khumalo, N., Glasser, D., Hildebrandt, D., Hausberger, B., Kauchali, S., 2006, "The application of the attainable region analysis to comminution", Chemical Engineering Science 61, 5969-5980.

Kokossis, A.C., Floudas, C.A., 1990, "Optimization of Complex Reactor Networks-I. Isothermal Operation", Chemical Engineeirng Science 45, 595-614

Lakshmanan, A., Biegler, L.T., 1996, "Synthesis of Optimal Chemical Reactor Networks", Industrial & Engineering Chemistry Research 35, 1344-1353.

Metzger, M., Glasser, B., 2007, "Teaching Reaction Engineering using the Attainable Region", Chemical Engineering Education 41, 258-264.

Omtveit, T., Tanskanen, J., Lien, K.M., 1994, "European Symposium on Computer Aided Process Engineering—3 Graphical targeting procedures for reactor systems", Computers & Chemical Engineering 18, S113-S118.

Mulenga, F.K., Chimwani, N., 2013, "Introduction to the use of the attainable region method in determining the optimal residence time of a ball mill", International Journal of Mineral Processing 125, 39-50.

- Nicol, W., Hernier, M., Hildebrandt, D., Glasser, D., 2001, "The attainable region and process synthesis: reaction systems with external cooling and heating: The effect of relative cost of reactor volume to heat exchange area on the optimal process layout", Chemical Engineering Science 56, 173-191.
- Nicol, W., Hildebrandt, D., Glasser, D., 1997, "Process synthesis for reaction systems with cooling via finding the Attainable Region", Computers & Chemical Engineering 21, Supplement, S35-S40.
- Okonye, L.U., Hildebrandt, D., Glasser, D., Patel, B., 2012, "Attainable regions for a reactor: Application of  $\Delta H - \Delta G$  plot", Chemical Engineering Research and Design 90, 1590-1609.
- Rooney, W.C., Hausberger, B., Biegler, L.T., Glasser, D., 2000, "Convex attainable region projections for reactor network synthesis", Computers & Chemical Engineering 24, 225-229.
- Schweiger, C.A., Floudas, C.A., 1999, "Optimization Framework for the Synthesis of Chemical Reactor Networks", Industrial and Engineering Chemistry Research 38, 744-766
- Scott, F., Conejeros, R., Aroca, G., 2013, "Attainable region analysis for continuous production of second generation bioethanol", Biotechnology for biofuels 6, 171.
- Smith, R.L., Malone, M.F., 1997, "Attainable Regions for Polymerization Reaction Systems", Industrial & Engineering Chemistry Research 36, 1076-1084.
- Vetter, T., Burcham, C.L., Doherty, M.F., 2014, "Regions of attainable particle sizes in continuous and batch crystallization processes", Chemical Engineering Science 106, 167-180.
- Waghmare, R.S., Moharir, A.S., 2006, "Isothermal PFR/PMR Networks", International Journal of Chemical Reactor Engineering, Vol 4, 1542-6580
- Wang, X., Wang, C., Jin, S., Chen, H., 2006, "Optimal operating conditions for reactor-separator-recycle system", Journal of Scientific and Industrial Research, Vol 65, 867-872